Politecnico di Torino

Master's Degree in Energy and Nuclear Engineering
A.a. 2024/2025
March 2025

Design and management of a hybrid system for a multi-dwelling building in the context of renewable energy communities

Relatori:
Viviana Negro
Michel Noussan

Candidato:
Stefano Pricop

Tutor Aziendale:
Abhinav Sawhney

Politecnico di Torino

Index

List of figures

List of tables

1 Introduction

In recent years, the transition to a more sustainable and decentralised energy system has become a key issue in global environmental policy. Renewable Energy Communities (RECs) are seen as a promising solution to facilitate the integration of renewable energy sources and promote active participation of citizens in energy production and management. In this context, the adoption of hybrid systems combining photovoltaic (PV) systems and battery energy storage systems (BESS) is a key element to maximise self-consumption, reduce dependence on the national grid and improve overall energy efficiency.

1.1 Scope of work

This thesis project focuses on the design and operational management of a hybrid system for a multi-dwelling building in an urban context. The first phase of the work includes the sizing of the PV and BESS system using commercial software to ensure a professional approach. The main objective is to optimise solar energy production and the storage of surplus energy storage to ensure a continuous and sustainable energy supply.

An Energy Management System (EMS) will be then developed to plan daily operations. The EMS will use predictive algorithms to estimate the next day's energy demand and optimise the use of available resources, thus improving the operational efficiency of the hybrid system.

The project will be implemented within the framework of RECs, which promote shared renewable energy production and consumption models. Through a critical analysis of the results, this thesis aims to demonstrate how advanced technological solutions can contribute to the realisation of a sustainable energy future, by enhancing the energy self-sufficiency of local communities and reducing the overall environmental impact.

To summarise, this project aims to design and manage a hybrid system for a multi-house building, incorporating PV and BESS technologies, managed by a day-ahead EMS, under the framework of RECs. This approach ensures an efficient, sustainable and community driven energy solution.

1.2 World energy market

The global energy market is undergoing a deep transformation driven by the accelerated deployment of renewable energy, due to the transition to a more electrified system, the challenges of energy security and climate change. Clean energy production is experiencing unprecedented growth, with investments in all kinds of renewable sources, gradually overtaking those in fossil fuels especially for electricity production. This expansion is being driven by national policies, increasingly lower technology costs and growing climate awareness.

In the last decade, the share of fossil fuels in the global energy mix has slightly decreased, from 82% in 2013 to 80% in 2023. Over the same period energy demand has increased by 15%, but it is important to note that approximately 40% of this growth has been met by clean energy sources (renewables, nuclear energy, and low-emission fuels supported by carbon capture and storage technologies currently under development and commercialization) [1].

Figure 1 shows an overview of the global energy mix from 1950 to 2023 and a forecast until 2050 [1]. On the right side, it is possible to observe different perspectives starting from the less optimistic (STEPS) to the most optimistic one (NZE) in terms of penetration of clean energy. In the Stated Policies Scenario (STEPS), the fossil fuels will represent the 58% of total energy demand in 2050. For the other two scenarios the forecasts are less conservative: in the Announced Pledges Scenario (APS) clean energy will meet 75% of global energy demand by 2050, while for the Net Zero Emissions by 2050 (NZE) almost all the global energy demand will be satisfied by energy derived from low-emission systems.

However, differences are relevant between advanced and developing economies separately. The data are collected from 2000 to 2050, considering an estimation for the future years. Regarding advanced economies, overall energy demand has been observed to decrease by 0.5% per year over the past decade, and renewables have an annual growth rate of 3% since 2013. For emerging and developing countries the situation is the opposite: energy demand extrapolated from the graph grew by 2.6% per year over the same period, driven by an increasing population [1].
The general trends for both types of economies are represented in Figure 2.

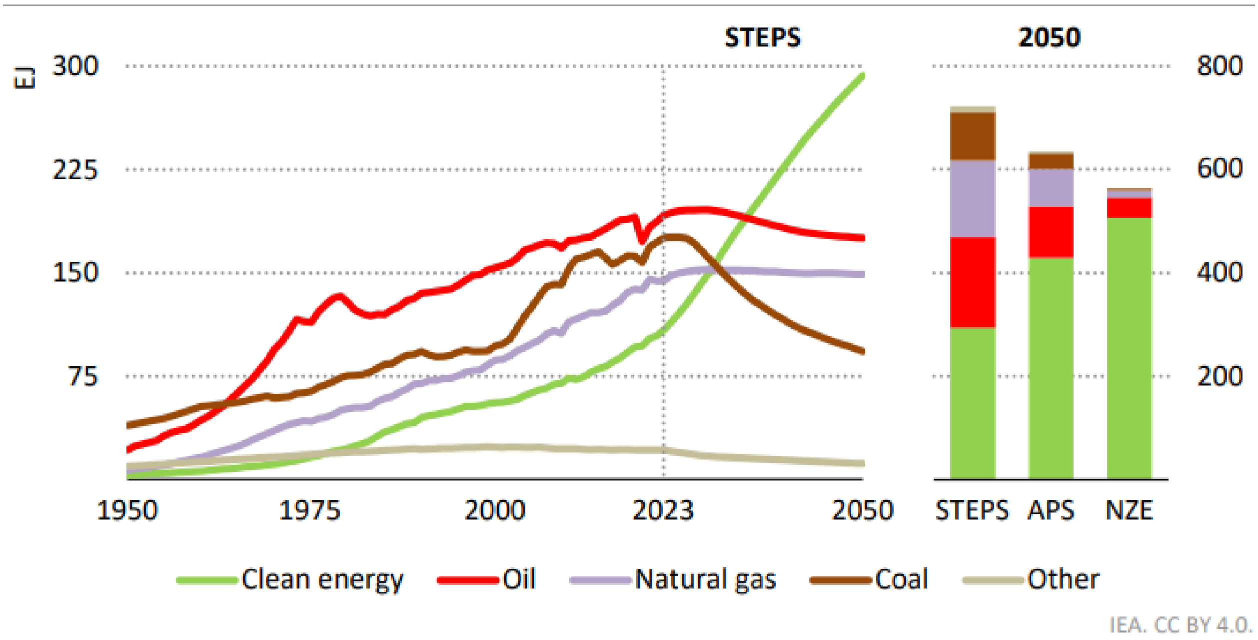

Figure 1: Global energy mix by scenario to 2050 [1]

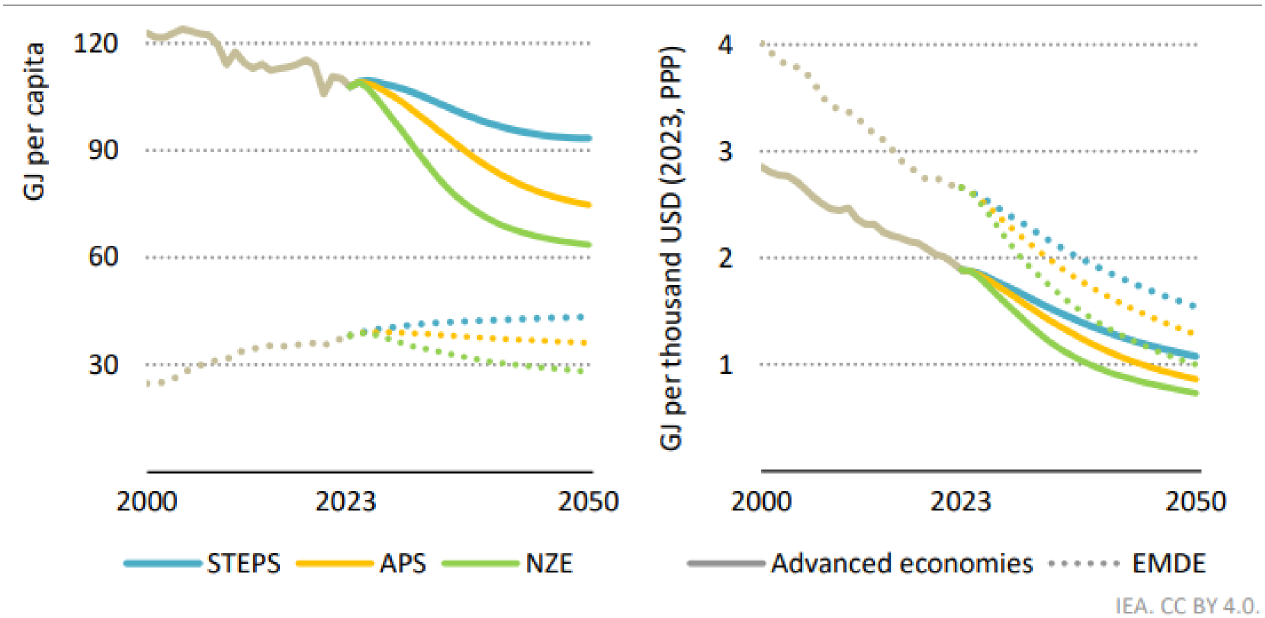

Figure 2: Total final consumption per capita and per unit of GDP by scenario [1]

It is quite clear that globally, the energy intensity has been falling thanks to technological progress, innovations, efficiency improvements and changes in the structure of global economy. Energy intensity refers to the amount of energy consumed per unit of output service, and it has been declining as energy resources are used more efficiently. The expansion of renewable energy and the increasing electrification of end-uses are important in order to improve the overall efficiency of the system. Energy efficiency, which measures the ability to achieve the same results using less energy, is crucial because the most advanced cutting-edge technologies, like heat pumps and electric vehicles, are able to perform their task using less energy than those that rely on fossil fuels.

1.2.1 Solar photovoltaic technology

Solar photovoltaic is a highly modular technology that can be manufactured in large plants, but it can be also used for small size applications. The modularity of this technology can permit to rely on a wide range of applications, from small residential systems up to power plants able to inject the electricity produced directly into the electric grids.

The global solar PV capacity increased by over 80% in 2023 in comparison with 2022, reaching the maximum nominal power capacity of 425 GW. About this aspect, China is the most influent country responsible for over 60% of all capacity increase. The European Union has been responsible for an addition of nearly 60 GW, while the USA accounts for over 30 GW. As shown in Figure 3, all the IEA's future scenarios point out that the capacity additions will continue over the period taken into consideration.
However, current solar PV generates just 5% of the total electricity generation in the world, but it should increase its share up to 17% in 2030 under the most realistic expectations. By 2035, electricity production from solar PV systems overtakes generation derived from coal and natural gas and will became the main source of electricity. This rapid growth of this technology will be beneficial in the next future because it ensures electricity security and more energy production from renewable energy sources, taking part to the energy transition towards electrification [1].

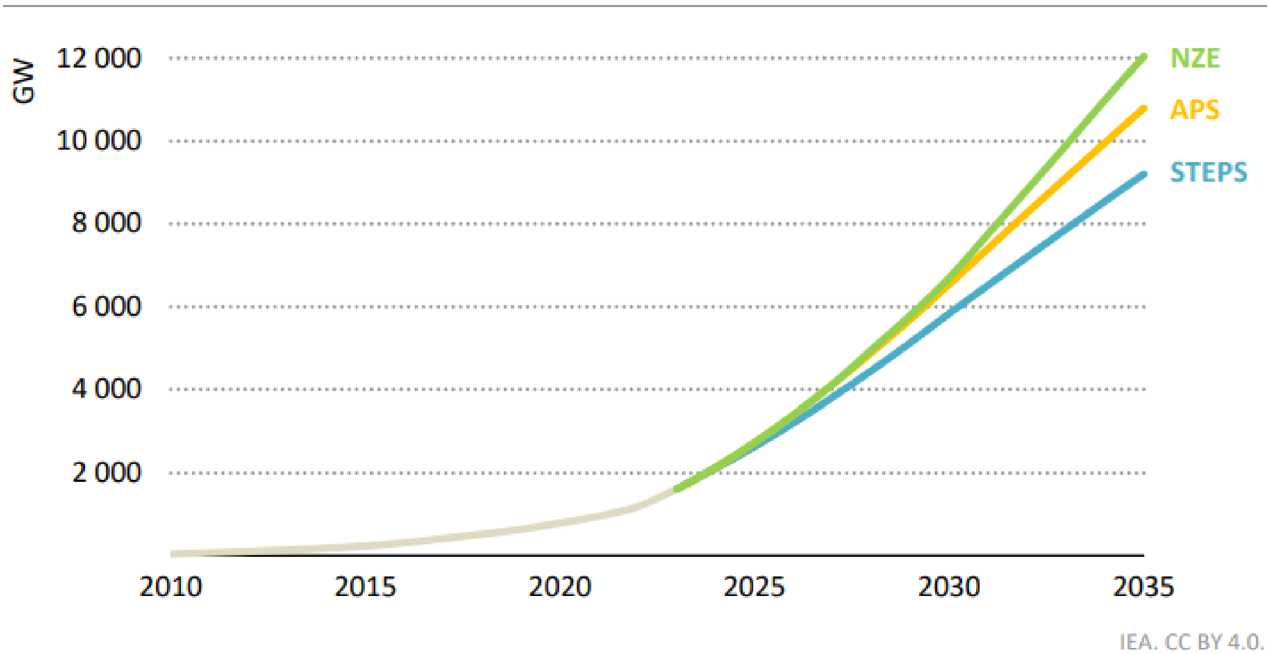

Figure 3: Scenario of solar PV capacity (2010-2035) [1]

1.2.2 Electricity demand and supply

As previously mentioned, the electrification process is extremely relevant in order to improve the total energy efficiency and to reduce as much as possible the CO_2 emission until 2050 [1]. In fact, the electricity sector is responsible for 36% of the energy-related CO_2 emissions in 2023. Nowadays, it is the largest emitting sector in the world. Therefore, the analysis of electricity demand and supply is useful to understand how these two parameters will be influenced by several political and economic factors.
[1]

1.2.2.1 Electricity demand

Global electricity demand rose by more than 2.5% in 2023 in comparison with the previous year, following a similar rate compared to those of the past years. China is the major contributor to the increase in demand for electricity, driven by an aggressive electrification in all the sectors of their industry [1]. Figure 4 provides a more detailed overview at the electricity demand by region and scenario.

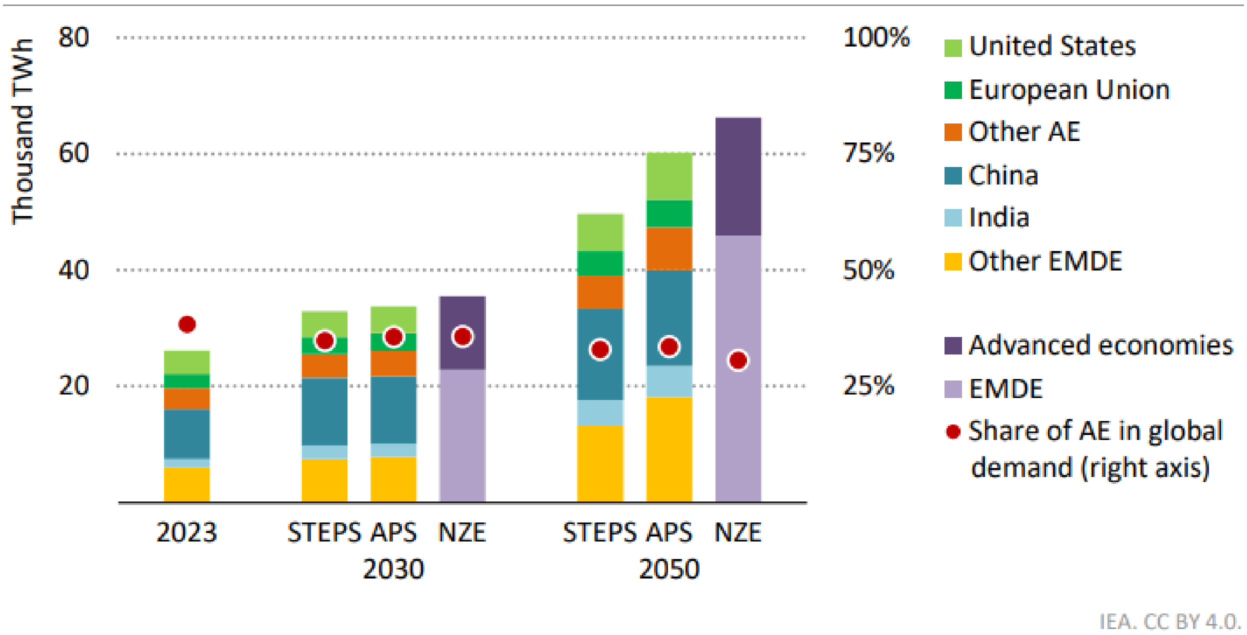

Figure 4: Electricity demand by region and scenario (2023, 2030, 2050) [1]

In addition, India, the Middle East and parts of Southeast Asia, where building sector has the greatest impact on demand growth, are also contributing significantly. Moreover, the advanced economies currently account for nearly 40% of global electricity demand, but in all scenarios their share will reduce in the next years.

It is also interesting to note how the electricity demand in the most energy-intensive sectors of advanced and developing countries is assessed. Figure 5 shows the electricity demand growth forecasts by application and scenario [1].

The automotive sector, in particular the electric vehicles, is driving growth in electricity demand in advanced economies. In emerging markets and developing countries needs are different, infrastructures are less developed and for this reason, the building sector will account for most of the additional growth by 2035. The increase in household appliances, rising demand for air conditioning and the electrification of industrial production are the other sectors that need to be considered for this analysis.

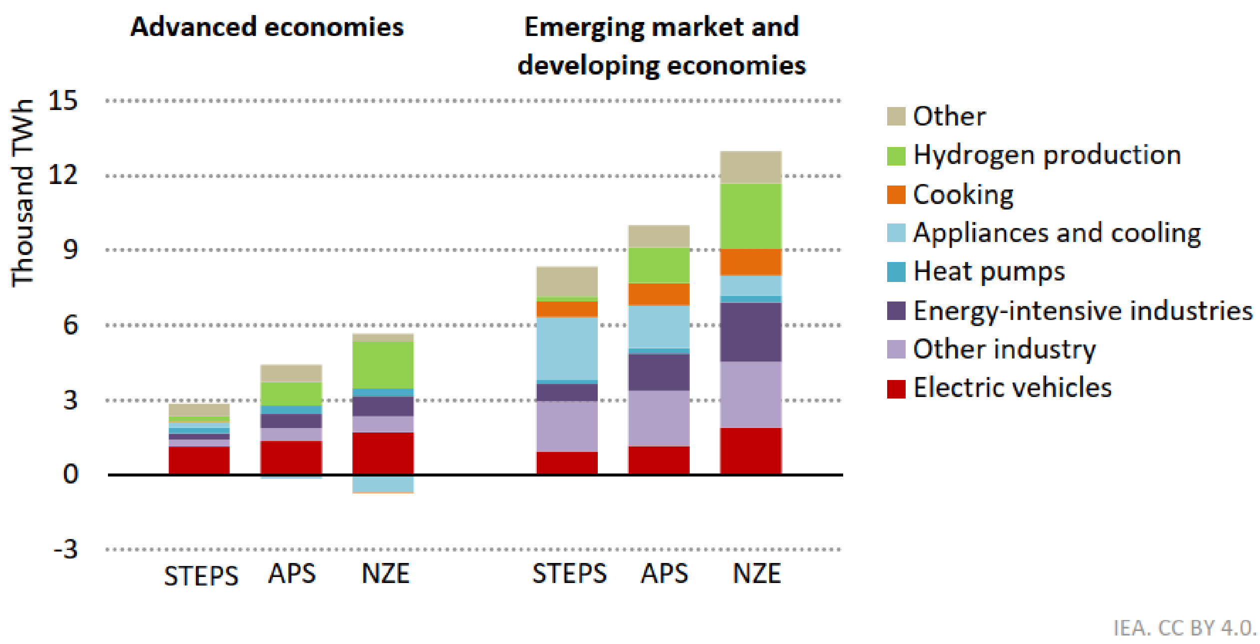

Figure 5: Electricity demand growth by sector and scenario (2023-2035) [1]

1.2.2.2 Electricity supply

In 2023, 60% of global electricity supply was provided by fossil fuels. Coal accounts for the largest share of the total with 36%, and also natural gas plays a major part at 22%. These numbers can be further reduced, they are representing the lowest share of the total electricity supply in the last 50 years. Although the production of nuclear and hydroelectric power is slightly declining, renewables has reached 30% of global generation, with wind and solar PV together providing the 13%. [1]

In Figure 6, a more detailed overview of the electricity generation by source and scenario is presented.

As shown, after decades of generating most of the world's electricity from fossil fuels, renewables will become fundamental for electricity generation worldwide.

At COP28, governments declared their intention to increase renewables capacity threefold. Many major economies are aiming to increase renewable energy by 50% or more by 2030, with a focus on capacity or electricity generation share [1].

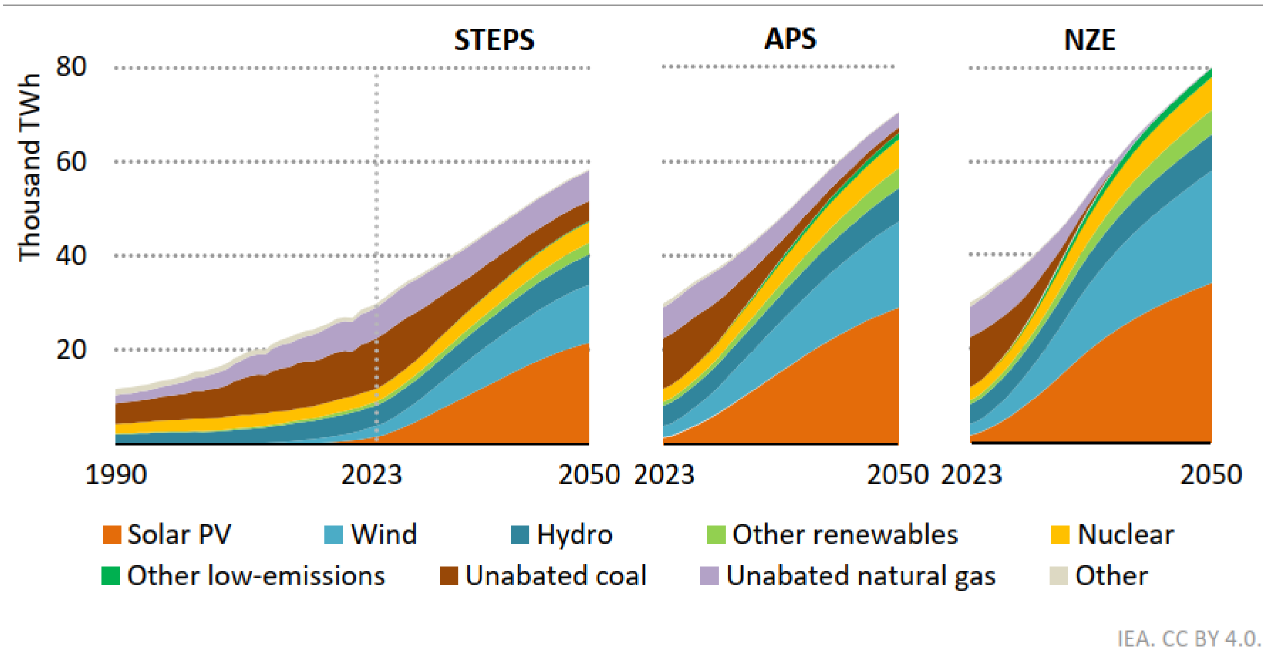

Figure 6: Global electricity generation by source and scenario (1990-2050) [1]

It is quite clear that policy sector is significant driver to increase renewable energy sources and to phase out the use of unabated coal power generation. Furthermore, another important point is related to energy storage, the G7 agreeing to contribute to a global target of 1500 GW of installed capacity by 2023. This initiative aims to improve the energy security and helping to integrate rising shares of renewables.

1.2.3 Carbon dioxide emissions

Carbon dioxide (CO_2) emissions are the primary cause of global climate change due to human activities like burning fossil fuels and industrial processes. Moreover, the deforestation cannot be considered as a direct source of emissions, but it contributes to reduce the amount of CO_2 that can be captured and stored inside the trees.
The global emissions began from the mid-18th century with the industrial revolution, growing rapidly year by year. Over the last century, the emissions of greenhouse gases

increased significantly, passing from 6 billion tons in 1950 to 20 billion tons just 40 years later [2].
The evolution of CO_2 emissions throughout the last two centuries is reported in Figure 7.

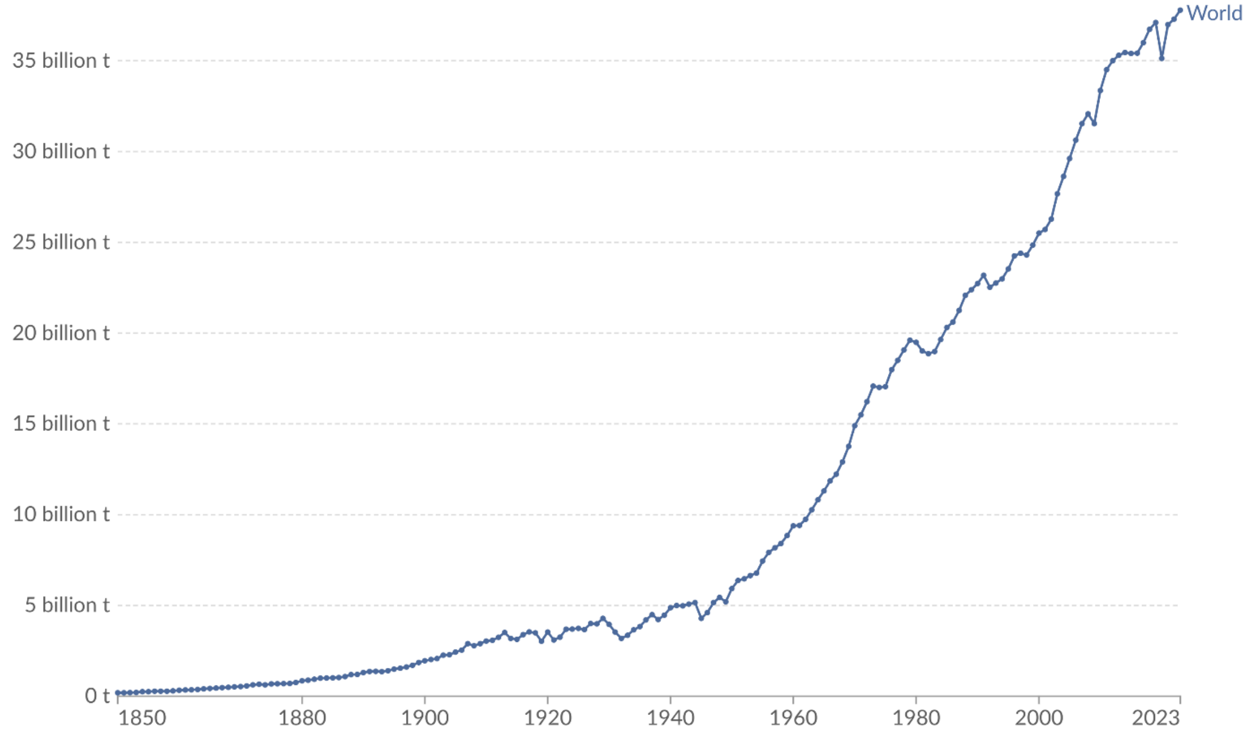

Figure 7: Annual carbon dioxide emissions [2]

Nowadays, we globally emit over 35 billion tons per year, but the trend has slowed over the last years. Unfortunately, apart 2020, where all the industrial and anthropic activities have been stopped by the Covid-19 pandemic, the trend of emissions is set to keep on growing because, according to forecasts, the emission peak still has to be reached in the future years.
The emissions are not equally distributed all around the world, emitters have changed over time. In 20th century, the global emissions were dominated by Europe and United States and this trend lasts until the half of the century. Nevertheless, as reported in Figure 8, in the recent decades the situation has changed significantly. In fact, many Asian countries, especially China, have sharply increased their emissions, due to the production of goods widely distributed and consumed in the US and EU [2].

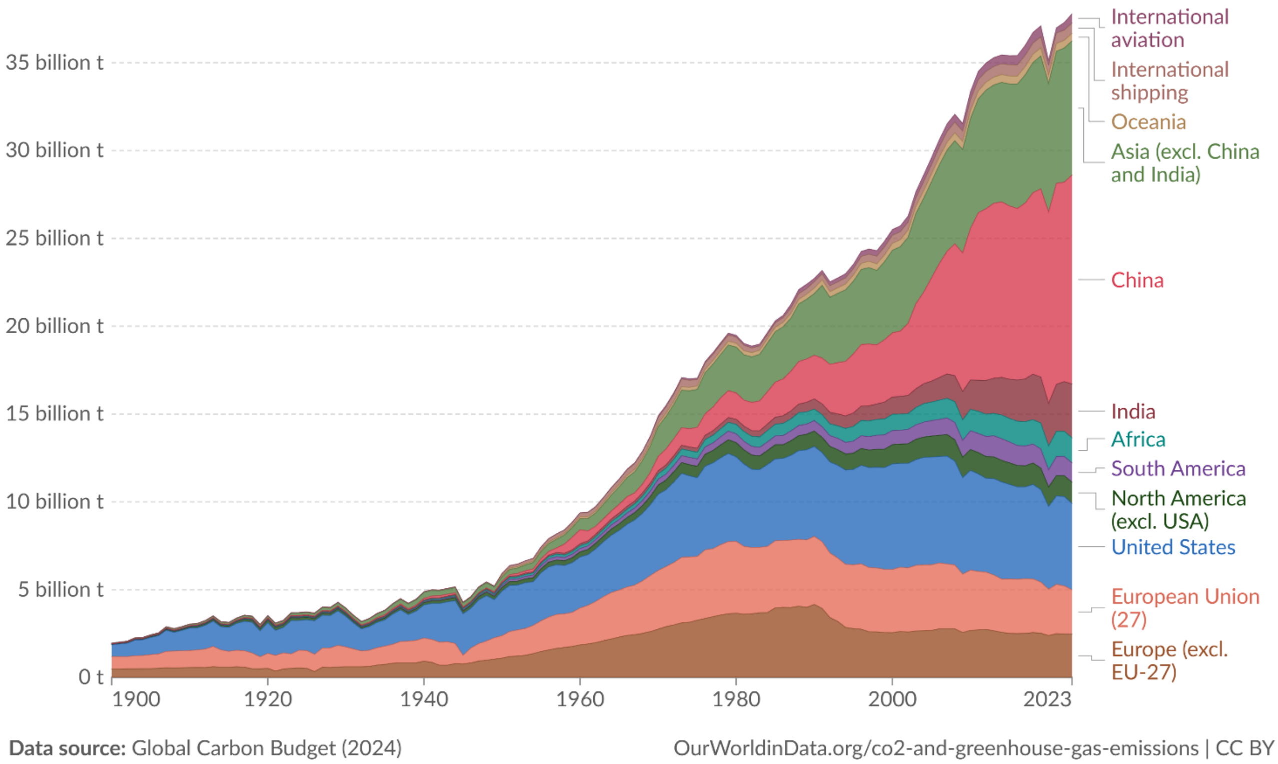

Figure 8: Annual CO_2 emissions by world region [2]

The comparison of CO_2 emissions between advanced and developing countries provide a clearer view about how different economies are dealing with the target of net zero emission, as displayed in Figure 9.

China and advanced economies (Europe, Japan, United States), whatever will be the future scenario, will reduce drastically their emissions by 2050. An increasing number of emerging and developing countries have announced goals to achieve net zero emissions, but high efforts and expensive investments are required in order to support the energy transition [1].

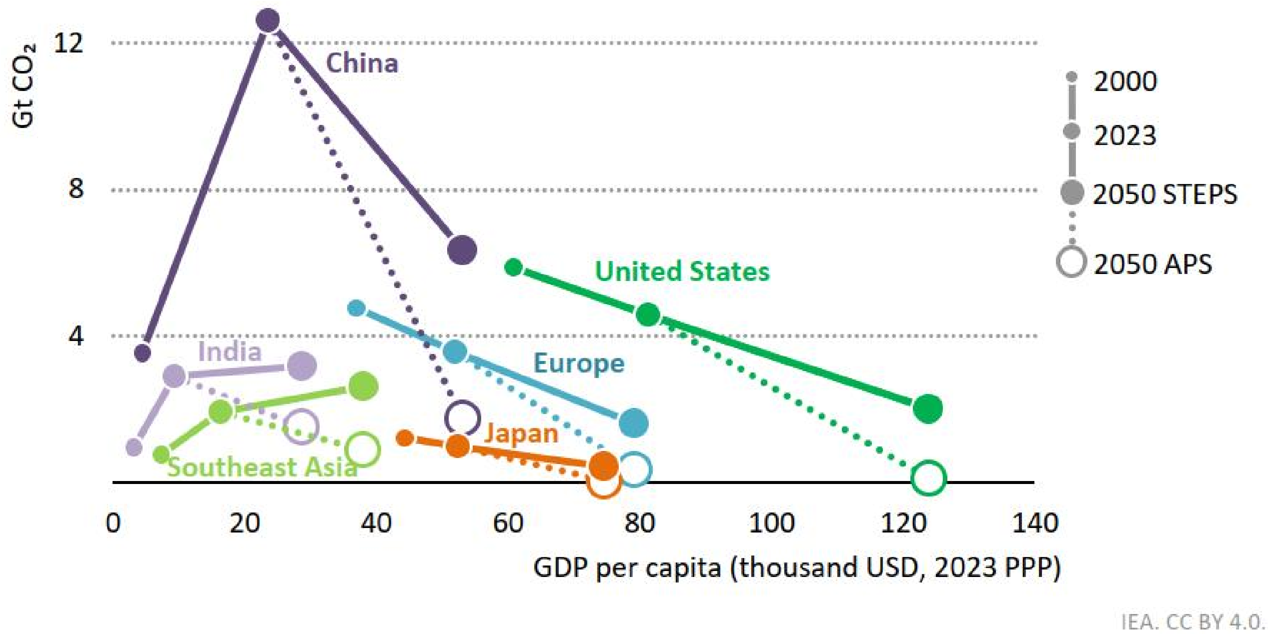

Figure 9: CO_2 emissions and GDP per capita in selected countries in STEPS and APS [1]

1.3 Renewable energy communities

The energy transition towards net zero emissions cannot be realized without the strong joint and management of technological, environmental, economic and social problems. New forms of collective action and collaborative economies, including several benefits due to cutting-edge digital technology, may lead to a new model able to accelerate the energy transition.

A Renewable Energy Community (REC) is a legal entity that enables local communities to share common energetic targets, aiming to provide environmental, economic and social advantages. According to the European Commission, energy communities allow local communities to join forces and invest in clean energy, acting as a single entity to access suitable energy markets on a level playing field with other market actors.
The concept of energy community is not new, the idea was already put in practice for isolated regions, such as islands and highlands [3]. Europe, Germany played a pivotal role with the creation of a bio-energy village in Jühnde in 2006 [4]. This country adopted

the Feed-In-Tariff, a policy mechanism designed to intensify investments in renewable energy systems by applying long-term contracts to producers [5].
In Italy, in particular in the northern regions like Aosta Valley, Lombardy and Friuli-Venezia-Giulia, the concept of energy community was well known since the last decades of 19th century. The initiatives were based on citizen participation to promote the energy sustainability and the development of the local community. Before the usage of PV technology, the first communities relied on hydroelectric systems, reinvesting the profits in local projects.

From a policy perspective, energy communities and similar initiatives have recently become more relevant for the European energy policy. In particular, RED-II (2018/2001/EU) [6] presents the definitions of collective self-consumption and of the REC, while IEMD (2019/944/EU) [7] defines the citizens' energy community. In these documents are included the specific terminology related to regulatory framework, summarized in Table 1.

Terms	**Definition**	**Main goal**
Renewable Energy Cooperatives (REC)	A collective of individuals who voluntarily participate in a democratically managed, non-profit organization.	To address shared economic and social needs within the energy sector, including production, distribution, and consumption.
Renewable Energy Communities (REC)	Legal entities, with voluntary and open participation managed by members or shareholders.	To provide environmental, economic, or social benefits for the community, rather than generating financial gains.
Citizen Energy Communities (CEC)	Like REC, with extended operational activity, to provide energy efficiency services or electric vehicle charging services for the members or shareholders.	To promote sustainable energy use and community-based solutions, following similar objectives as Renewable Energy Communities.

Table 1: Definition of community led-energy initiatives [5]

Regarding the Italian legislation, Italy has implemented both aforementioned European directives, 2018/2001/EU (RED-II) and 2019/944/EU (IEMD), starting from the Milleprorogre

legislative decree of 2020 (DL 162/19) [8]. In particular, the Art. 42-bis [9] had introduced regulations with the aim of regulating the first experimental phase. The RECs were thought to include plants powered by renewable energy sources with a power capacity of less than 200 kW each. Furthermore, the perimeter of plant aggregation was limited to those under the same secondary transformer substation.
A more significant evolution in Italian regulatory framework occurred with the introduction of legislative decree 199/2021 [10] and implementing decree 414/2023 [11]. These two aimed to transport the RED-II into the Italian law, improving the previous regulatory landscape for REC. The power capacity was changed from 200 kW up to 1 MW of power installed and more primate and public entities were allowed to take part to the local energy communities.
Recently, the CER decree of 2023 implemented a new system of incentives to enhance the RECs operation. The incentive tariff on shared energy is up to 120 €/MWh for plants under 200 kW and PNRR funds will permit to use up to 40% of non-repayable grants plants in disadvantages areas.

1.3.1 Emerging Distribution System

Due to its characteristics, a REC can be considered as an Emerging Distribution System (EDS). An EDS refers to the framework of electrical distribution networks that combine advanced technologies, decentralised energy resources and innovative management strategies in order to improve reliability, efficiency and sustainability.
Therefore, this kind of system ensures the incorporation of Distributed Energy Resources (DERs) into the network. DERs refers to energy sources such as solar panels, wind turbines, and battery storage systems. Another interesting feature is the bidirectional energy flow, enabling the energy flux to flow both from and to consumers. Hence, there are no longer only producers and consumers, but also “prosumers” who both produce and consume energy.
About the market structure, it is intrinsically based on competition because of the presence of self-interest players which aim to maximise their profits. This goal can be achieved through the shift from centralised decision making to distributed decision making. All the players interact with a physically constrained network thanks to several ICT technologies [12]. A schematic representation of a self-sustainable prosumer community is presented in Figure 10.

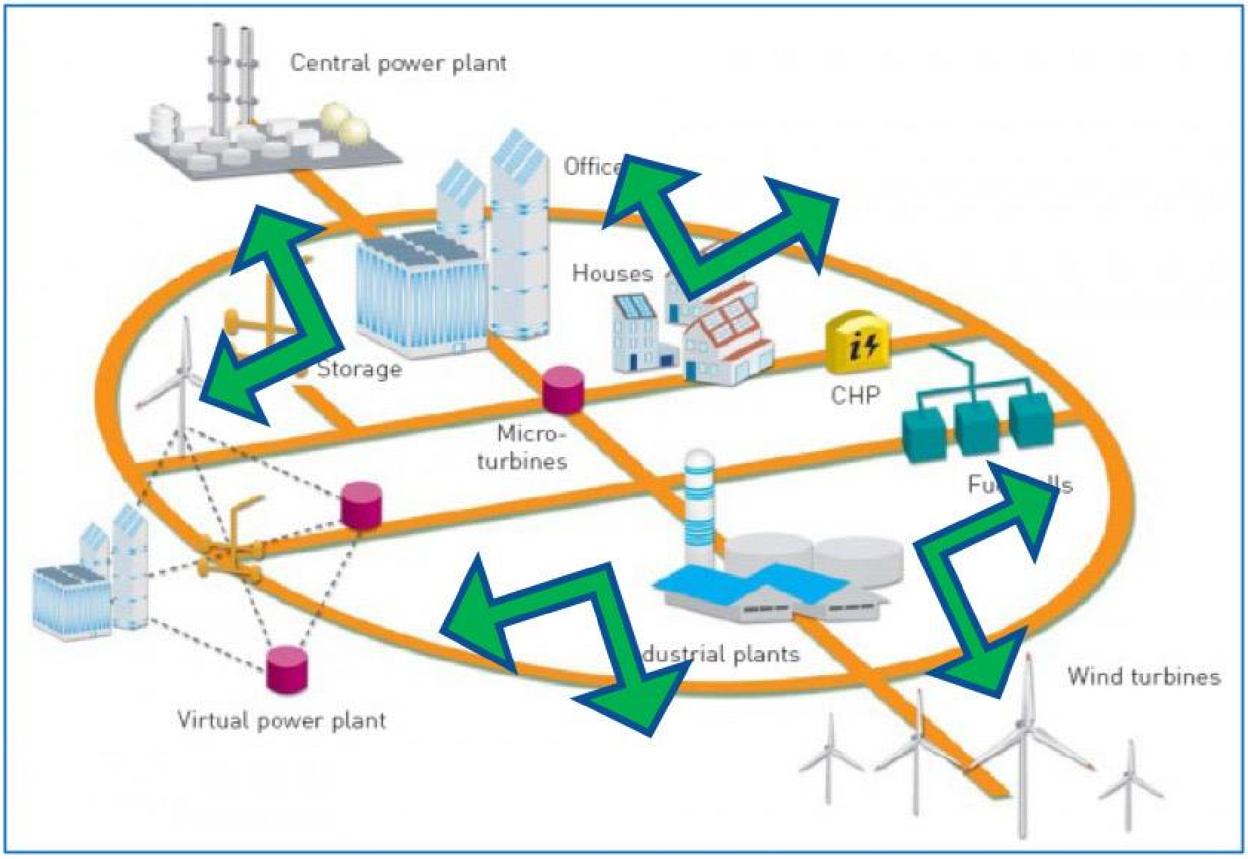

Figure 10: Scheme of a self-sustainable prosumer community [12]

1.3.1.1 General framework for modeling EDS

As previously anticipated, the EDS operation and performances are influenced by social, psychological, technical, economic and environmental aspects. Hence, the model can be schematized by three main layers (Figure 11):

- Social: it provides a virtual place where people exchange information and strategies for the individual profit and comfort.
- Cyber (ICT): it is the part devoted to gather and send data about operational states, bidirectional transactions, real-time market prices and current regulation. The smart grids rely on ICT control system able to provide commands, control actions and transfer technical data to human or automatic decision makers. An

important example is the smart metering, an important device used for measuring bidirectional communication between consumers and producers.

- Physical: it consists of the power systems in the network, including power grids with active and reactive power injection/withdrawal. To this layer also belong grids, which must operate within predefined operational limits.

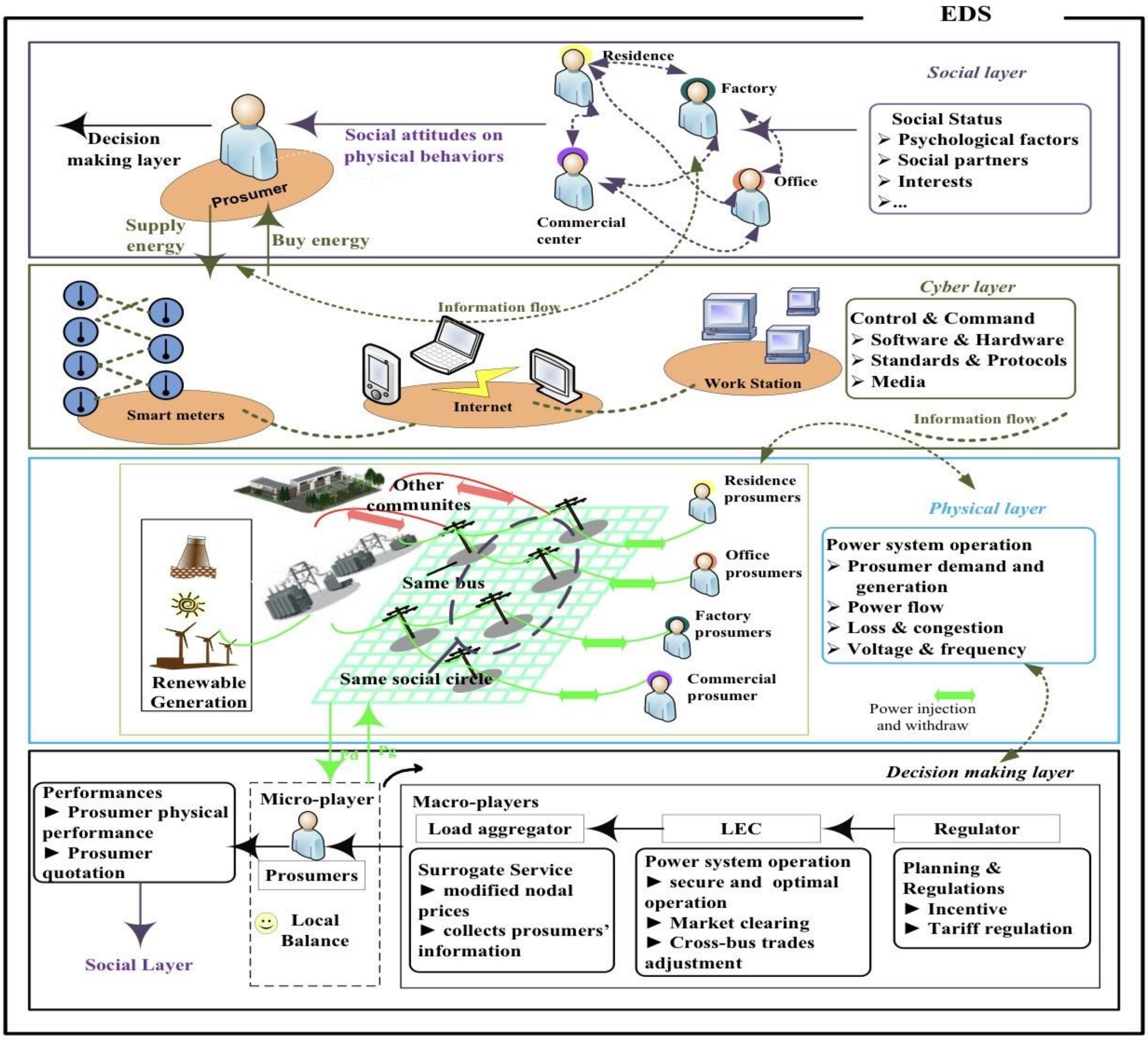

Figure 11: General EDS modelling [12]

In addition, it is possible to include the decision-making layer which implement laws and regulations in order to influence the behaviour of the players, so it permits a sort of overall system control. The decision-making layer deals with the network structure with physical and operational constraints, defining its active and reactive flow.

The layers interact each other and with external inputs to assess the overall performance of the system measured by a set of metrics like energy saving, environmental efficiency or market efficiency.

In conclusion, the emerging distribution grids are changing completely the way of thinking about this topic.

People are not just limited to passively purchase electricity but can participate in scheduling the demand and power generation. This model is beneficial even for the local economy, new market roles and business model for existing players in the market can be adopted [12].

1.4 Hybrid system combining PV and BESS

The hybrid system taken into consideration for our purposes (Figure 12), is composed of photovoltaic panels (PV) and a battery energy storage system (BESS).

The inverter is a fundamental component of the system under analysis, it is devoted to manage the energy fluxes between PV system, BESS, residential load and electrical grid. This advanced solution is designed to maximize the energy production from renewable sources and improve grid stability.

This technological solution, adopted for this case study, addresses the problem related to the intermittency of solar energy. The system can store locally the excess produced energy in periods characterized by high solar irradiance, while it can supply completely or partially the local demand when the PV generation is insufficient. In this way, the local energy production can cover a higher percentage of building's demand.

This kind of technology solution is not the only possibility to optimize the energy distribution. In fact, it is also possible to adopt large-scale storage systems at grid level able to further enhance the grid stability. These storage facilities aim to collect surplus energy from multiple decentralized sources and release it in case of higher demand, in order to contribute to a more resilient and efficient energy network.

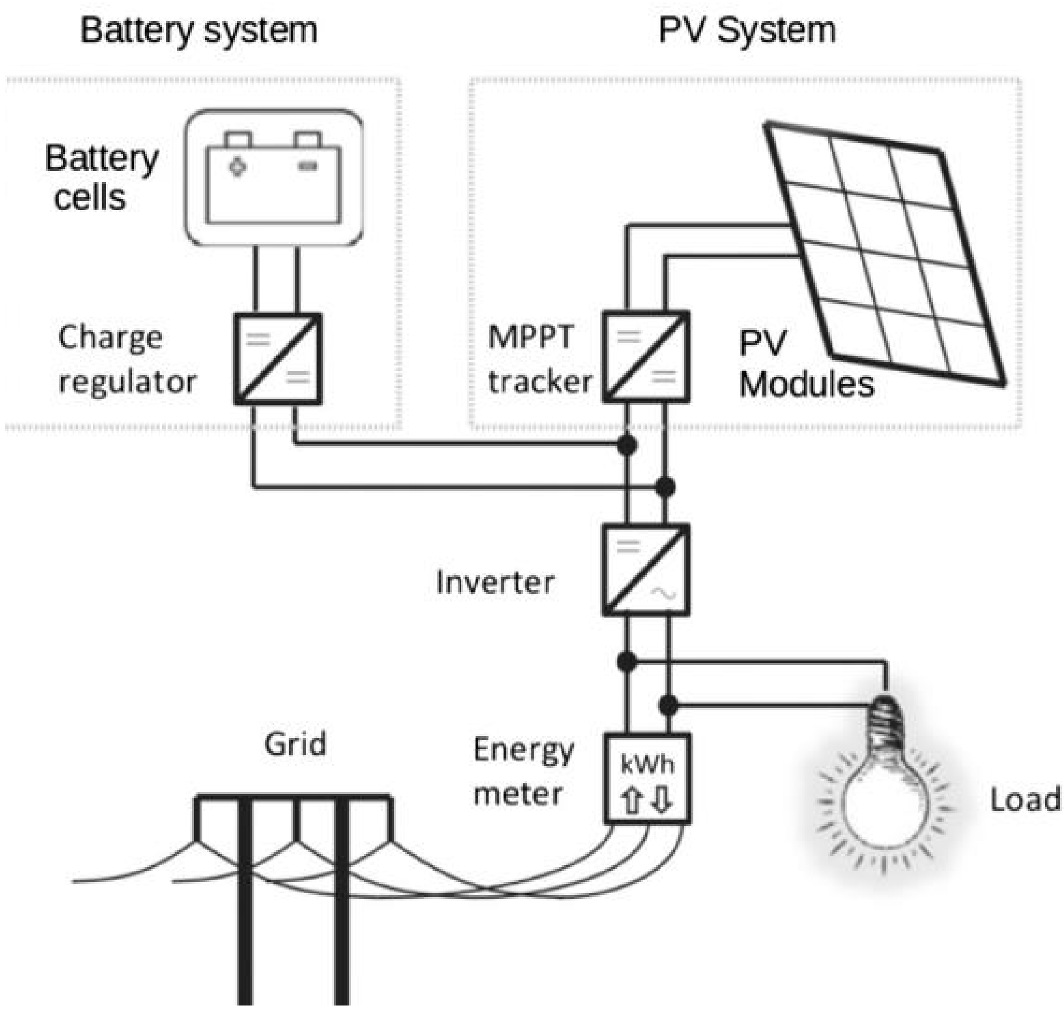

Figure 12: Hybrid system (PV + BESS) [13]

The two most relevant parameters about this aspect are the self-consumption (SC) and the self-sufficiency (SS), making a comparison between local demand and generation under different perspectives [14].

The self-consumption is defined as the percentage of the local generation used to cover the demand:

$$SC = \frac{E_{SC}}{E_{PV}}$$

E_{SC} represents the self-consumed energy while E_{PV} is the total energy produced from the PV system, exiting from the inverter.

The self-sufficiency is calculated as the percentage of the demand covered by local generation:

$$SS = \frac{E_{SC}}{E_{load}}$$

E_{load} is the total energy consumed by AC load. To better understand the meaning of the two ratios, in Figure 13, is reported a graphical representation of a household power dispatch for a typical week of July.

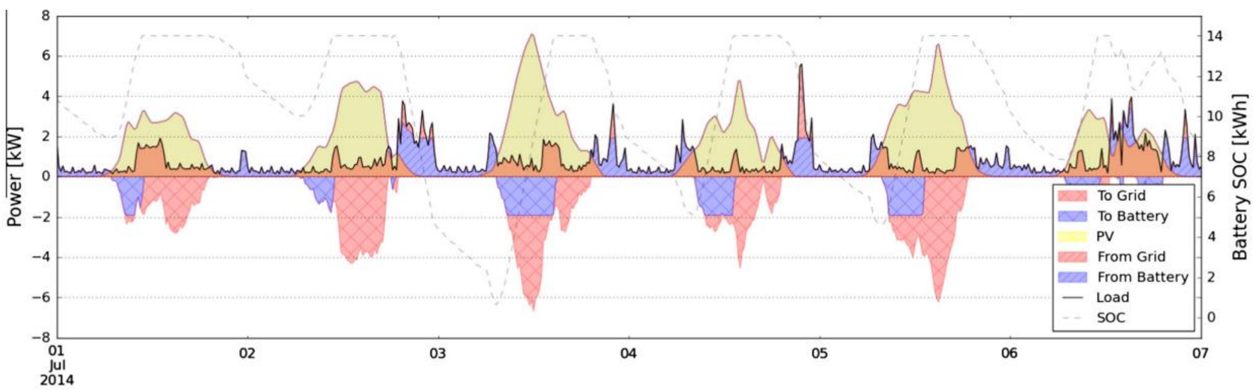

Figure 13: Power dispatch for a typical week of July [13]

The storage system can adopt different strategies according to the operational conditions, such as self-consumption, peak shaving and islanding. The first strategy is the most interesting one for the purposes of the analysis, it aims to reduce the energy taken from the grid, optimizing the cost of energy and enhance the grid management. When the PV power is higher than load, the battery is charged until it is completely full. If the battery is fully charged, the surplus production is sold and sent to the electric grid. Otherwise, as soon as the PV power is not able to satisfy the load, the battery is discharged until empty.

Therefore, the SS is a key parameter that must be maximized, it represents how much of the total demand is covered by local production. The SS depends on PV system power production and size of batteries, so the design of these two elements is crucial in order to obtain the desired result.

2 The role of microgrids in RECs

The microgrids are a fundamental part of a REC, they can be defined as a group of interconnected loads and distributed energy resources that acts as a single controllable entity with respect to the grid. It can connect and disconnect from the grid to operate in grid-connected or island mode. Hence, it is important to analyse the electrical distribution systems and in particular, the different types of microgrids and their main functions.

2.1 General overview of electrical distribution systems

The electrical systems are classified according to their nominal voltage. Generally, the transmission systems are at high voltage (HV) level, while the distribution systems are at medium voltage (MV) and low voltage (LV) levels. In Table 2, is reported the categories and the ranges for AC and DC systems [15].

Categories	**Rated voltage for AC systems**	**Rated voltage for DC systems**
Category 0	$V \leq 50$ V	$V \leq 120$ V
Category I	50 V $< V \leq$ 1000 V	120 V $< V \leq$ 1500 V
Category II	1 kV $< V \leq$ 30 kV	1.5 kV $< V \leq$ 30 kV
Category III	$V >$ 30 kV	$V >$ 30 kV

Table 2: Rated voltages for AC and DC systems [15]

The first three categories are associated with the distribution systems while the category III is related to transmission systems, it is typically denoted as high voltage. The categories 0 and I are denoted as low voltage, whereas the category II as medium voltage.

2.1.1 MV distribution systems

The MV distribution systems are the fundamental link between high voltage transmission network and low voltage consumer systems, ensuring reliable power delivery across wide areas. A typical example of MV distribution system is represented in Figure 14.

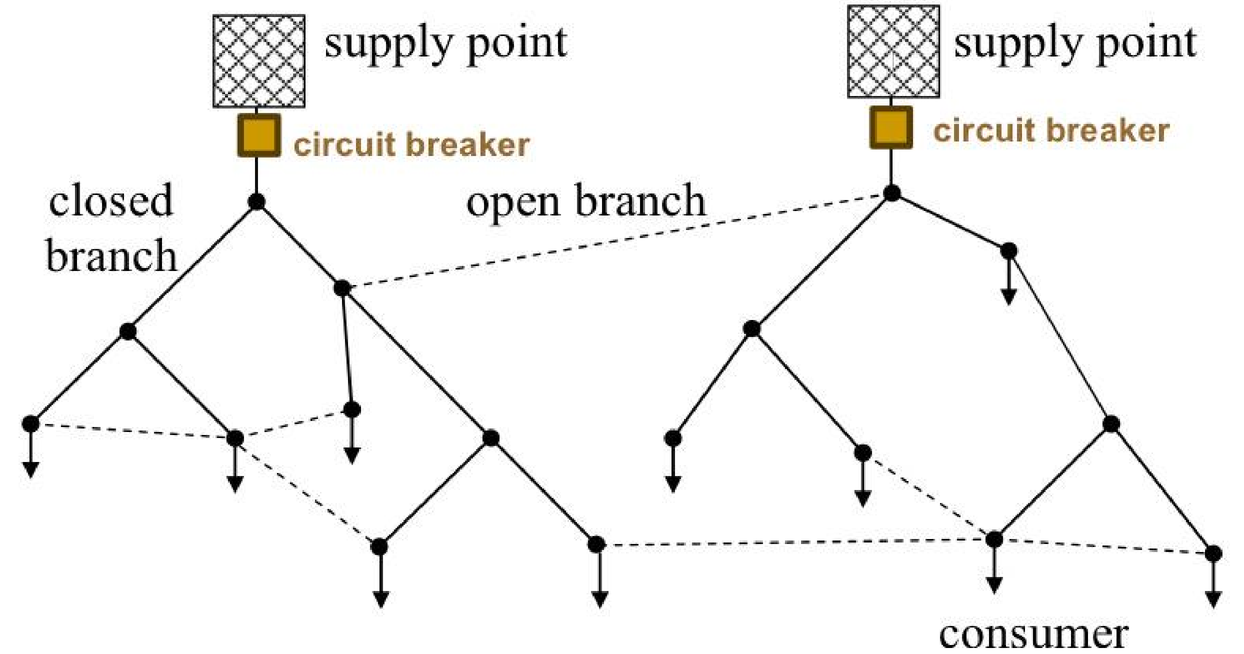

Figure 14: Structure of MV distribution system [15]

The structure is weakly meshed, it is operated with radial configurations in order to simplify the protection schemes. This particular configuration of the structure is obtained by opening the redundant branches.
As it can be seen, the circuit breakers are located only at the starting point of each line connected to the supply point, at the other line terminals there are only switches that are not able to interrupt high currents. This aspect is a major difference with respect to distribution system, which is protected at both ends by circuit breakers [15].

2.1.2 LV distribution systems

The low voltage distribution system (Figure 15) presents a radial structure and there are generally no redundant branches. The circuit breakers are positioned at the beginning of the lines and after the medium voltage supply point is required a step-down transformer able to reduce the voltage level from medium to low.
It is the final stage in the electrical power distribution network, delivering power directly to all the possible different kinds of end-users [15].

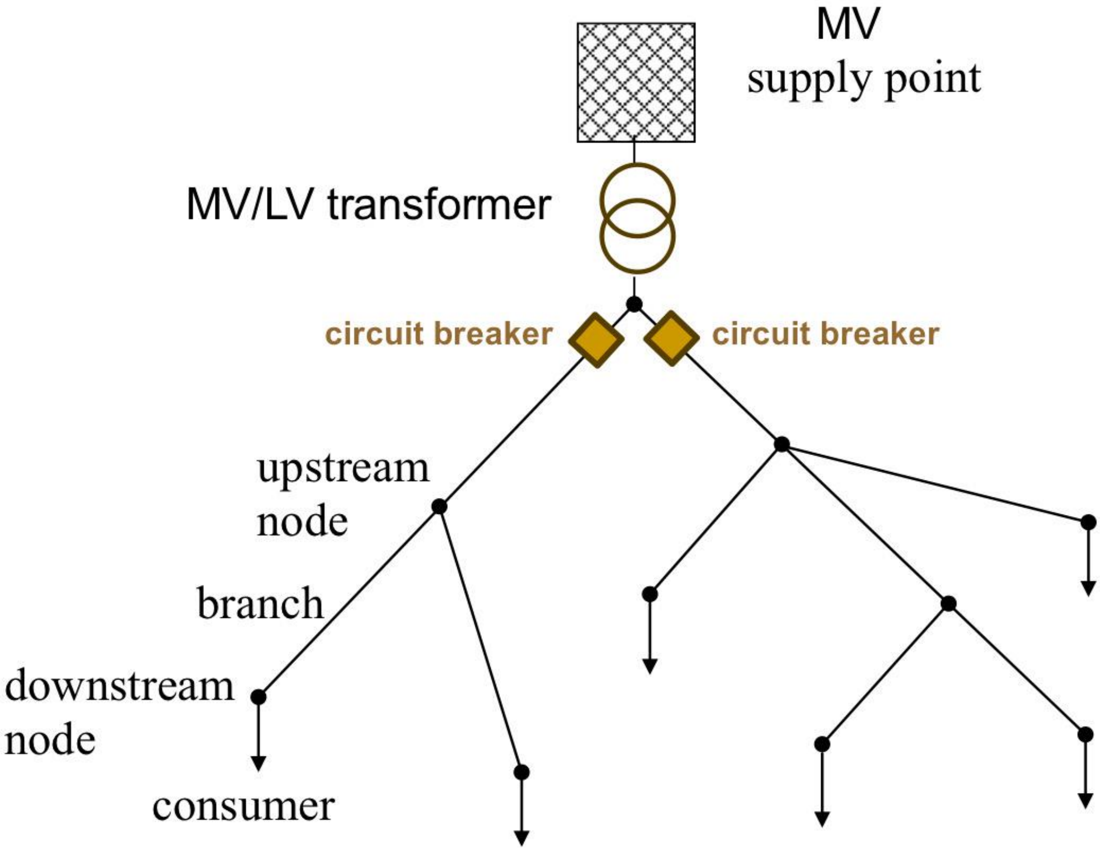

Figure 15: Structure of LV distribution system [15]

2.2 Microgrids

Microgrids are small distribution systems containing generation and load, whose operation can be totally separated from the main distribution system, and they are defined as either autonomous, or connected to it - non-autonomous. The autonomous microgrids working operation is critical because of possible issues in voltage, frequency control and regulation.

Microgrids generally work as independent systems, but they can be eventually connected to the electric network in emergency cases to improve the continuity of supply in case of fault. The connection can also be justified according to economic advantages due to electricity prices for energy or reserve service.

The demand and supply of energy within the microgrid is managed from a control center to optimise the use of distributed energy resources, in particular distributed generation, demand response and distributed storage.
Thanks to these features, the microgrids are characterised by many advantages, such as high availability of service, possible combined management of energy mix, economic efficiency with cost reductions for the consumers. All the benefits of the microgrids are particularly suitable for different types of applications, especially for particular areas far from urbanised territories. The most popular uses are associated to rural communities, island communities and large industries with local and scattered sites. In developing countries like Indonesia, Africa and India, this kind of solution is progressively spreading access to electricity even in regions far from the main electricity network [16].
In our case, the study is focused on urban distribution system, characterised by its robustness, relatively short lines, redundant connections and voltage control prevailing from HV/MV substation. Furthermore, low variations of voltage profiles are detected and voltage control from distributed generation is generally not so efficient.

2.2.1 AC, DC and hybrid microgrids

Even if the first ever power system was thought to be DC, nowadays the industry is more familiar with AC power systems. The definitive adoption of this kind of systems is due to the usage of transformer, that permits to transform the power from one voltage level to another one increasing the voltage (step-up) or reducing it (step-down).
The change of voltage level is important for power transmission in order to reduce as much as possible the conversion losses. Due to AC generation and transmission, the distribution and utilization systems were reasonably developed in alternate current, including commercial and residential applications.
Nevertheless, the increasing attention for green-energy production systems are put in evidence the DC power systems once again. Furthermore, new highly efficient DC loads are favoring the penetration of DC power systems. The storage technologies, especially electric vehicles (EVs), represent a clear example of the importance of DC power systems in building applications.
Anyway, the AC power systems are already spread all over the world, therefore it is almost impossible to change completely the electricity network according to the new purpose. The difference between AC and DC systems is due to the power used to serve

the load and to the load itself. For hybrid systems, there are no concern regarding the types of loads because they are able to drive AC loads through AC power and DC load through DC power [17] [18]. An example of a hybrid AC/DC microgrid structure for residential application is reported in Figure 16.

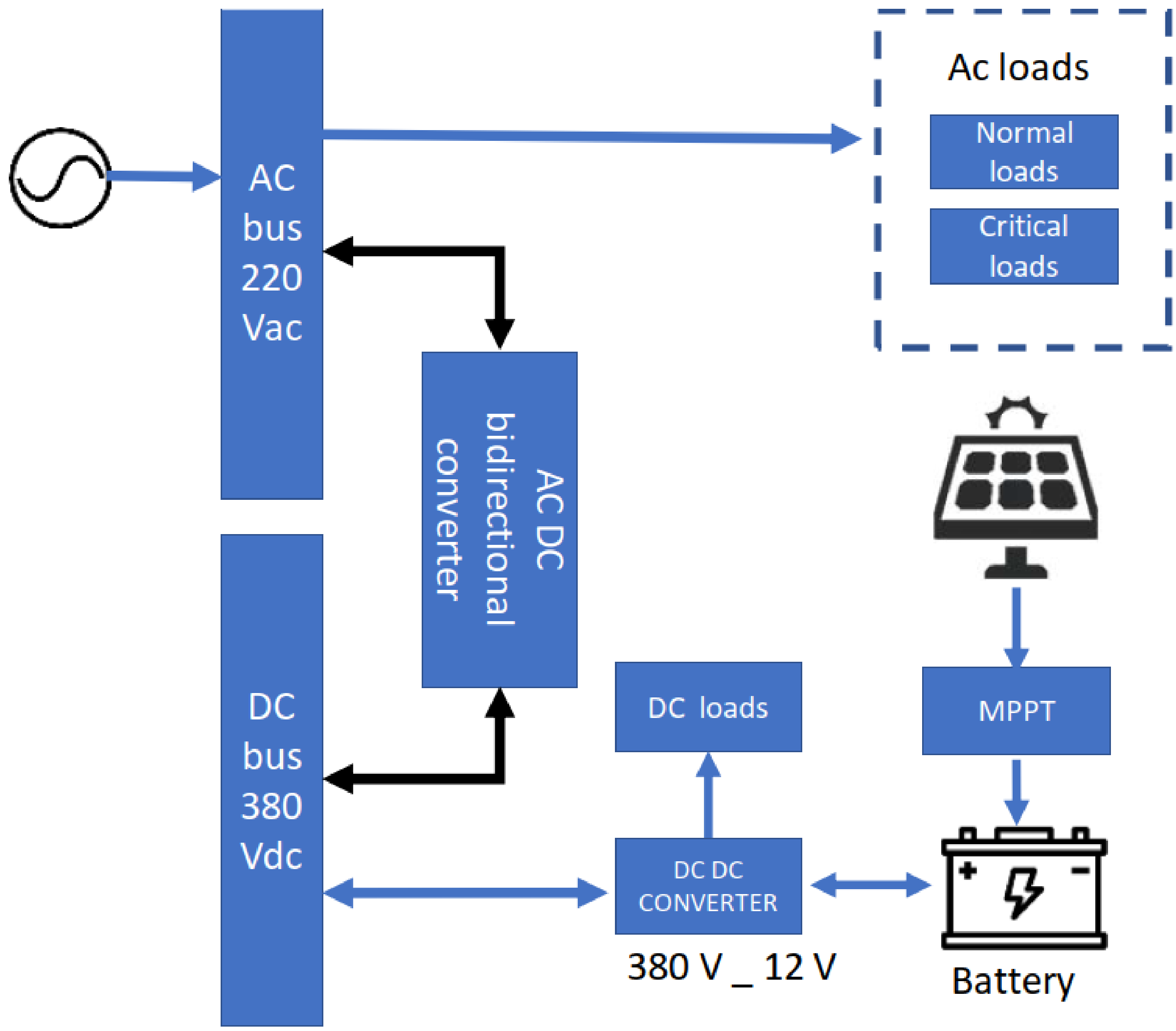

Figure 16: Diagram of a hybrid AC/DC microgrid [18]

In this case, the integration of solar PV is performed via DC bus and a DC/DC converter increase the voltage level from 12V to 380V in order to serve the DC load or to inject the power into the DC bus.

The system aims to minimise the distribution as well as AC/DC conversion losses, therefore DC and AC power must drive the respective kind of loads.
To ensure the optimization of PV power production, a bidirectional AC/DC converter is employed. When an excess of PV generation occurs, it converts the surplus of DC power and inject it into the AC bus.
Therefore, the hybrid system offers many advantages with respect to the other two micrograds as previously mentioned. One of the most interesting benefits of this kind of system is the high efficiency gained from the complete optimization of the process. As reported by Ameer Hamza, et alt., considering a simulation based on a PV installation capacity of 1 kW_p, a comparison between efficiencies of AC, DC and hybrid systems has been performed and showed in Figure 17.

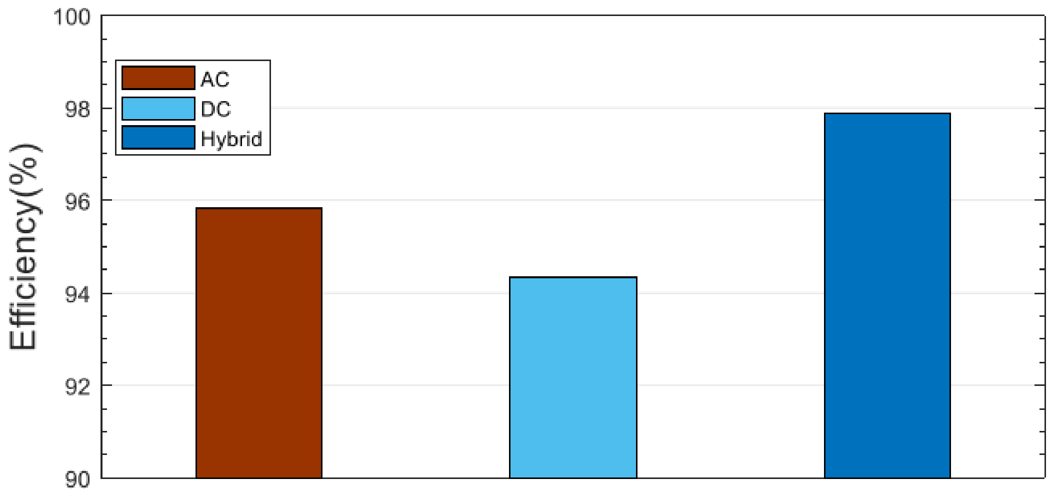

Figure 17: Efficiencies comparison of AC, DC and hybrid systems with 1 kWp PV integration [18]

As can be easily noticed, the hybrid system can obtain the highest efficiency value, reaching about 98% of efficiency. The other two systems are characterised by lower performances but the AC microgrids result to be better with respect to DC power transmission systems, as could be expected.
In Figure 18, is displayed the same graphical analysis, but plotted hour by hour.

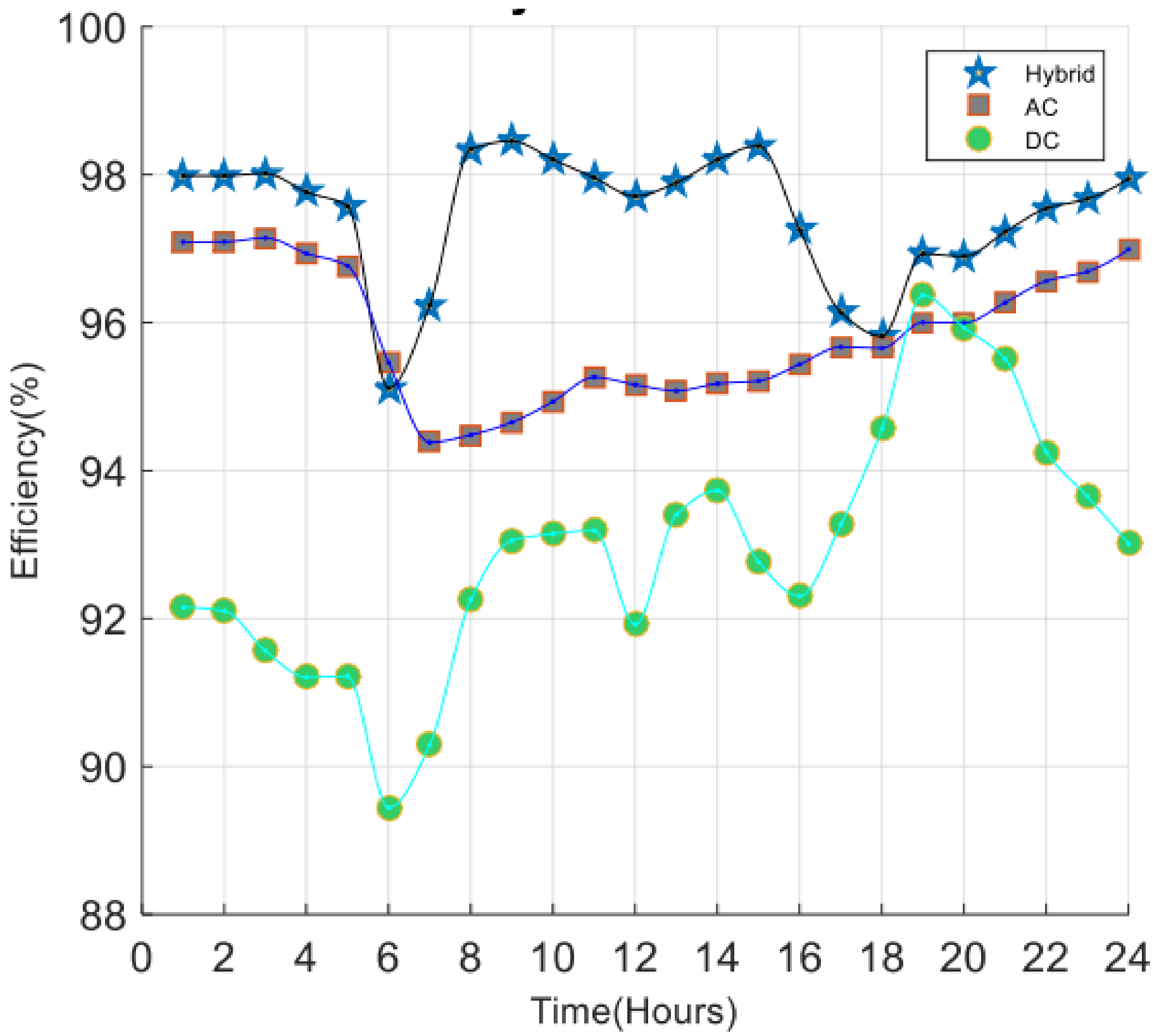

Figure 18: Efficiencies comparison of AC, DC and hybrid systems with 1 kWp PV integration (hourly variations) [18]

3 Design of the hybrid system

This chapter will examine the design of the hybrid system in depth. In particular, the analysis will cover all the most relevant steps in order to perform a detailed and reliable simulation through a dedicated PV design software, namely PVsyst, and weather databases, namely Solargis.
After a brief introduction of the tool utilized, the simulation will be carried out using the PVsyst software and the main results will be shown.

3.1 Site location

The site location of the multi-dwelling building under study will be located in Italy, in the city of Genoa (Figure 19).

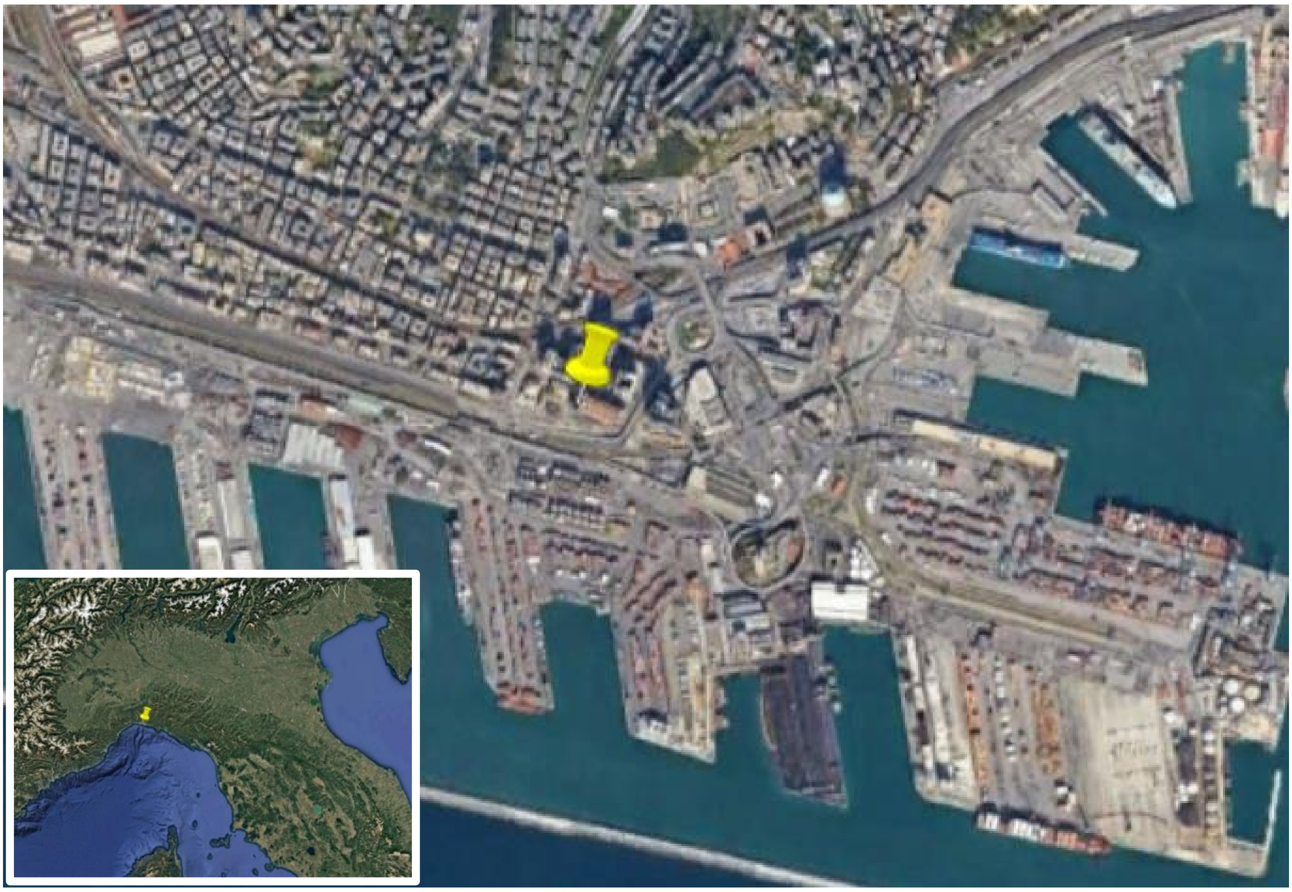

Figure 19; Site location from Google Earth

The geographical coordinates are the following:

- Latitude: 44°24'27.05"N
- Longitude: 8°53'59.07"E

The location of the building is very important to assess the weather parameters which influence the performance and electric energy production of the hybrid system. Those values are taken from a well-known commercial weather database named Solargis.

3.2 Solargis Prospect database

Solargis Prospect is a satellite database with a high spatial resolution of approximately 250 m, sub-hourly temporal resolution to better represent typical and extreme weather, and 1 km resolution for temperature. The validity of these values has been demonstrated in more than 220 locations where high-quality measurements were available.
This database is fundamental for the calculation of long-term monthly averages of solar radiation and meteorological parameters, as the global horizontal irradiance or the albedo. All these values are measured according to different methodologies, those will be presented and described in the following paragraph.

3.2.1 Relevant meteorological parameters

Among all the possible meteorological data provided by Solargis, some of them are particularly important for the purpose of the analysis:

- Global Horizontal Irradiance (GHI): Average monthly sum of global horizontal irradiation [kWh/m^2]
- Diffuse Horizontal Irradiance (DHI): Average monthly sum of diffuse horizontal irradiation [kWh/m^2]
- Global incident irradiation on collector plane (GlobInc): Average monthly sum of incident global irradiation in the collector plane [kWh/m^2]
- Temperature (T_amb): Average diurnal (24-hour) air temperature at 2 m above ground, calculated from outputs of ERA-5 model [°C]
- Albedo (ALB): Fraction of solar irradiance reflected by surface; it is calculated as the ratio of upwelling to downwelling (GHI) radiative fluxes at the surface

Furthermore, another relevant parameter is the specific yield [kWh/kW$_p$], which represents the amount of energy produced per kWp of nominal power installed in the power system. In Figure 20, is represented a map of the specific yield production in Italy taken from Solargis.

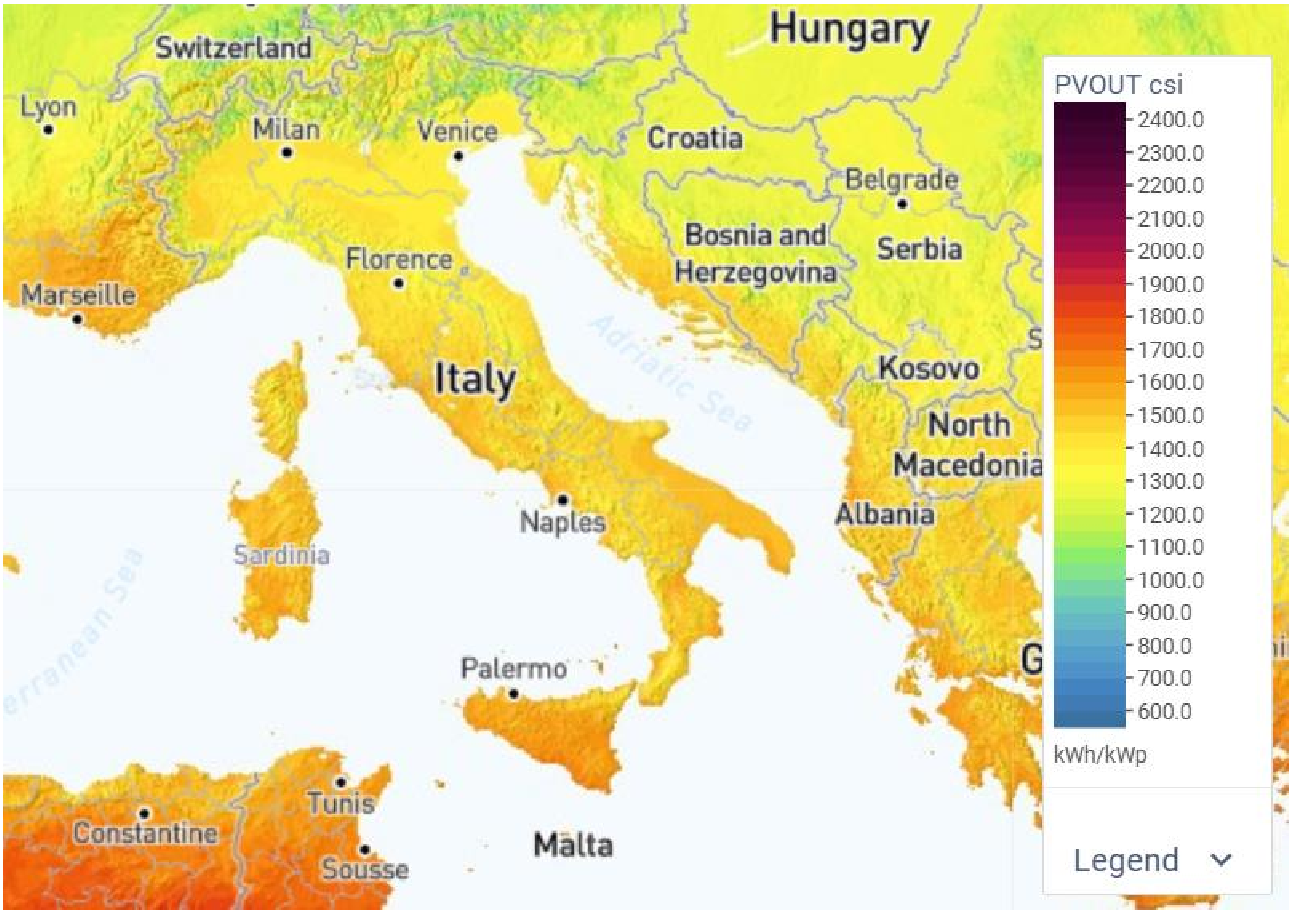

Figure 20: Map showing the specific yield production in Italy [19]

As could be expected, the southern regions are more productive with respect to the northern ones, this is due to the higher amount of solar irradiance reaching the ground. On average, Italy is characterized by specific yield values in the range between 1100 kWh/kW$_p$ and 1800 kWh/kW$_p$.

Anyway, the specific yield will be calculated precisely through the PVsyst simulation.

3.2.2 PVsyst simulation

As previously mentioned, the simulation of the hybrid system associated with the multi-dwelling building will be carried out through the PVsyst software.
PVsyst is a widely used software tool designed for the simulation and analysis of PV systems. It offers exhaustive functions for designing, optimizing and evaluating solar photovoltaic projects, from small rooftop installations to large-scale utility plant.
PVsyst allows users to assess energy yields, system losses, shading effects and financial performance under various environmental constraints.
In this paragraph, all the most important inputs required by the software will be described and listed in order to provide a clear view of the necessary steps to get the report developed by PVsyst. This final report will be analysed in the final paragraph, it gives the most relevant output results and a loss diagram to understand the main sources of system losses. Moreover, will be carried out a sensitivity analysis in order to modify some design parameters and observe how the results are influenced by the changes.

3.2.3 Multi-dwelling building description

The building is oriented towards the south (azimuth 0°) and is assumed to be one of the most common housing types in Italy, namely a multi-dwelling structure. For this case, the total number of flats is 8 and they have a surface ranging from 80 m^2 to 100 m^2.
The width, the length and the height are deemed as common for the majority of the existing multi-family buildings, these can be retrofitted to improve their energy efficiency. The dimensions are listed as follows:

- Width: 17.50 m
- Length: 15.50 m
- Height: 12.00 m

The roof tilt angle has been adopted as 20°, this is a reasonable value for the roofs slope in the geographic area in which the building is located. The structure is faced towards the south direction, so the panels rows are orientated in east and west direction. In figure 21, is shown its representation obtained in the construction phase of the shading scene.

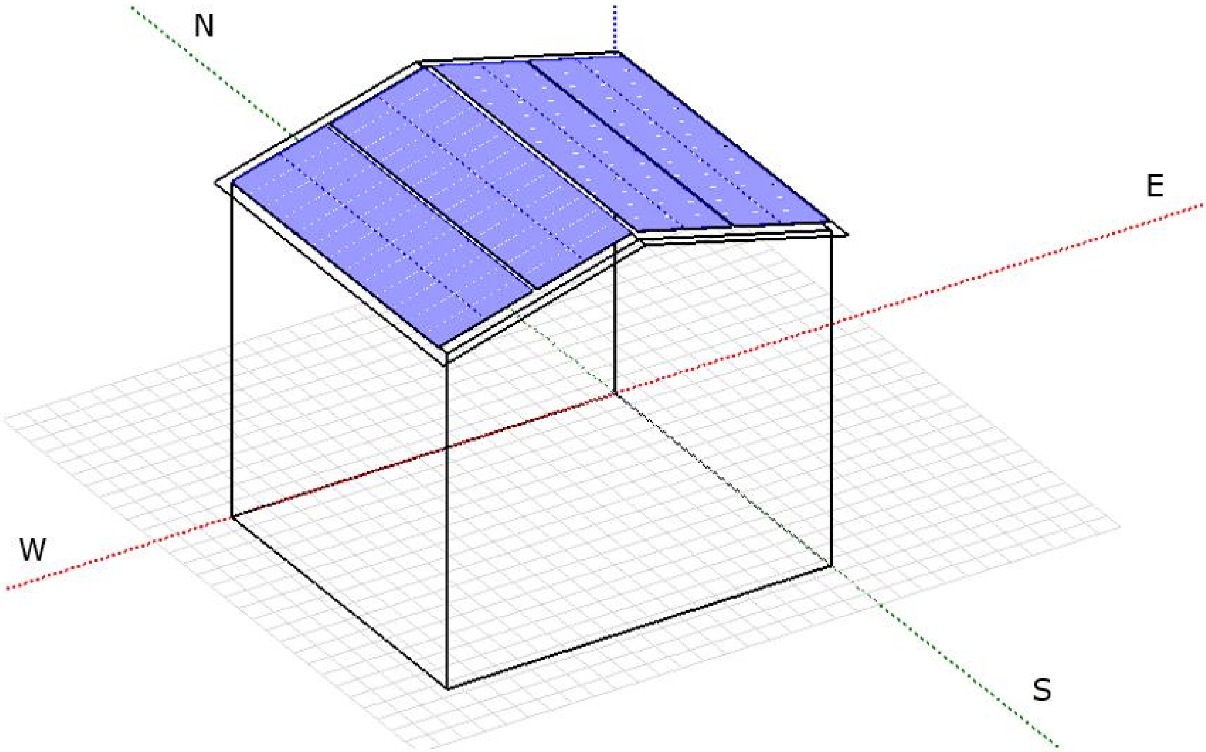

Figure 21: Multi-dwelling building representation

The apartments are supposed to have 3 or 4 people each, hence the total number of inhabitants are supposed to be in the range between 24 and 32. This information is useful for determining the energy output needs and to size the hybrid system in order to cover as much as possible the users' energy demand.

3.2.4 User energy needs

The definition of the daily consumption is crucial for the sizing of PV ad BESS systems, hence it is necessary to estimate the amount of energy required on a daily basis. Therefore, the load profile has been obtained considering all the electric household consumptions, it is supposed that every flat has the same number and types of electric devices. The domestic appliances include microwave, electric oven, washing machine, dishwasher, vacuum cleaner, hair dryer and iron. Those devices account for the largest

part of the energy demand because are particularly energy-intensive but are used just for a limited amount of time.
The following tables (from 3 to 6) report the daily consumption for each season of the year, starting in summer up to spring. The daily household profiles are developed on a seasonal basis in order to keep the analysis as reliable as possible.
The power requested from each item has been calculated by using a time-weighted average, and the reported power do not refer to the best market option in terms of efficiency, in order to keep the analysis conservative.

The hourly profile was selected from the PVsyst template taken from the BDEW website [20], the German grid operator association. It represents the typical profile for a private household which can be considered reliable also for this case study. As illustrated in the following figures, the weekdays show the same trend while the weekends are characterised by higher consumption. Furthermore, the load profile is normalized to a consumption of 1 MWh per year, therefore it will be rescaled with respect to the total users' energy needs.
The hourly profiles vary according to the season, due to the hours of daylight during the day and the outdoor temperature. The figures from 22 to 25 shows in detail the differences in energy load demand throughout the seasons for 3 days selected for each season.

Number	**Appliance**	**Power**	**Daily use**
40	Lamps (LED)	10 W	3 h/day
16	TV and PC	150 W	2.5 h/day
56	Domestic appliances	1575 W	2.5 h/day
8	Fridge	62.5 W	24 h/day
8	Fan coil (cooling)	2000 W	5 h/day

Table 3: Daily consumptions estimation for summer season

In the summer season, for the week 3rd to 9th of July, the energy demand of the entire building accounts for about 272 kWh/day. This value is one of the lowest one throughout the year because the energy consumption is quite reduced due to the higher availability of soral irradiation and lower need of electricity. Moreover, the hybrid system is able to use and store more energy for covering the energy needs as much as possible.

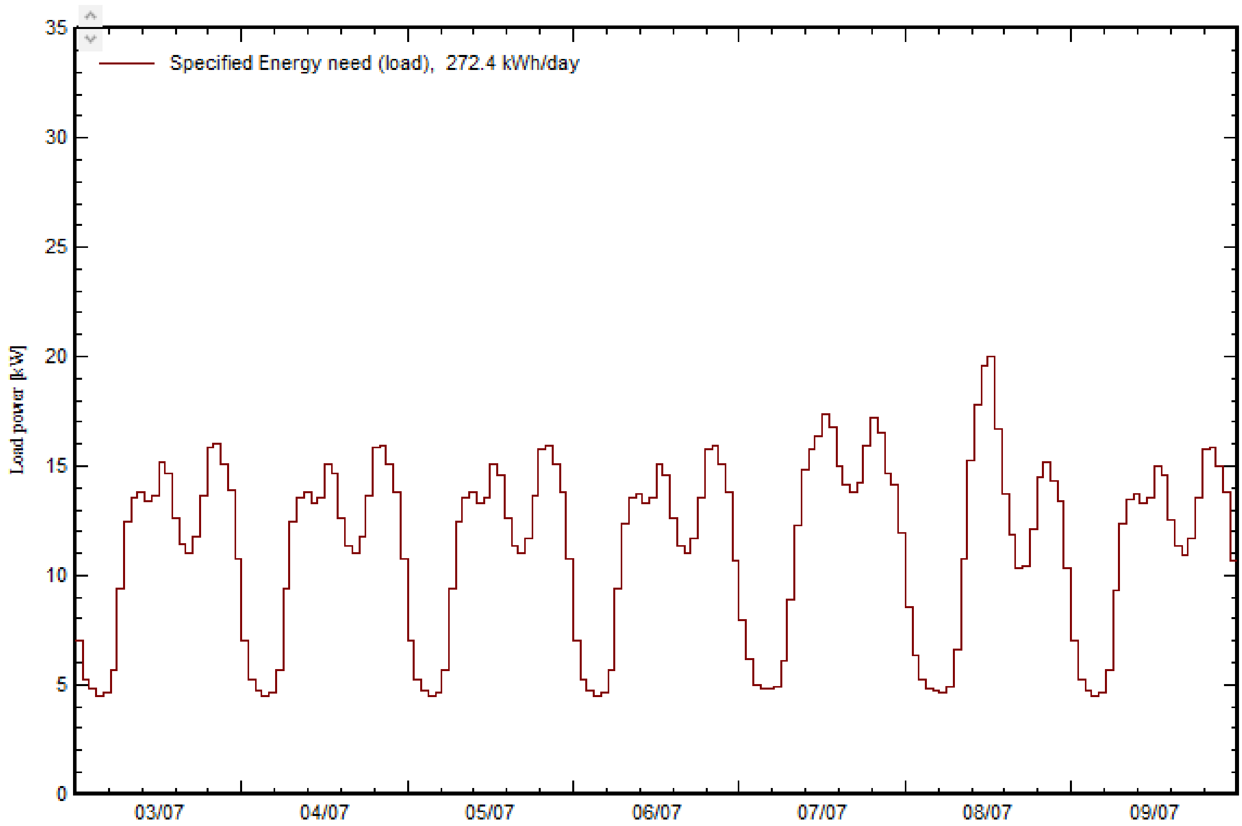

Figure 22: Load power for a week in summer period for the entire building

In the autumn period, as could be expected, the power needs to satisfy the loads are increasing while the electricity production is progressively decreasing. The load power reaches 20 kW when peaks demand occurs.
The energy need for the time period, from 10th to 16th of October, is about 320 kWh/day.

Number	**Appliance**	**Power**	**Daily use**
40	Lamps (LED)	10 W	5 h/day
16	TV and PC	150 W	3.5 h/day
56	Domestic appliances	1575 W	3.5 h/day
8	Fridge	62.5 W	24 h/day
8	Fan coil (heating)	2000 W	3 h/day

Table 4: Daily consumptions estimation for autumn season

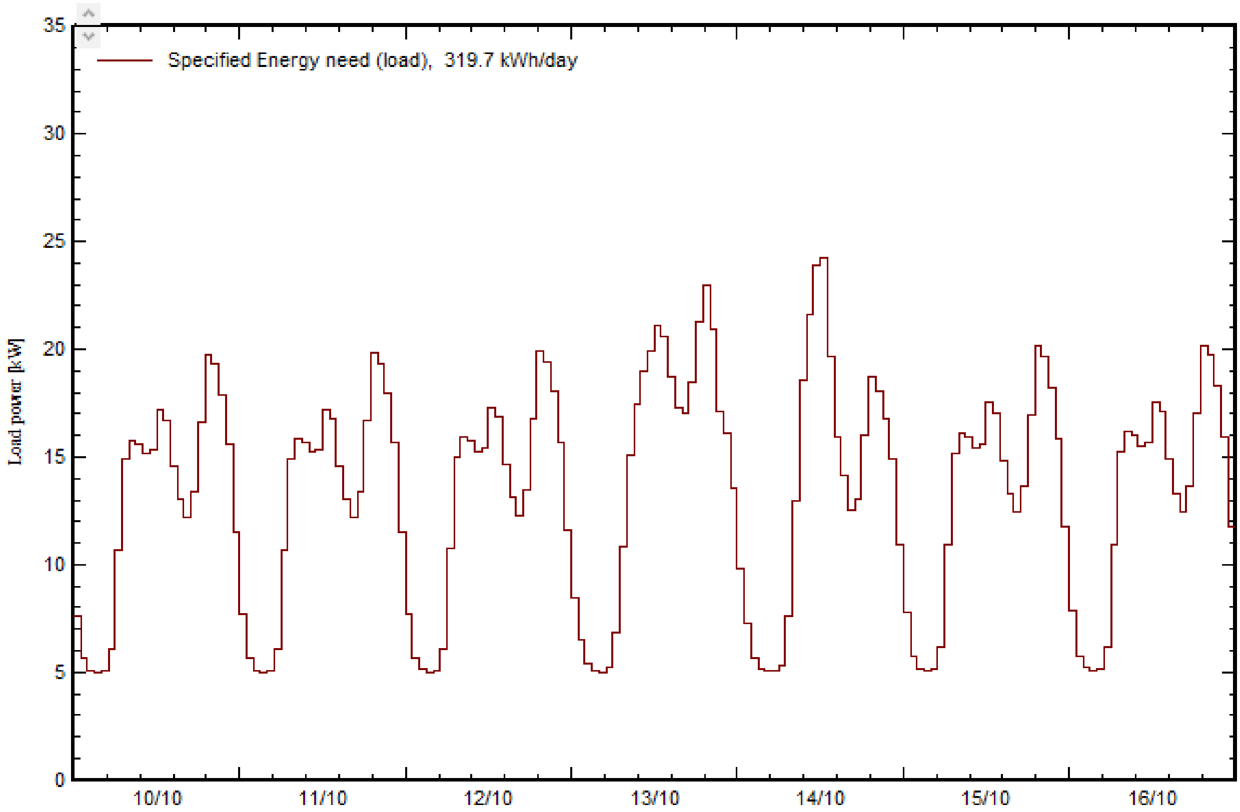

Figure 23: Load power for a week in autumn period for the entire building

The winter period is characterised by the highest load power request, while at the same time the hybrid system is not particularly productive. Especially for these winter months, the building has to rely mainly on the external electric grid to meet the demand.
The energy need for the time period, from 1st to 7th of January, is about 395 kWh/day.

Number	**Appliance**	**Power**	**Daily use**
40	Lamps (LED)	10 W	7 h/day
16	TV and PC	150 W	3.5 h/day
56	Domestic appliances	1575 W	3.5 h/day
8	Fridge	62.5 W	24 h/day
8	Fan coil (heating)	2000 W	8 h/day

Table 5: Daily consumptions estimation for winter season

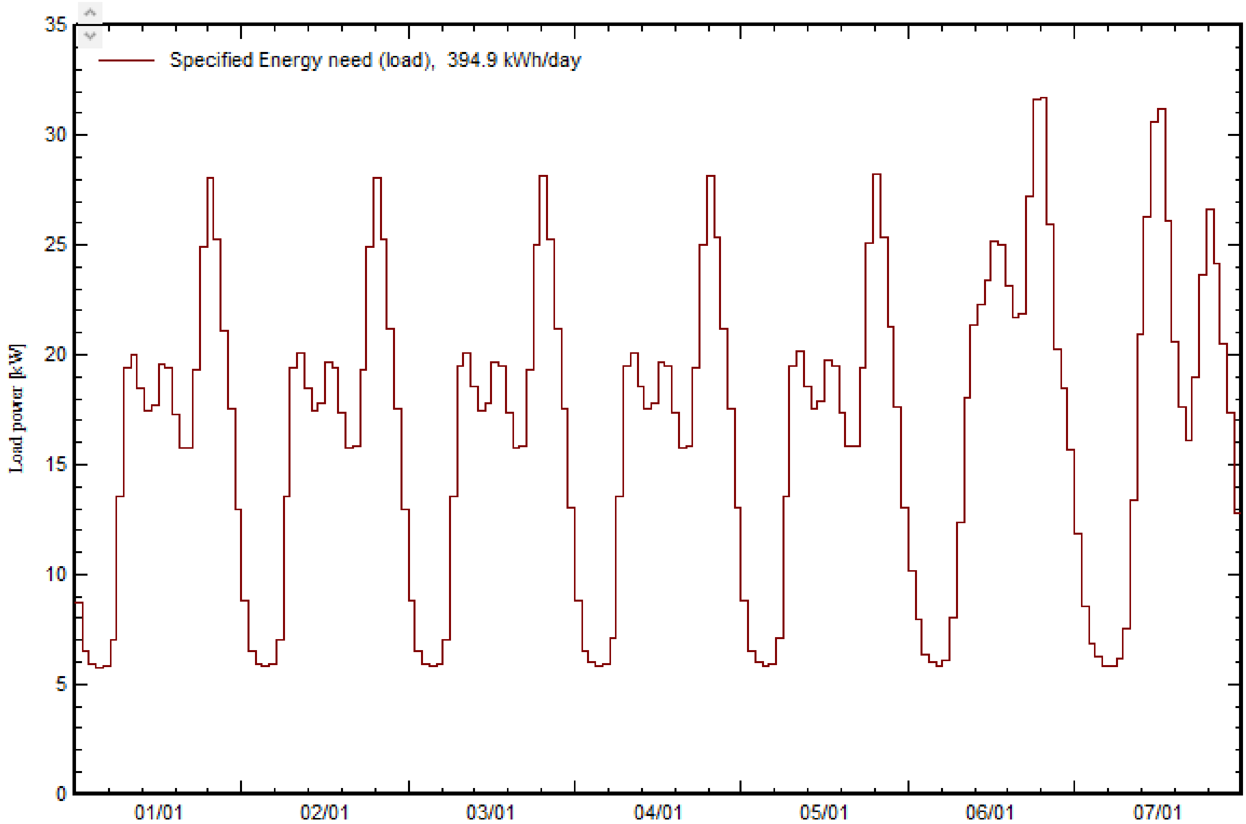

Figure 24: Load power for a week in winter period for the entire building

Finally, in the spring period can be noted a power need between the ones for summer and autumn. The demand peaks reach values up to 30 kW in the weekend, but the average energy demand is generally lower with respect to the winter period.
The energy need for the time period, from 5th to 11th of April, is about 345 kWh/day.

Number	Appliance	Power	Daily use
40	Lamps (LED)	10 W	4.5 h/day
16	TV and PC	150 W	3.5 h/day
56	Domestic appliances	1575 W	3.5 h/day
8	Fridge	62.5 W	24 h/day
8	Fan coil (heating)	2000 W	4 h/day

Table 6: Daily consumptions estimation for spring season for the entire building

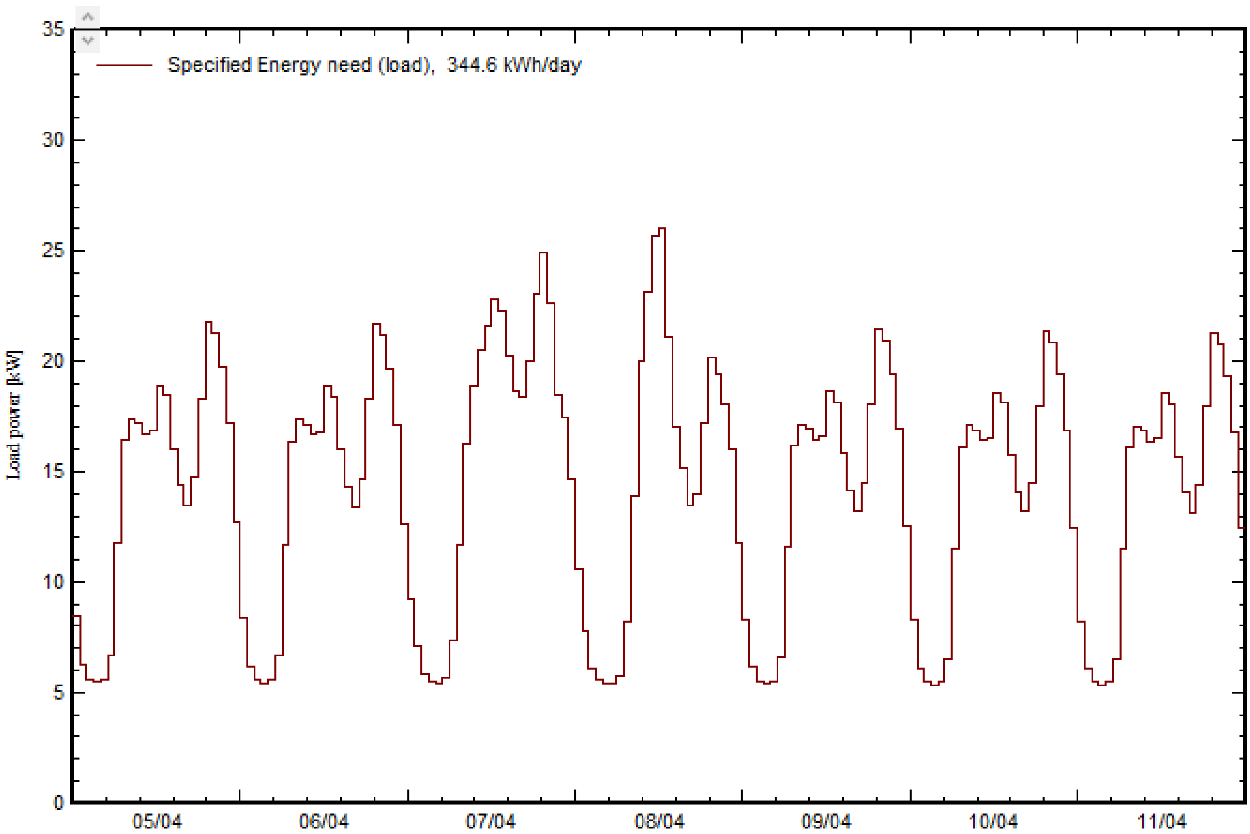

Figure 25: Load power for a week in spring period

The total yearly energy demand for the building accounts for about 121 MWh/year. The average load for the entire year is around 13.80 kW, while the maximum load reached during the winter period is equal to 31.90 kW.

3.2.5 Sizing of PV and BESS systems

The sizing of PV and BESS systems are one of the most important parts of the simulation because it has to be performed in a precise manner. The PV system must produce as much power as possible, covering all the available surface area of the roof for the installation of modules. At the same time, the battery storage system stores the excess energy production, therefore its capacity must be technically and economically optimized in order to offer the maximum flexibility and reduce the electricity consumption for the grid. The design part will focus on a technical analysis of the hybrid system, while the economic considerations related to the trading of electricity will be considered in the following chapter. The design is valid for both the orientations because they are projected in the same way, therefore the description will be carried out just for one of them.

3.2.5.1 Photovoltaic system design

Basically, the PV system is composed of photovoltaic modules and inverters. The modules produce electricity in DC current, while the inverters transform the DC current into AC current to be supplied to the loads.
Hence, the module choice is crucial because of the wide number of models available on the market, each one characterised by different nominal powers and properties.
For this case of study, the selected model is JKM-530M-7TL4-V manufactured by Jinkosolar (Figure 26). This model has been selected for its features, the reliability of the producer, and they permit to cover the largest part of the roof surface.
The monocrystalline models, like the selected one, are crafted from high-purity silicon crystals offering the highest efficiency with respect to other solar panel types. Their efficiency is remarkable, reaching values between 18% and 22%, especially in comparison to polycrystalline panels. They are particularly suitable for residential and commercial applications even when the roof space is limited. Due to the complex manufacturing process and the higher efficiency provided, they are more expensive than all the other PV technologies but ensures higher energy production and less degradation.
In the following table the most relevant features are listed, taken from the module datasheet. All the specifications are calculated at standard test conditions (STC).

Figure 26: PV module JKM-530M-7TL4-V

List of specifications JKM-530M-7TL4-V (mono-facial)	
Cell type	P type mono-crystalline
Dimensions	2206 x 1122 x 35 mm
Weight	28.2 kg
Power tolerance	0~+3%
Maximum power (Pmax)	530 Wp
Maximum power voltage (Vmp)	41.80 V
Maximum power current (Imp)	12.68 A
Open-circuit voltage (Voc)	49.34 V

Short-circuit current (Isc)	13.41 A
Module efficiency	21.41 %
Operating temperature	~40 °C~+85 °C
Nominal operating cell temperature (NOCT)	45 ± 2 °C

Table 7: List of specification for the selected PV module

After the assessment of PV module, the array has to be designed. It consists of defining the number of modules in series and the number of strings. The number of modules in series are defined according to the roof dimensions and aims to cover as much suitable roof surface as possible, taking in account that the open circuit voltage (Voc) at -10 °C must be lower than the inverter absolute maximum input voltage.

For this case of study, the following design parameters have been chosen for each side:

- Modules in series: 13
- Number of strings: 4

The total number of modules is 104 and the total module area is equal to 257 m^2. The ground cover ratio (GCR), which represents the percentage of roof area covered by modules, is very close to the maximum and is equal to 98.5%.
All the modules are able to provide a total nominal DC power of 55.1 kWp.

As previously mentioned, the DC power must be converted by the selected inverters which will be briefly described, focusing on their main features.
The inverter model is SUN2000-12KTL-M2 manufactured by Huawei Technologies, it is a three-phase smart string inverter. The general characteristics are reported below in Table 8.

List of specifications SUN2000-12KTL-M2	
Rated output power	12 kW
Rated AC output power	12 kVA
Max. efficiency	98.5 %

European weighted efficiency	98.0 %
Max. input voltage	1080 V
Operating voltage range	160 V ~ 950 V
Number of MPP trackers	2
Max. number of inputs	4
Max. output current	20 A
Operation temperature range	~25 ~+60 °C
Cooling	Natural convection

Table 8: List of specification for the selected inverter

The total number of inverters used in the simulation is 4, therefore the total nominal AC power is equal to 48 kWac. Both nominal AC and DC power can be considered acceptable according to the Pnom ratio, which is equal to 1.148.
This value is the ratio between the nominal AC power and DC power, it is within the acceptable range between 1.1 and 1.3.
Each inverter can be considered as a multi-MPPT (Maximum Power Point Tracker) inverter, so the single inverter is treated as several independent identical inverters. In our case, every inverter has 2 MPPT inputs, therefore every string is associated with one MPPT input. This kind of configuration allows the power sharing of the single inverter across two strings, each string will have a nominal power of half the power of the full inverter (6 kW). Furthermore, this configuration allows to avoid the usage of further systems of protection. The balance of strings on MPPTs is a relevant aspect in order to increase the overall efficiency under the same solar irradiance condition.

3.2.5.2 BESS design

The battery energy storage system aims to store the excess of electricity production and use it when the power requested by the load is increasing. The self-consumption strategy may have different objectives, such as the minimization of the energy supplied by the grid, optimizing the cost of electricity and re-injecting the energy when needed by the community. This kind of strategy allows to charge the batteries when excess of solar power is available and to discharge them as soon as the user needs power.

The two most diffused BESS technologies are lithium-ion batteries and lead-acid batteries. The lead-acid batteries are a mature and cost-effective option but with lower energy density and shorter lifespan. On the other hand, the lithium-ion batteries are the most widely used technology due to high energy density, efficiency and long cycle life. Despite the advantages, this kind of batteries also have several drawbacks such as high initial costs, challenges in raw material supply and safety concerns. Anyway, the advancements in battery management systems (BMS) are improving their management and efficiency.
The battery set chosen for the simulation is a lithium-ion battery named Battery Box Premium HVS 12.8 kWh, manufactured by BYD (Figure 27). The battery size was chosen interactively in order to obtain an appropriate contribution from the BESS.
The following table resume the main features of the battery set.

List of specifications Battery Box Premium HVS 12.8	
Number of modules	5
Usable energy	12.8 kWh
Max. output current	25 A
Peak output power	50 A
Nominal voltage	512 V
Operating voltage	400 ~ 576 V
Dimensions	1411 x 585 x 298 mm
Weight	205 kg
Operating temperature	-10 °C~+50 °C
Battery cell technology	Lithium iron phosphate (cobalt free)
Round-trip efficiency	≥96 %
Static lifetime at 20 °C	10 years

Table 9: List of specification for the selected battery pack

The design parameters for the battery set are reported as follows:

- Racks in series: 1
- Racks in parallel: 24
- Initial state of wear (number of cycle): 96%
- Initial state of wear (static): 98%

- Maximum charging (OFF): 98%
- Minimum discharging (OFF): 15%
- Maximum charging power: 27 kW
- Maximum discharging power: 33 kW

Figure 27: BESS model Battery Box Premium HVS 12.8 kWh

The battery pack voltage is 512 V, the global capacity (C10) accounts for 600 Ah.
The operating battery temperature is kept fixed at 20 °C, the air-conditioning is used to maintain the same temperature and avoid decreasing the batteries efficiency.

3.2.6 Photovoltaic system layout

The PV modules have to be installed in a proper way in order to cover the total area of the two sides of the roof. The two directions (E-W) are chosen to maximise the solar irradiation during the day considering the house's orientation, therefore the first one is oriented towards the east while the second one towards the west. The azimuth angles are respectively -90° and 90°. For the sake of simplicity, photovoltaic modules are mounted above the roof to reduce installation and maintenance costs. In Figure 28 is provided a more detailed view of the PV modules layout.
The modules are mounted on fixed structures characterised by the same roof tilt angle (20°). For each side of the roof are installed two fixed structures with the following relevant measures:

- Table height: 4.47 m
- Table length: 14.87 m
- Sensitive area: 65.71 m^2

For each table are mounted 13 modules in length and 2 modules in height, so there are 26 modules per structure. The orientation of modules is portrait as shown in Figure 28.

Figure 28: PV modules layout

The partitioning is important for electrical shading calculations, for this reason the definition of rectangles representing one string of modules has been carried out. The partitions are fully defined by setting the number of rectangles in width is 1, while the number of rectangles in height is 2.

3.3 Simulation results and sensitivity analysis

After providing to the PVsyst software all the necessary information to perform the analysis, the simulation can be run in order to obtain a final report including all the main results and graphs.
Firstly, will be presented the main data related to weather conditions, together with solar irradiance and system production outputs. Then, will be shown the loss diagram, describing all the kinds of losses in detail and their percentage value. Finally, a sensitivity analysis will be also carried out to understand how the main system parameters vary when the roof slope changes.

3.3.1 Balances and main results

The first results to be displayed in Table 10 are those associated with the solar irradiation collected by the photovoltaic modules. These variables are helpful to give an idea of how much energy per unit of area is available in our location and how the slope of the roof can increase or decrease the incident irradiation. Furthermore, it is also reported the average monthly ambient temperature.

	T_amb [°C]	**GHI [kWh/m²]**	**DHI [kWh/m²]**	**GlobInc [kWh/m²]**	**GlobEff [kWh/m²]**
Jan	6.5	47.5	21.8	46.6	42.0
Feb	7.4	65.2	29.0	63.9	59.2
Mar	10.1	112.9	47.3	110.2	103.5
Apr	13.0	140.7	61.2	137.4	129.9
May	16.7	176.0	78.2	171.0	162.4
Jun	20.6	196.3	81.6	191.0	180.7
Jul	23.1	210.4	78.6	205.1	194.4
Aug	23.3	178.9	69.8	174.2	165.5
Sep	19.8	127.9	55.3	124.6	117.4
Oct	15.8	80.3	39.3	78.6	73.2
Nov	11.1	48.4	24.0	47.4	43.1
Dic	7.5	38.6	18.5	38.1	33.9

Year	-	1423.1	604.6	1388.0	1305.1

Table 10: Monthly solar irradiance and external temperature data

Ambient temperature (T_amb): due to the geographical location, the hottest season is summer when the highest values are registered, in line with expectations. This value influences the efficiency of solar panels, higher temperatures can reduce their performance.

Global Horizontal Irradiance (GHI): as previously discussed in paragraph 3.2.1, it is the average daily sum of diffuse horizontal irradiation and includes both direct and diffuse radiation. The highest value is reached in July, when the solar beams are more perpendicular with respect to the ground.
This parameter is one of the most representative, a better visual representation is pictured in Figure 29.

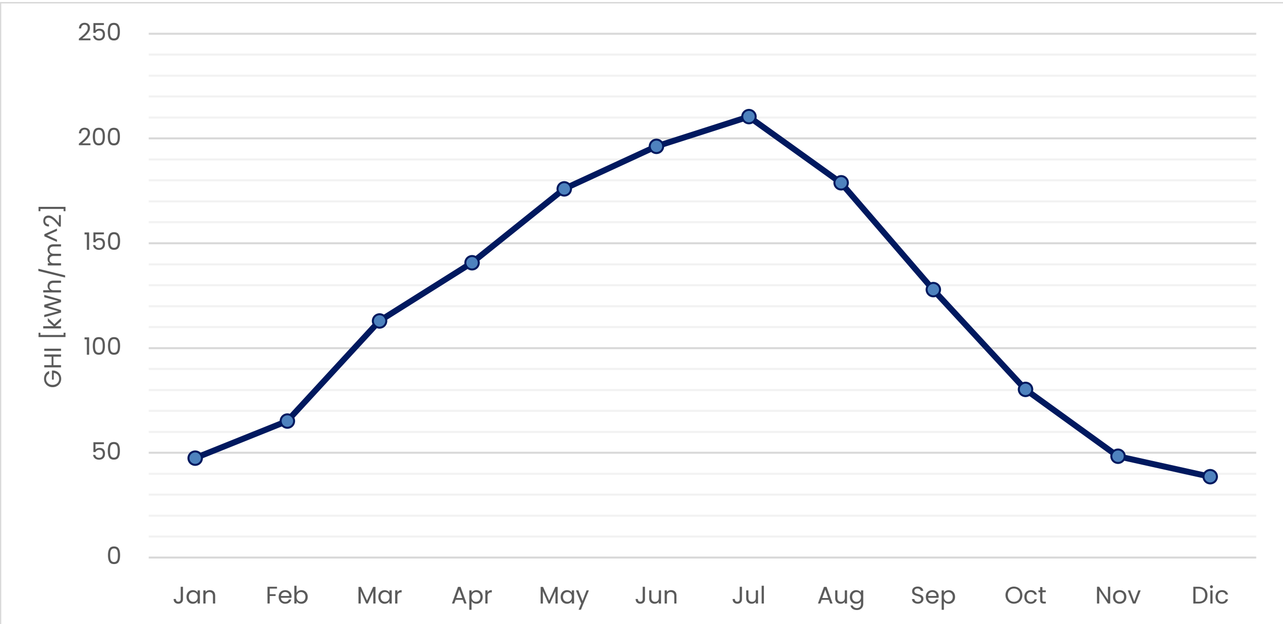

Figure 29: Global Horizontal Irradiance (GHI)

Diffuse Horizontal Irradiance (DHI): it represents the portion of solar radiation scattered by the atmosphere and received on a horizontal surface, excluding the direct sunlight.

Global incident in collector plane (GlobInc): this parameter accounts for the total solar radiation received on a tilted surface, taking into account both direct and diffuse components. It is possible to note that the monthly values are slightly lower than GHI ones, so the tilted surface is able to collect lower energy than the horizontal one.

Effective Global irradiance (GlobEff): it represents the portion of the incident irradiance that is effectively converted into usable energy by PV modules, after accounting losses related to factors like shading, reflection and temperature effects. In fact, these monthly values are lower but very close to the ones associated to GlobInc.

After evaluating the main parameters related to monthly solar irradiance, it is possible to consider the results related to balances of energy produced and exchanged within the system. In Table 11 are reported the main variables of interest.

	EArray [MWh]	**E_User [MWh]**	**E_Solar [MWh]**	**E_Solar_BESS [MWh]**	**E_Grid [MWh]**	**EFrGrid [MWh]**
Jan	2.19	12.26	2.24	0.65	0.0	10.02
Feb	3.08	10.79	2.95	0.86	0.0	7.84
Mar	5.34	11.60	5.07	1.47	0.0	6.54
Apr	6.62	10.04	6.21	1.80	0.0	3.83
May	8.14	9.25	7.57	2.20	0.0	1.68
Jun	8.89	8.50	7.85	2.28	0.364	0.65
Jul	9.50	8.40	8.26	2.40	0.351	0.14
Aug	8.10	8.58	7.48	2.17	0.136	1.10
Sep	5.84	8.71	5.46	1.58	0.0	3.25
Oct	3.71	10.02	3.51	1.02	0.0	6.51
Nov	2.21	10.92	2.12	0.61	0.0	8.80
Dic	1.75	11.93	1.68	0.49	0.0	10.25
Year	65.38	121.00	60.39	17.51	0.852	60.61

Table 11: Monthly energy production

Effective energy at the output of the array (EArray): Total energy generated by the PV array, this parameter represents the gross energy production before losses or conversions.

Energy supplied to the user (E_User): Total energy consumed by the users, it includes both solar-generated energy and energy collected from grid when needed. The total yearly energy consumption is the same reported in paragraph 3.3.2, namely 121 MWh. The variations in energy demand follow the same trend of the load profile, therefore the winter months are those characterised by higher need of energy as expected. The monthly energy supplied to the users is the summation of the energy from the sun (E_Solar) and the energy from the grid (EFrGrid), as can be seen in Figure 30.

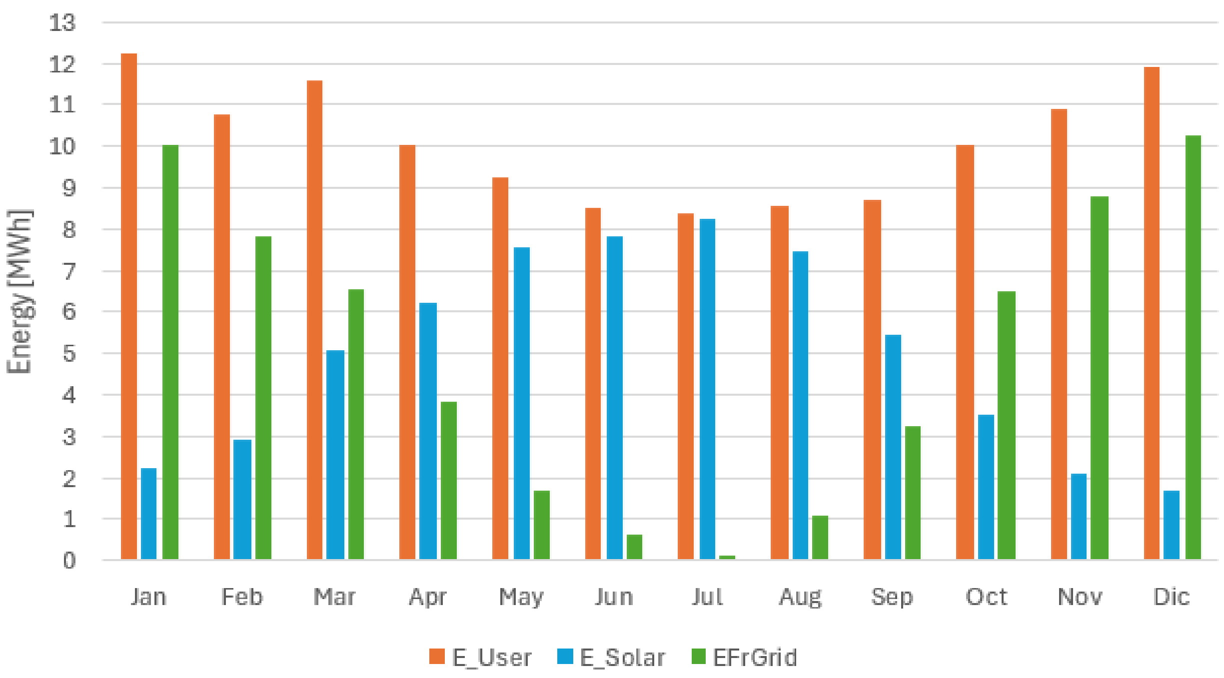

Figure 30: Monthly comparison between E_User, E_Solar and EFrGrid

Energy from the sun (E_Solar): Portion of the generated solar energy that is directly used for internal consumption. When the energy production is higher, the hybrid system is able to provide almost all the energy required by the building. For instance, in July the PV system cover the 98.3% of the total demand. The amount of energy stored in the BESS (E_Solar_BESS) accounts for the 29% of E_Solar.

Energy injected into the grid (E_Grid): amount of energy exported to the grid, representing the excess solar that was not consumed locally. Unfortunately, the total energy injected into the grid accounted only for 852 kWh (less than 1.5% of E_Solar) because the excess production occurs mainly during the summer period.

Energy from the grid (EFrGrid): energy imported from the grid to meet the user demand when solar generation is insufficient. Its trend is the opposite one with respect to E_Solar, therefore when energy from the sun is lower, the energy from the grid is higher and vice versa. This can be better analysed through the observation of graphical representation in Figure 31.

Finally, the last results to be analysed are those related to system energy production.
The produced energy throughout the year accounts for 61242 kWh, while the used energy is 121000 kWh as reported in paragraph 3.3.2. Another important parameter is the specific production, it amounts to 1111 kWh/kWp. This result is underestimated with respect to the average values for the selected geographical location, but it can be considered reliable and conservative as well. Moreover, the orientations selected are not the best options, in fact the south direction would maximise the specific production.
In Figure 31 is visible the picture reporting the performance ratio for each month, while the average value is equal to 80.05%

The performance ratio PR is adopted as dimensionless indicator of the availability of solar energy for final uses. This parameter points out how much energy can be actually supplied to the users with respect to the theoretical expected production without losses. The performance ratio is calculated as follows:

$$PR = \frac{E\_Grid + E\_Solar}{GlobInc \cdot PnomPV}$$

E_Grid, E_Solar and GlobInc are parameters already described and shown in Table 10 and Table 11. PnomPV represents the nominal DC power of the PV system, accounting for

55.1 kWp. The first three values (E_Grid, E_Solar and GlobInc) vary month-by-month, therefore the monthly performance ratio depends on their monthly values, while the nominal power system is constant throughout the life of the entire system.

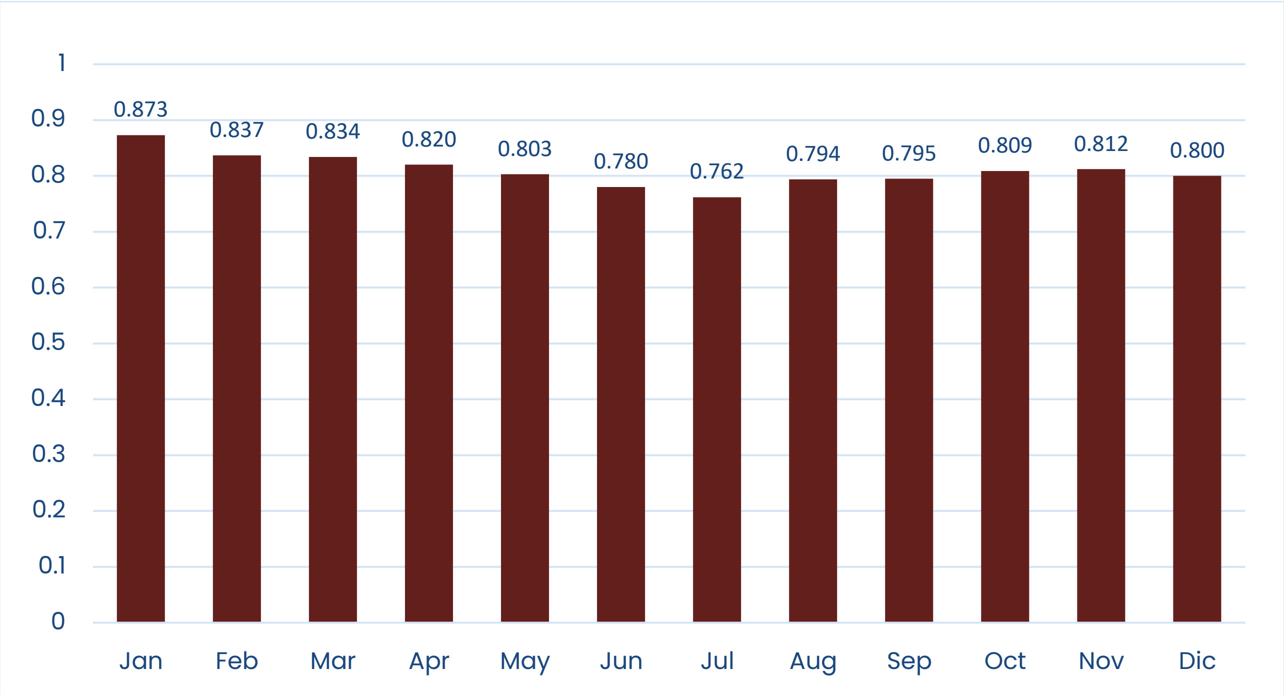

Figure 31: Performance ratio PR

The summer months are characterized by lower PR values, the numerator results to be increased due to higher energy production, but also the incident solar radiation collected on tilted structures is increased remarkably.
The same concept can be also visualized in Figure 32 under another perspective.
The useful energy produced per kWp of installed power, namely the inverters output, is higher in summer period than in winter period as expected. However, it is possible to note that higher electricity production leads to higher losses in percentage terms, while lower production causes lower amounts of losses. The losses are aggregated in system loss (represented in green) and collection loss (represented in purple). In particular, the latest one is the major responsible for energy loss, while the system loss is almost negligible thanks to very high efficiency of energy conversion components, especially when the solar irradiance is less available.

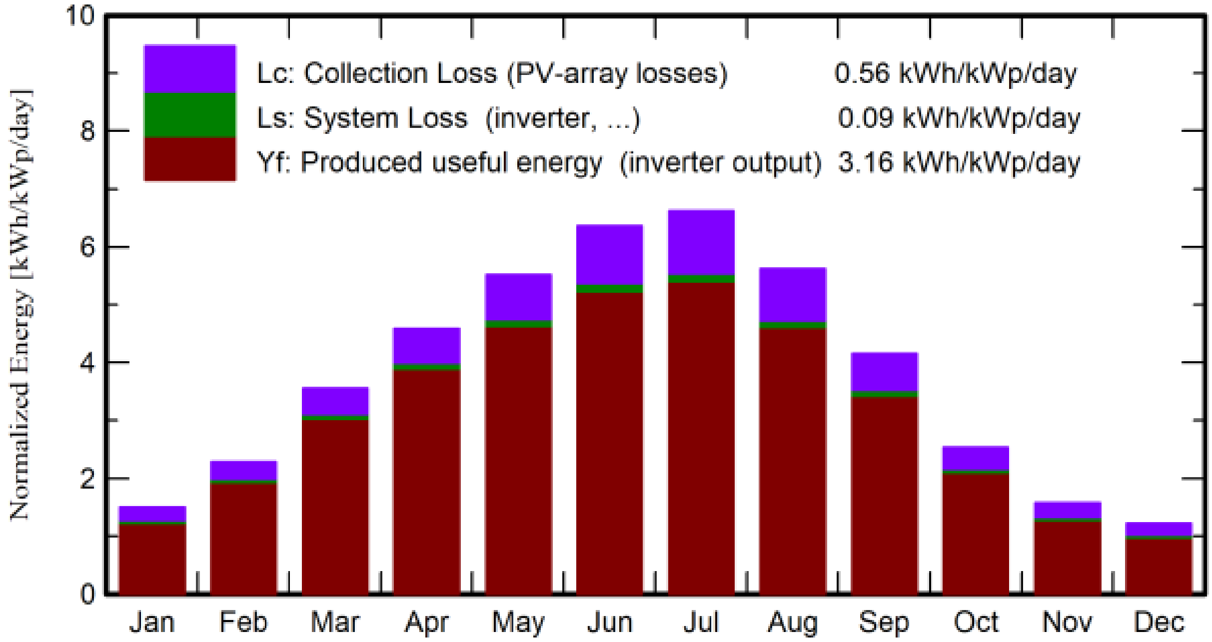

Figure 32: Normalized production per installed kWp

3.3.2 Loss diagram

The loss diagram represents all the possible kind of losses occurring during the process of transformation of solar irradiation to electricity delivered to users, batteries and electric grid. The graphical representation in Figure 34 also permits to understand how the final electric production is shared among the different parts of the system. In particular, the most relevant source of losses will be briefly analysed and described:

Global incident in collector plane: -2.46%
This negative value points out that the PV modules slope is not optimised, namely the global horizontal irradiation is higher than irradiation collected by tilted modules. This can be also observed by the results reported in Table 10.

Far shadings: -0.83%
This loss is referring to shadings of objects sufficiently far from the PV field, and their accounting is performed define a Horizon line. Since at a given time, the sun is over or

under such line, PVsyst determines the time of the crossing of the horizon line within the simulation hour and applies this fraction of hour as loss to the beam component. The horizon line drawing has been imported from PVGIS, in Figure 33 is shown the sun height at different azimuth angles for both the orientations.

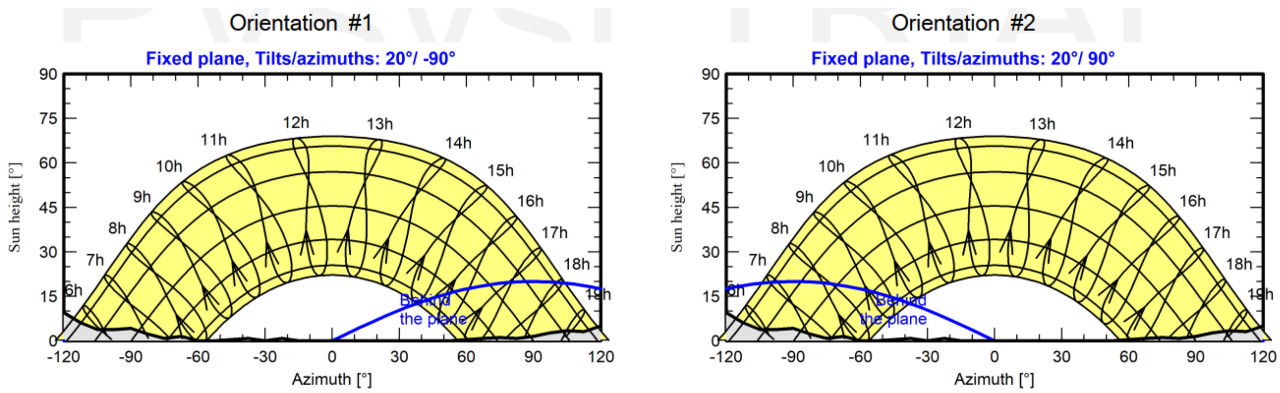

Figure 33: Sun path for both the orientations

Near shadings: -0.09%

This loss is extremely low and is almost negligible because it is due to the partial mutual shading occurring between the modules mounted on fixed structures belonging to the orientations taken into consideration.

Soil loss factor: -2.00%

Although the modules' coatings are dust repellent, they will invariably collect dirt over their lifetime which will restrict the sunlight available to the cell and cause a small loss when compared to rated power. The modules should have to be cleaned regularly in order to reduce this source of losses as much as possible, but this value can be considered conservative and reliable.

IAM factor: -3.17%

The loss of power associated with the angle of incidence occurs when the light falls on the module at an angle other than 90 degrees. Losses are due to reflection of the light and to spectral reflectance and the current generated by the modules is varying with the radiation wavelength and the angle of incidence.

Losses due to irradiance level: -1.96%
Usually, module efficiency decreases with decreasing light intensity. The extent of these losses depends on several module characteristics and site environmental conditions.

Losses due to temperature level: -3.92%
The efficiency of a crystalline silicon PV cell decreases non-linearly with the module's temperature. The natural air ventilation of the panels also has an effect on the performance of the PV installation.

Shadings electrical loss according to strings: -0.01%
The partial shading effect on electrical production of PV modules is not linear and it depends on interconnections between the modules. As the current of each string is the same as the current of less irradiated cell, hence this phenomenon has high impact on the full string performance. This loss was calculated by the simulation tool taking into consideration the strings per shed as defined in 3D modeling of shading scene in PVsyst.

Module quality: +0.75%
Since in the datasheet of the photovoltaic module, it is indicated a positive tolerance of the modules (0/+3%), the effect of module quality applied as a gain for the system performance.

Light Induced Degradation (LID): -2.00%
Silicon PV modules have a natural degradation due to the electrons flow through the p-n junctions of a module. This initial degradation occurred when modules are exposed to sunlight. Considering the datasheet of the PV module and type of cells, this value can be considered as reasonable.

Module array mismatch loss: 1.50%
Losses due to the mismatching of modules are associated with a difference in performance of each single module, due to the electrical parameters of cells not being identical, tolerances in the manufacturing process and non-uniformity of the radiation over a string of modules. Cells and modules are connected in series, with the result that each string works at the power level of its worst module.
Ohmic wiring loss: -0.82%

Resistance losses must be considered for the DC cables from the panel to inverter of the entire PV plant. In this case, the cables length is unknown, therefore the loss fraction at STC has been chosen equal to -1.5% as reference value.

Inverter loss during operation: -2.61%
This source of loss takes into account that the inverters operations are not ideal, therefore it's need to account this non-negligible loss associated to this component of the system. Correctly sizing the inverters is very important to minimize inverter losses. The main inverter roles in a photo-voltaic plant are tracking of maximum power point and DC/AC conversion.
The -0.16% related to night operation considers the stand-by operation of inverters when the solar irradiation is absent.

Battery IN, charger loss: -1.30%
It represents the operating loss in the battery charger; therefore, it is a kind of inefficiency related to the charging phase of batteries that lead to waste a portion of energy produced from PV system.

Battery OUT, inverter loss: -1.29%
It represents the operating loss in the battery charger, so it is a kind of inefficiency related to the discharging phase of batteries, when the energy is withdrawn from batteries and converted from DC to AC currents through the inverters.

Battery global loss: -1.31%
This loss represents the battery energy loss due to charging/discharging efficiency, internal resistance or over-current due to overcharging. The global loss is equivalent to the other two sources of loss related to battery operation.

The availability of the plant is assumed to be equal to 100%, so it is supposed that the system is always in operation for sake of simplicity.
Moreover, the loss diagram provides in its final part the energy amount delivered to the users directly from the PV system, stored in the batteries and withdrawn from the electric grid. In Figure 34 is shown a graphical representation able to clarify the energy final destinations in percentage, reporting their values in kWh. As can be observed, the division of the total energy supplied to the users is equally divided between the grid and direct production contribution.

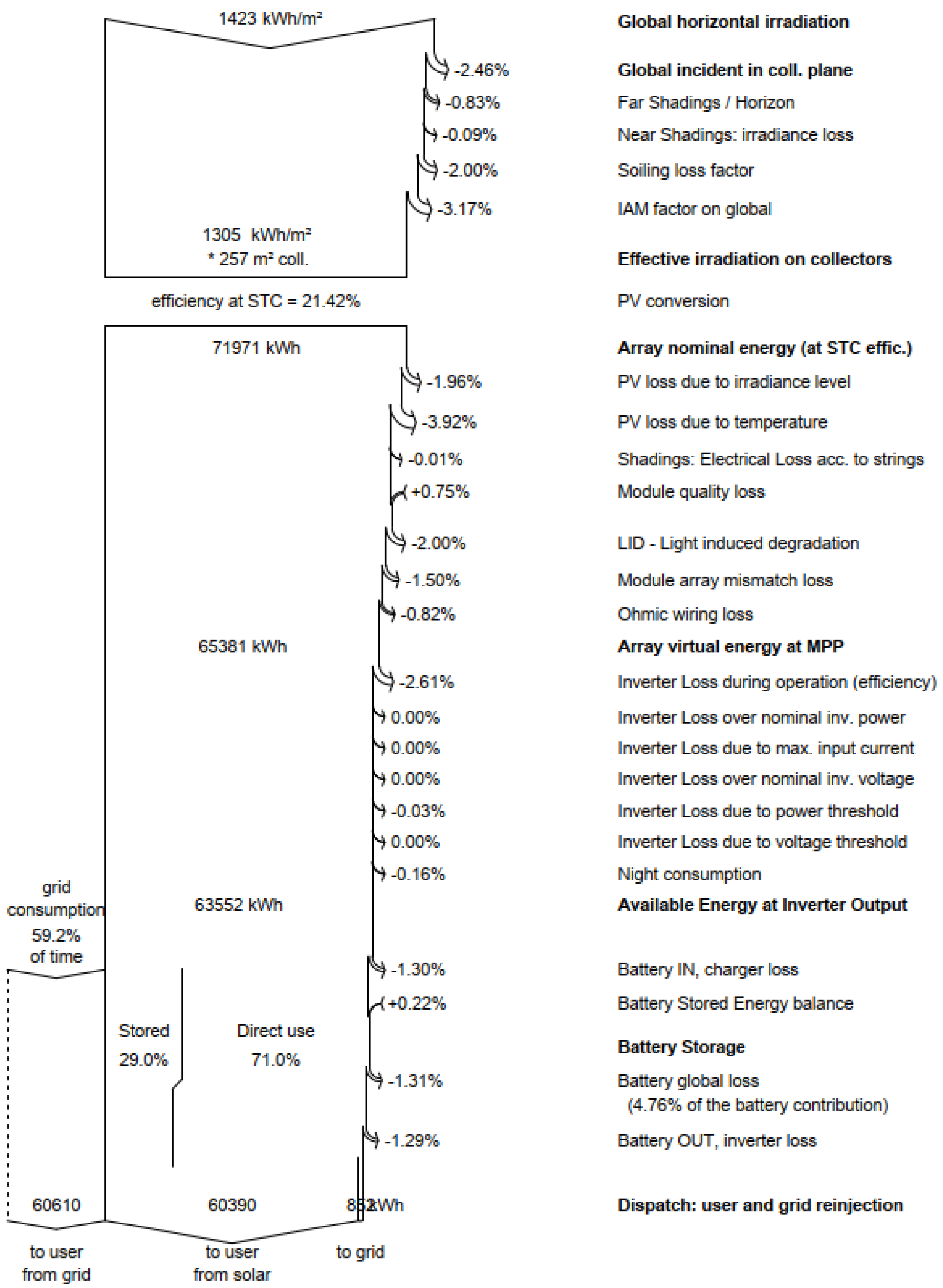

Figure 34: Loss diagram

The pie chart in Figure 35, shows the absolute equilibrium between the energy produced from solar and withdrawn from the electric grid, 49.9% and 50.1% respectively.
The first item accounts for 60390 kWh/year, the second one for 60610 kWh/year. This calculation does not consider the 852 kWh/year of energy injected into the grid that is considered as an energy production surplus.
The energy generated from solar source can be further divided into energy stored through the batteries and directly consumed by inhabitants. The energy stored throughout the year is the 29.0% of the energy provided by the PV system and the 14.5% with respect to the total amount of electricity supplied to the users. The energy directly consumed by users is the largest amount of electricity generated from the renewable energy system, accounting for the 71.0% of energy exiting from inverters.

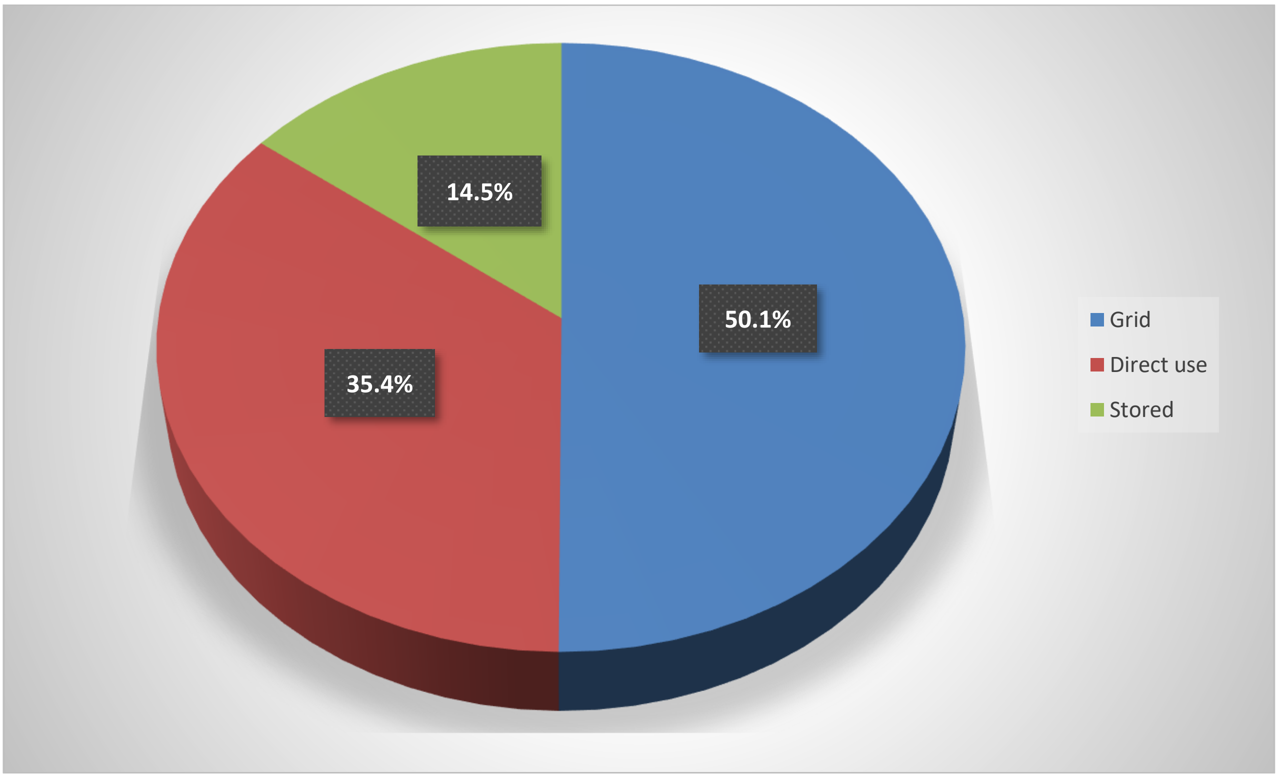

Figure 35: Pie chart of energy supplied to end-users

Anyway, the time utilization of energy coming from grid and hybrid system is less balanced, with the grid being used for the 59.2% of time and the other just 40.8%.

3.3.3 Sensitivity analysis

In the sensitivity analysis part, some design changes will be made in order to assess the differences related to the most relevant results. The variations will regard the slope of the roof and will be performed new simulations taking into account lower and higher values with respect to the one taken as reference in the previous paragraph. The main scope of this analysis is to understand how the energy system production is affected by design change, aiming to maximise the energy produced and managed by the whole system.

3.3.3.1 Roof slope variations

This sensitivity analysis is particularly interesting for what concern the energy supplied thanks to solar irradiance. The design features are kept unchanged and the slopes taken into consideration are:

- Case 1: 15°
- Case 2: 30°

Lower tilt angles should enhance the global incident irradiance in collector planes, so this positive effect will lead to higher total energy production. On the contrary, higher tilt angles causes more losses and less expected energy output. It is important to note that in this geographical area the roofs cannot be completely flat, otherwise their structural function would be compromised. Indeed, the sloped is designed to optimize rainwater drainage and snow load management. Hence, the 20° configuration will be also taken as reference for the management part in the next chapter.
The main results are summarized in Table 12.

Parameters	**Reference**	**Case 1**	**Case 2**
GlobInc	1388.0 kWh/m^2	1403.1 kWh/m^2	1348 kWh/m^2
Produced energy	61222 kWh	61932 kWh	59417 kWh
Specific production	1111 kWh/kWp	1124 kWh/kWp	1078 kWh
E_Solar	60381 kWh	60845 kWh	59013 kWh
EFrGrid	60619 kWh	60154 kWh	61986kWh
E_Grid	841 kWh	1086 kWh	404 kWh

Table 12: Results comparison for different roof slopes

The results follow the expected trend, for the first case with lower roof slope are registered higher produced energy and specific production. In fact, the energy production increases by 1.16% with respect to the reference case. The opposite for the second case, the percentage reduction accounts for -2.95%.
The differences between energy produced from solar irradiance, injected and withdrawn from the grid for each case are better visualised in Figure 36.

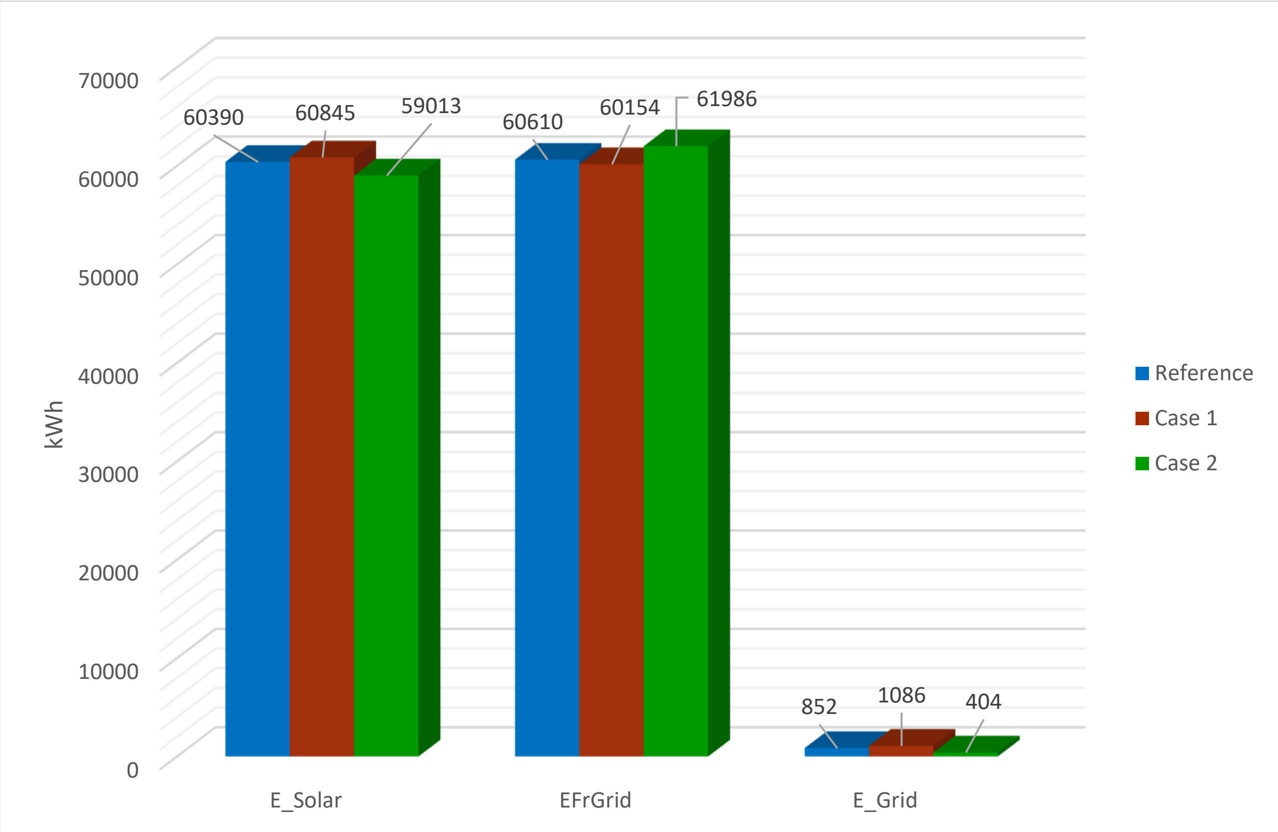

Figure 36: Comparison between the three cases results under analysis

It is possible to note the correlation between energy production and energy withdrawn and injected into the grid. In case 1, with higher solar energy production, the energy demand can be met using less energy from the grid. Furthermore, the increasing produced energy leads to a further excess of electricity that can be sold and injected into the electric grid. The case 2 follows the opposite trend, lower production causes an increasing energy coming from the grid and less electricity surplus can be sold.

The utilization time of the hybrid system and the electric grid are slightly modified according to the differences in internal energy production. The contribution of direct use mode and battery storage also remain the same since the technical features of the operating system are unchanged.

4 Energy Management System (EMS)

In this chapter, the main focus is on developing EMS for the buildings, taken as reference in the previous chapter, in the context of REC. For this case of study, the simulation is performed taking into account just two buildings within this hypothetical energy community: the reference case analyzed in the previous chapter (building 1) and another one that will be briefly described (building 2). Both are also connected to the external electric grid for the purchase and sale of electricity. The number of participants is rather limited, but it is the minimum number that guarantees a trade-off between simplicity and reliability of the analysis. Indeed, the methodology used can be applied to whatever number of members using the same reasoning.

The building 2 is designed differently from the first one, in fact the roof area is wider and consequently there are more PV modules installed. Furthermore, it is assumed without the BESS in order to include this kind of system in the simulation environment that can interact with the other building.
The most relevant characteristics of the technologies installed and consumption of the building 2 are listed in Table 13.

Building 2	
Geographical location	Genoa
Dimensions	37 x 18.5 x 15 m
Module	JKM-530M-7TL4-V (Jinkosolar)
Modules in series	16
Number of strings	16
Number of modules	256
Unit nominal DC power	530 Wp
Inverter	SUN2000-15KTL-M2 (Huawei)
Number of inverters	8
Unit nominal DC power	15 kWac
Total DC power	136.0 kWp
Total AC power	120.0 kWac
Pnom ratio	1.13

Specific production	1162.0 kWh/year
Performance ratio PR	83.71%
EArray	160.9 MWh
Produced energy	157.6 MWh
E_User	151.0 MWh

Table 13: General characteristics of building 2

The building is oriented towards the same direction (south), the PV modules are installed in E-W orientation. A graphical representation of the building 2 is reported in Figure 37. The size of the building has increased, hence the number of inhabitants is higher as well as the annual electricity consumption.

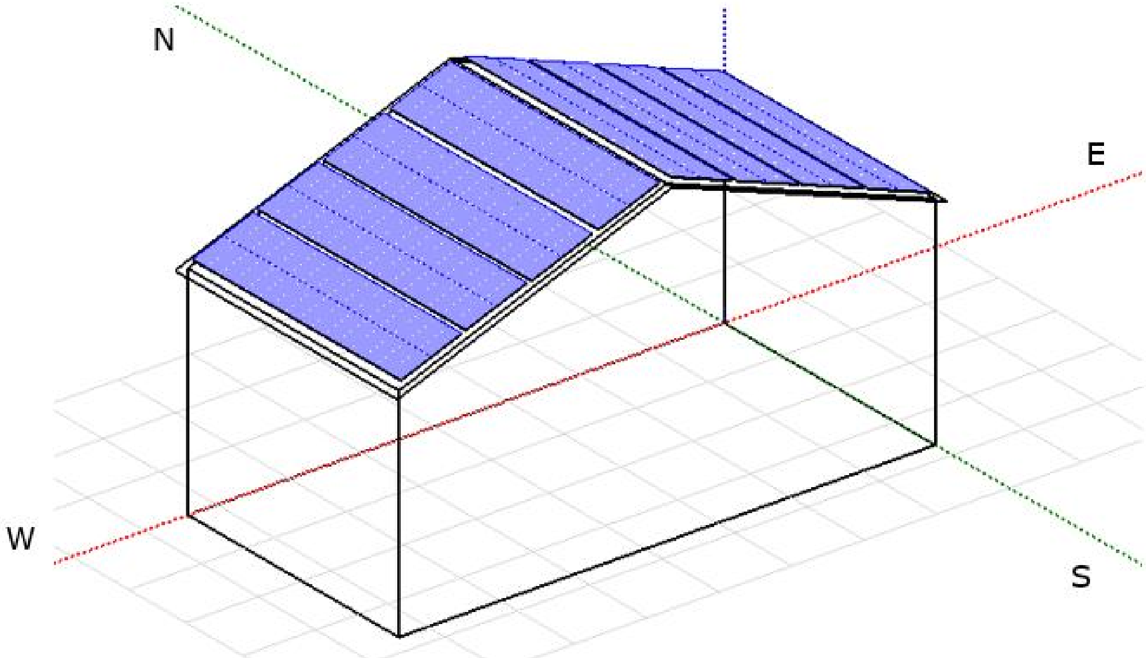

Figure 37: Building 2 representation

Once defined the two buildings taking part to the local energy community, it is necessary to clarify the general model to develop in MATLAB environment.

MATLAB is a powerful computing environment widely used for numerical analysis, data visualization, and algorithm development. For this kind of application, a particular toolbox named Yalmip is necessary. It is designed for modeling and optimization problem and is coupled with a numerical solver, like Gurobi.
The general model representing the basic microgrid architecture and its components is illustrated through a graphical representation in Figure 38.

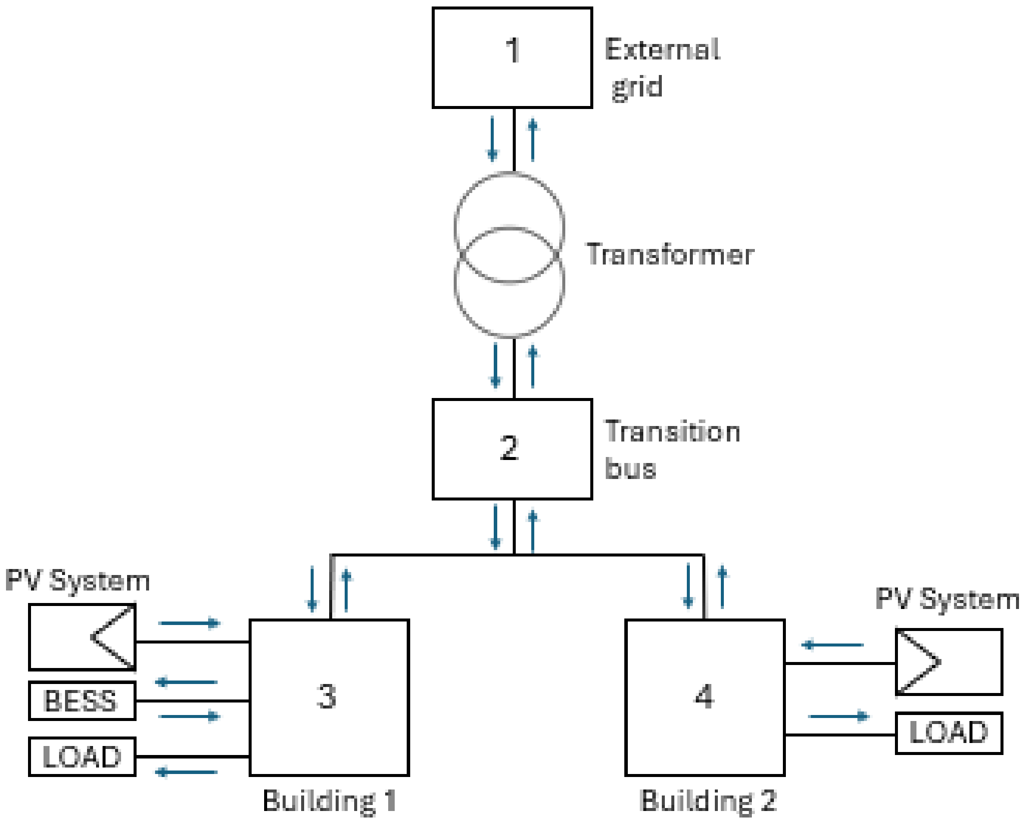

Figure 38: Graphical model of REC

The building 1 and 2 are denoted with the blocks 3 and 4. These two are not directly linked, the transition bus (block 2) aims to collect and distribute the active power according to the energy needs. All this electric structure is connected to the external electric grid managed by the distribution system operator (DSO). It is represented by the block 1, the connection is permitted thanks to the MV-LV transformer able to increase and decrease

the voltage level. The low voltage level is assumed to be equal to 0.4 kV, while the medium voltage level 15 kV. Each block taken into consideration will be modelled as a bus from an electric point of view, to be analysed individually.
The external grid is a fundamental part of the system, it ensures the energy supply from outside the energy community which act as a slack bus as an unlimited source of energy and is crucial for the energy selling.

The Matlab algorithm has been realised importing and setting some essential parameters, like those listed in paragraph 4.1. Moreover, the mathematical model related to the electrical aspects was included in the code, establishing constrains and ensuring the power flow across the buses is balanced. The algorithm is expected to take into account the minimization of the total costs, with the help of Yalmip toolbox. Finally, the output consists of decision variables got by the processing of input data provided. The final results are represented and discussed by means of the plots reported in paragraph 4.5.

4.1 Inputs

In this paragraph the crucial information that needs for the Matlab simulation is reported. Those are mainly technical features of PV modules, MV-LV transformer and batteries, but are also included relevant data regarding the non-manageable electrical load, like the revenue for the electricity sold to the national grid.

PV:

$P_{b,t}^{PV,av}\ \forall b = 1..B\ \ \forall t = 1..T$, Available power PV [kW]
$A_b^{PV}\ \forall b = 1..B$, Nominal apparent power of the PV inverter at nodes b [kVA]

Electrical Load (non-manageable):

$P_{b,t}^{el,active}\ \forall b = 1..B\ \ \forall t = 1..T$, Active Power Electrical demand at different BUS [kW]
$P^{buy,max}$, Maximum power that can be bought from the national grid [kW]
$P^{sell,max}$, Maximum power that can be sold to the national grid [kW]
$B_t^{el}\ \forall t = 1..T$, Price of electricity bought from the national grid [€/kWh]

$r_t^{el}\ \forall t = 1..T$, Revenue for the electricity sold to the national grid [€/kWh]
$C^{curt,PV}$, Cost of curtailment for PV [€/kWh]

The electricity purchased and sold, for the time period of 3 days taken into consideration, shows a dynamic behaviour as reported in the following two figures.
Figure 39 represents the cost associated with the selling of energy is quite discontinuous for the 36 hours, then the curve increases up to 0.53 €/kWh. The linear part of the curve is intended to simulate the selling price when geopolitical and economic events, like wars and catastrophic events, increase the price of imported energy.

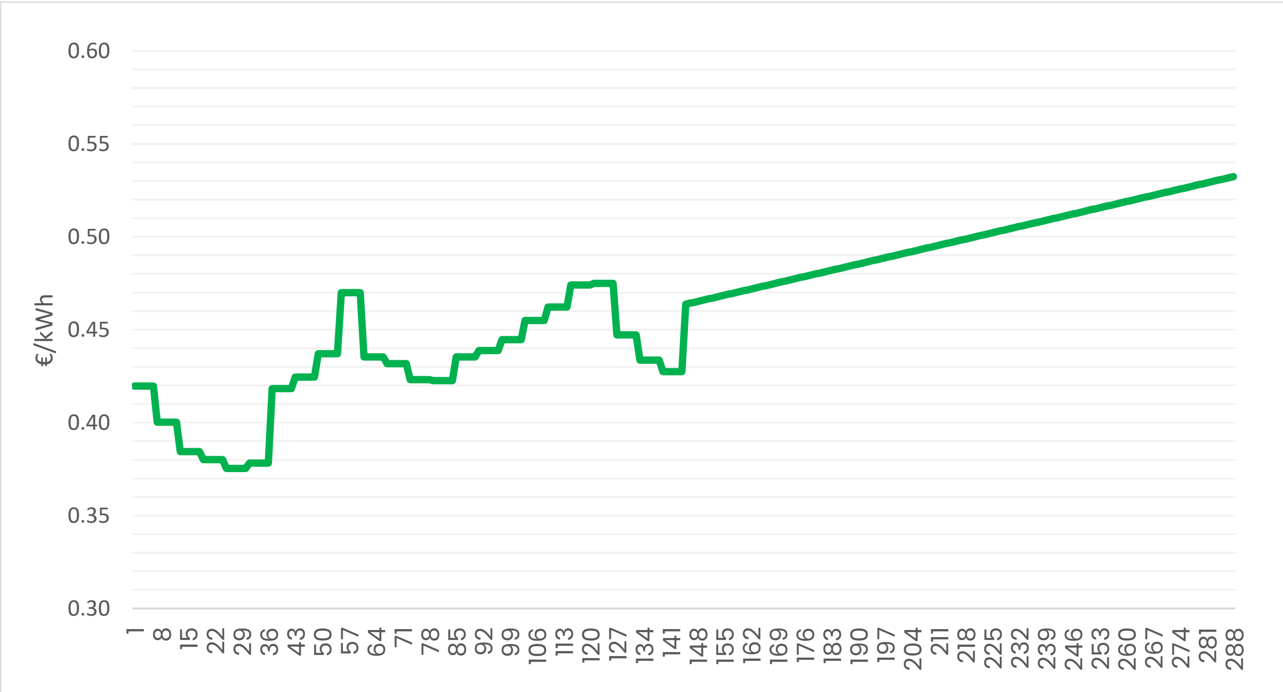

Figure 39: Selling price of electricity for the time period considered

In Figure 40 is displayed the buying price of electricity taken from the national grid.
The curve exhibits a stable price around 0.40 €/kWh for most of the time, except for a period where it increases to approximately 0.55 €/kWh, forming a peak. This peak suggests a time frame during which electricity prices rise before returning to the baseline level.

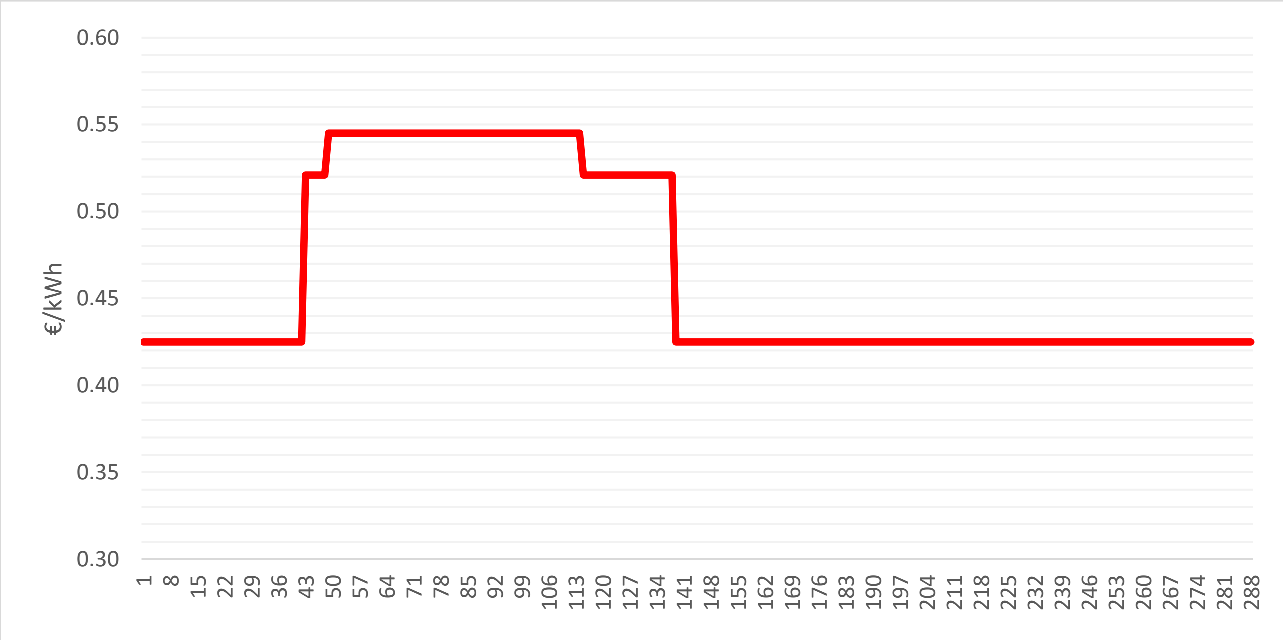

Figure 40: Buying price of electricity for the time period considered

Transformer:

A^T , Nominal apparent power of the transformer [kVA]
V^{N1}, Nominal voltage (line to line) of the primary side of the transformer[kV]
V^{N2}, Nominal voltage (line to line) of the secondary side of the transformer[kV]
P^{SC} , Short circuit power of the transformer [W]
v^{SC} , Short circuit voltage of the transformer [-]

Storage batteries:

$\eta^{ch,ESS}$, $\eta^{dch,ESS}$, Batteries charging and discharging efficiencies
$\mathrm{P}_b^{max,ch,ESS}$ $\forall b = 1..B$, Maximum power that can be provided to each battery of ESS [kW]
$\mathrm{P}_b^{max,dch,ESS}$ $\forall b = 1..B$, Maximum power that can be discharged from each battery of ESS [kW]
$\mathrm{P}_b^{min,ch,ESS}$ $\forall b = 1..B$, Minimum power that can be stored into ESS [kW]
$\mathrm{P}_b^{min,dch,ESS}$ $\forall b = 1..B$, Minimum power that can be taken from ESS [kW]

A_b^{ESS} $\forall b = 1..B$, Nominal apparent power of the electrical storage inverter [kVA]
C_b^{ESS} $\forall b = 1..B$, Rated Capacity of the storage system [kWh]
N^{ESS}, Number of batteries
$SOC^{min,ESS}$, Minimum state of charge of batteries [%]
$SOC^{max,ESS}$, Maximum state of charge of batteries [%]
τ^{ESS} , Ideal self-discharging rate
Δt, time interval

4.2 Decision variables

The decision variables are associated with the parameters that are obtained by the Matlab algorithm. Those are in a close relationship with the constraints, with the aim of providing the calculated solution that respects all the theoretical limits.

Load Flow variables:

$p_{b,k,t}^{node}$ $\forall t = 1..T$, where b and k represent all the connected nodes and Active power flowing from node b to node k. [p.u]
$q_{b,k,t}^{node}$ $\forall t = 1..T$, where b and k represent all the connected nodes and Reactive power flowing from node b to node k. [p.u]
$v_{b,t}^{node}$ $\forall t = 1..T$, Voltage module at node b.[p.u.]
$\delta_{b,t}^{node}$ $\forall t = 1..T$, Phase angle at node b.[p.u.]

Grid connection variable:

P_t^{buy} $\forall t = 1..T$, Active Power withdrawn from the national grid [kW]
P_t^{sell} $\forall t = 1..T$, Active Power injected into the national grid [kW]
x_t^{buy} $\forall t = 1..T$, binary variable equal to 1 if Active Power is withdrawn from the national grid
x_t^{sell} $\forall t = 1..T$, binary variable equal to 1 if Active power is injected into the national grid

PV:

$P_{b,t}^{PV}$ $\forall b = 1..B$ $\forall t = 1..T$, PV Active power output at bus all buses [kW]

$P_{b,t}^{PV,curt}$ $\forall b = 1..B$ $\forall t = 1..T$, PV Active power curtailment at different bus [kW]

Battery

$P_{b,t}^{ch,ESS}$ $\forall b = 1..B$ $\forall t = 1..T$, Active Power charged into ES [kW]
$P_{b,t}^{dch,ESS}$ $\forall b = 1..B$ $\forall t = 1..T$, Active Power discharged from ES [kW]
$x_{b,t}^{ch,ESS}$ $\forall b = 1..B$ $\forall t = 1..T$, binary variable equal to 1 if ESS is charging
$x_{b,t}^{dch,ESS}$ $\forall b = 1..B$ $\forall t = 1..T$, binary variable equal to 1 if ES is discharging
$E_{b,t}^{ESS}$ $\forall b = 1..B$ $\forall t = 1..T$, ESS energy content [kWh]

4.3 Constraints

Here are shown the theoretical limitations applied to the simulation. It is important to note that the reactive power flow calculations have not been taken into consideration for this analysis.

Load flow constraints:

$$p_{b,k,t} = \frac{r_{b,k}}{(r_{b,k})^2+(x_{b,k})^2} * (v_{b,t} - v_{k,t}) + \frac{x_{b,k}}{(r_{b,k})^2+(x_{b,k})^2} * (\delta_{b,t} - \delta_{k,t}), \forall t = 1..T$$
$$q_{b,k,t} = \frac{x_{b,k}}{(r_{b,k})^2+(x_{b,k})^2} * (v_{b,t} - v_{k,t}) - \frac{r_{b,k}}{(r_{b,k})^2+(x_{b,k})^2} * (\delta_{b,t} - \delta_{k,t}), \forall t = 1..T$$

Where b and k represent two connected nodes, these are linearized version of the real load flow equations.

Active power balance:

$$P_{b,t}^{PV} + P_{b,t}^{dch,BESS} = P_{b,t}^{ch,BESS} + L_{b,t}^{el,active} + S * \sum_{\substack{k\in B \\ k\neq b}} p_{b,k,t}^{node}$$

Grid:

$$0 \le P_t^{buy} \le P^{buy,max} * x_t^{buy}, \quad \forall t = 1..T$$
$$0 \le P_t^{sell} \le P^{sell,max} * x_t^{sell}, \quad \forall t = 1..T$$
$$x_t^{buy} + x_t^{sell} \le 1, \forall t = 1..T$$

PV:

$$P_{b,t}^{PV,av} = P_{b,t}^{PV} + P_{b,t}^{PV,curt}, \forall b = 1..B \ \ \forall t = 1..T$$
$$0 \le P_{b,t}^{PV,curt} \le P_{b,t}^{PV,av}, \ \ \forall b = 1..B \ \ \forall t = 1..T$$
$$0 \le P_{b,t}^{PV} \le P_{b,t}^{PV,av}, \ \ \forall b = 1..B \ \ \forall t = 1..T$$
$$0 \le P_{b,t}^{PV} \le P_{b,t}^{PV,av}, \ \ \forall b = 1..B \ \ \forall t = 1..T$$

Battery:

$$P_t^{ch,ESS} \ge 0 \, , \forall t = 1..T$$
$$P_t^{ch,ESS} \le P^{max,ch,ESS} * N^{ESS} * x_t^{ch,ESS} \, , \forall t = 1..T$$
$$P_t^{dch,ESS} \ge 0 \, , \forall t = 1..T$$
$$P_t^{dch,ESS} \le P^{max,dch,ESS} * N^{ESS} * x_t^{dch,ESS} \, , \forall t = 1..T$$
$$x_t^{ch,ESS} + x_t^{dch,ESS} \le 1 \, , \forall t = 1..T$$
$$E_t^{ESS} \ge \frac{SOC^{min,ESS}}{100} * N^{ESS} * C^{ESS} \, , \forall t = 1..T$$
$$E_t^{ESS} \le N^{ESS} * C^{ESS} \, , \forall t = 1..T$$
$$E_{t+1}^{ESS} = E_t^{ESS} + \Delta * \left(P_t^{ch,ESS} * \eta^{ch,ESS} - \frac{P_t^{\mathrm{dch},ESS}}{\eta^{dch,ESS}} \right)$$
$$\forall \ t = 1..(T-1)$$
$$E_1^{ES} = E_T^{ES} + \Delta * \left(P_T^{ch,ESS} * \eta^{ch,ESS} - \frac{P_T^{dch,ESS}}{\eta^{dch,ESS}} \right)$$
$$\forall \ t = 1..(T-1)$$

Voltage and phase angle constraints:

$$v_t^1 = 1$$
$$\delta_t^1 = 0$$
$$0.9 \le v_t^k \le 1.1 \ \ \forall t = 1..T$$

4.4 Objective functions

The objective function is designed to model the total costs associated with electricity trading. It accounts for the amount of electricity purchased minus the amount sold and includes all curtailment costs. This ensures that the PV plant is actively producing energy and incurs penalties if it fails to do so. The optimization of this function is performed with the help of the Yalmip toolbox and inbuild solver.

$$\min\{Total\ costs\}$$

$$\text{Total costs} = \Delta * \sum_{t=1}^{T} \left(B_t^{el} * P_t^{buy} - r_t^{el} * P_t^{sell}\right) + \Delta * \sum_{t=1}^{T} \left(C^{PV,curt} * P_{b,t}^{PV,curt}\right)$$

Δt , time interval [h]

4.5 Results and discussion

This final paragraph will outline the main results, together with their comments and comparisons. In particular, the discussion will be focused on the active power balance of each bus (2, 3, 4), the active power flowing in and out of the microgrid, the power and the state of charge of the batteries. The results will be shown for 3 random days of each season, the summary of the selected days is visible in Table 14.

Winter	15/01 – 17-01
Spring	5/04 – 7/04
Summer	7/07 – 9/07
Autumn	12/10 – 14/10

Table 14: Days selected for each season

4.5.1 Active power through the microgrid

The active power (inlet and outlet) of the microgrid provides a general overview of how the users' energy needs are met by the local energy community. The power load, pictured in blue, is satisfied in different ways (PV, purchase from the grid, storage) proportionally according to the season.

Electricity production from PV directly influences the contribution of BESS in covering the energy demand, the surplus energy is sold to the external grid when possible and energy is purchased from the outside when necessary.
Figure 41 represents the active power in and out of the microgrid for winter season. As could be seen, the energy derived from PV model is less significant than that purchased from the external grid. The batteries are used in a negligible and occasional manner and energy is sold for very limited periods of time, namely when peaks in electricity production occur.

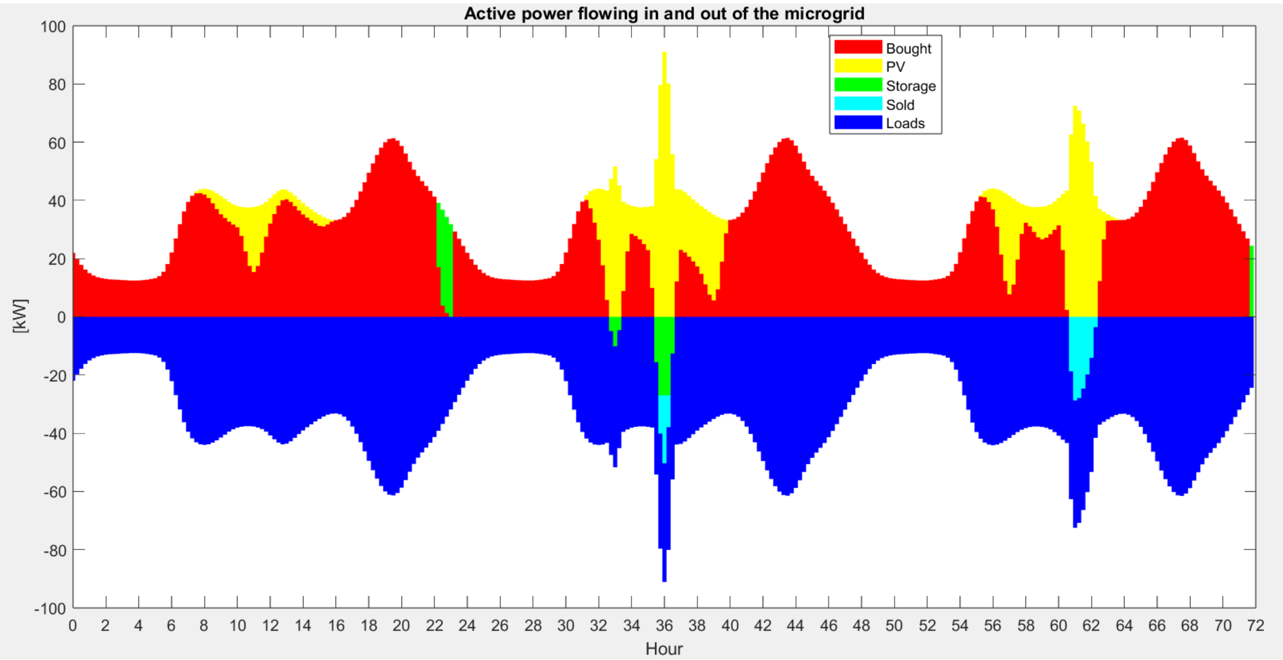

Figure 41: Active power flowing in and out of the microgrid during winter season

In Figure 42 and 43 is displayed the active power flowing through the microgrid for spring and summer periods.

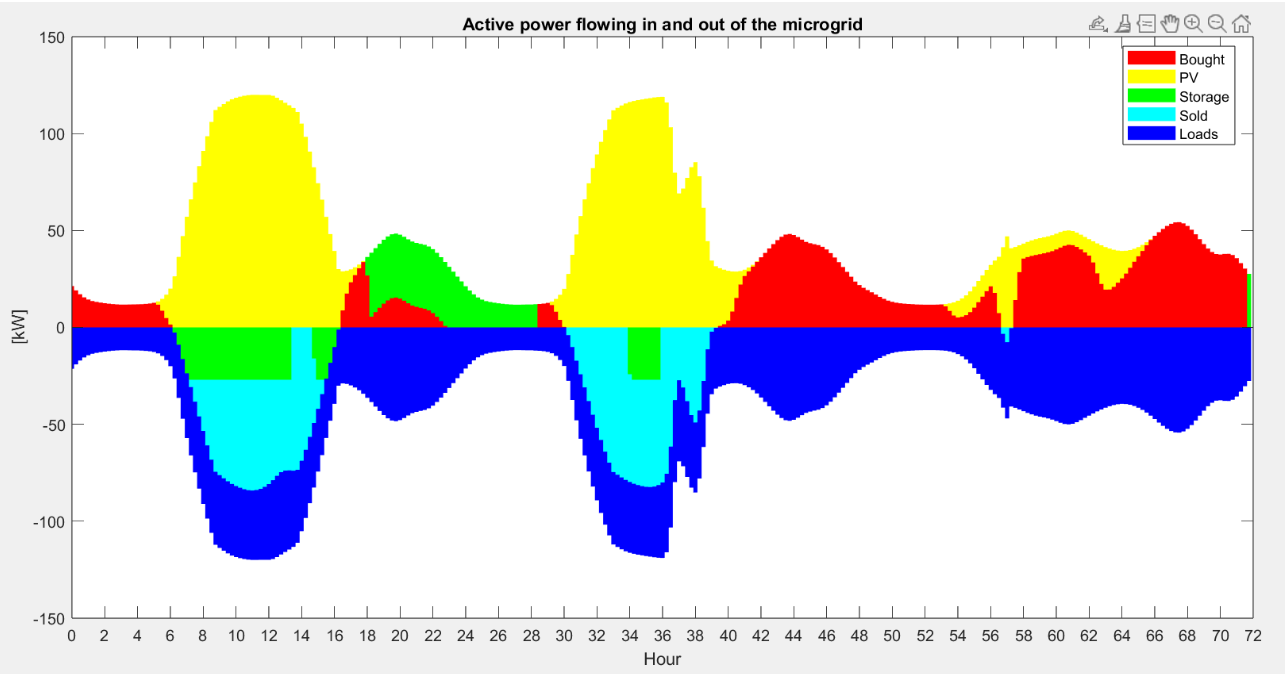

Figure 42: Active power flowing in and out of the microgrid during spring season

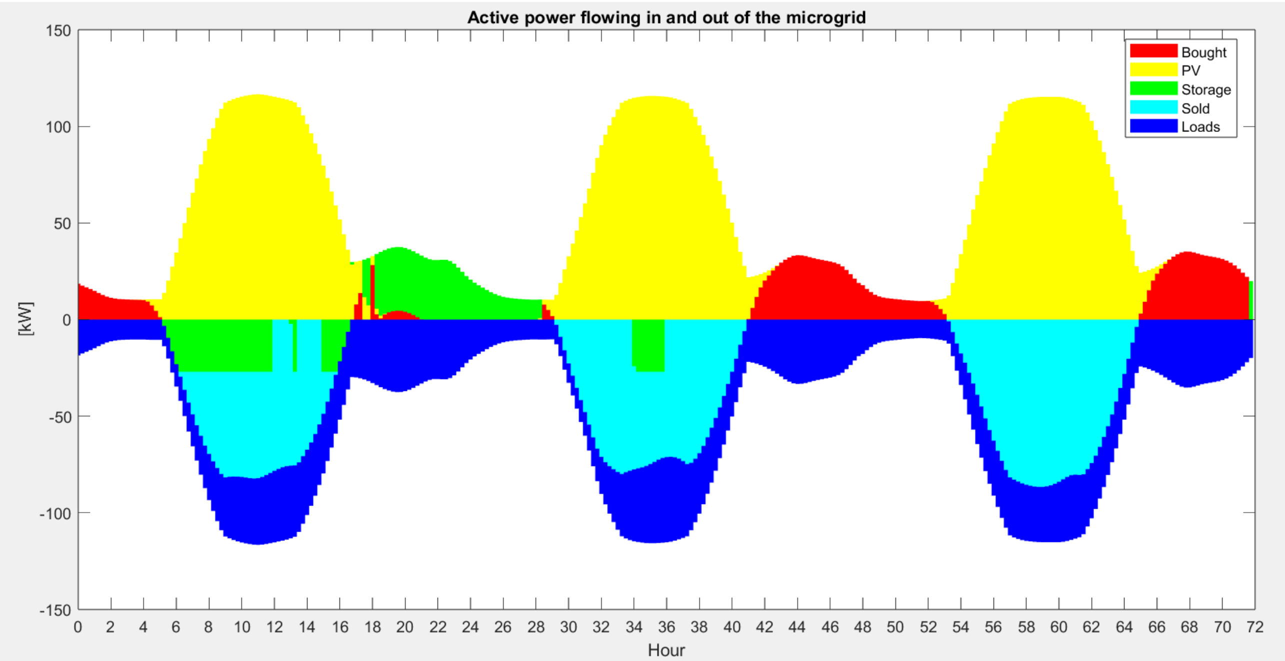

Figure 43: Active power flowing in and out of the microgrid during summer season

The findings for the two periods are similar, although energy production in spring is not as high as in summer.
In both cases (spring and summer), the energy purchased is lower compared to colder seasons, due to the decrease in electrical loads and the increase in energy production from PV systems.
The surplus energy produced, and not stored in BESS, is largely sold and is profitable for the whole community. The utilization of storage system is also increased and is able to meet all or part of the users' needs for a few hours, such as between 18th and 28th hour. In absence of sunlight, on the other hand, the electrical load is still fulfilled by purchased energy.

The autumn season, reported in figure 44, shows a similar behaviour compared to the winter period. By increasing electricity production, the batteries can be charged more and used to cover the consumer load, limiting the amount of energy derived from the transmission grid. This, however, is not yet high enough to sell energy and make a significant profit for the community.

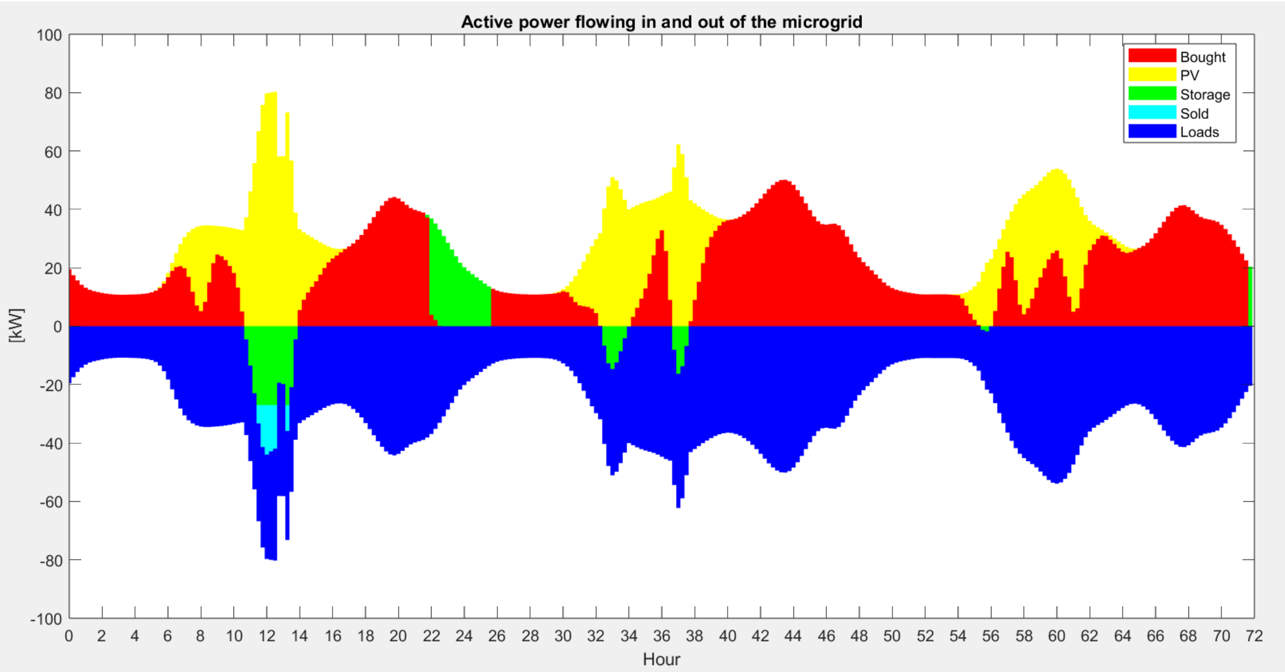

Figure 44: Active power flowing in and out of the microgrid during autumn season

In order to better understand which part of the total energy load is covered by the solar production contribution, an analysis related to SS parameter is performed. In particular, will be presented the better and the worst scenario, hence summer and winter seasons. In summer season (Figure 45), the PV production is really relevant and the SS results to be 100% when sunlight is available. The charging and discharging phases of the batteries are regulated according to buying and selling electricity price.

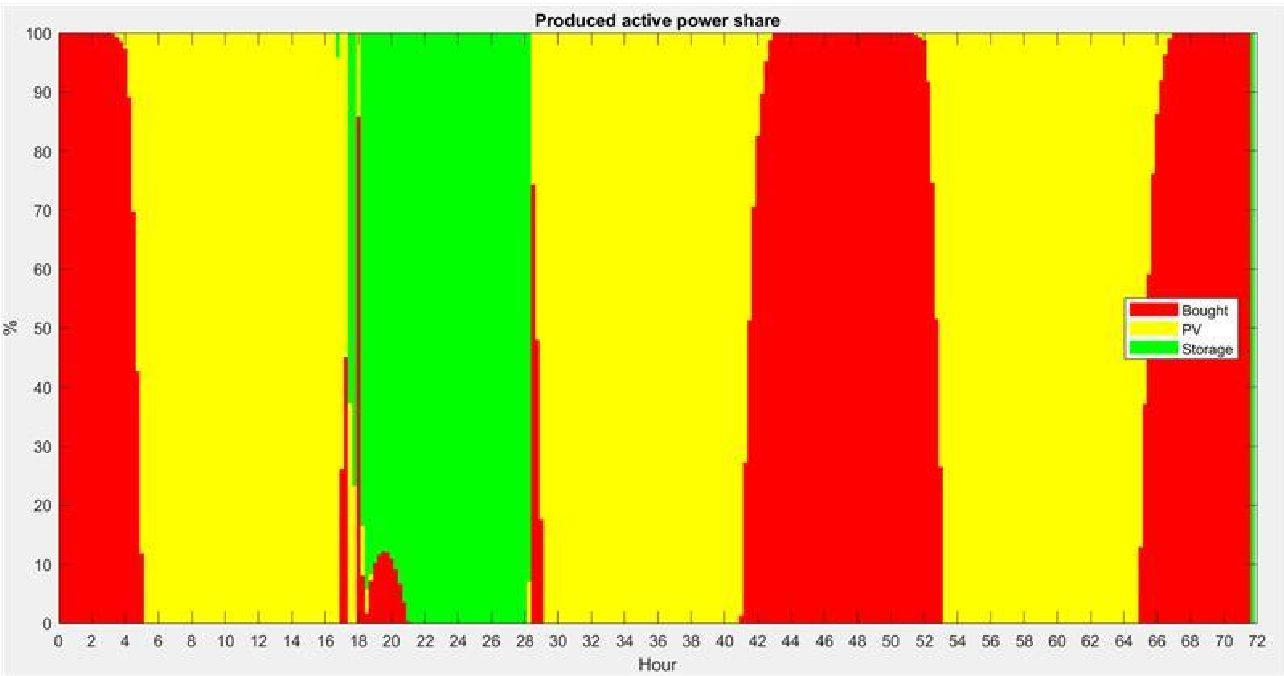

Figure 45: Produced active power share for summer season

The winter season, pictured in Figure 46, represent a different situation with respect to the previous case. The energy purchased from the grid is dominant for most of the time, while the share of solar energy production is intermittent during the daytime. Therefore the SS value is equal to 0% the majority of hours taken into account, showing a wide range of values up to 100% when peaks of solar production occur.

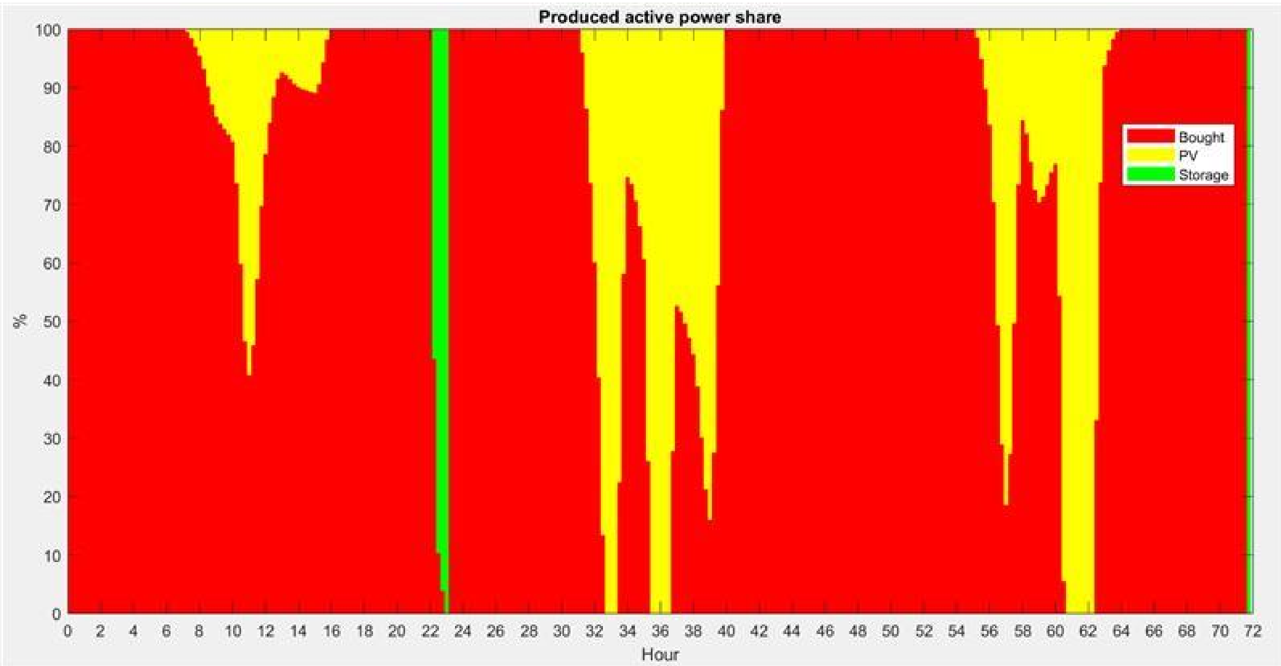

Figure 46: Produced active power share for summer season

4.5.2 Active power balance: bus 2

The bus 2, that is the transition bus, is the connection point between the external grid and the two buildings. This is the most important element of whole microgrid and the active power balance on this bus will be evaluated in the best condition (summer) and in the worst one (winter).

Figure 47 shows the active power balance for the winter season. The energy is represented in yellow coming from the electric grid due to the insufficient electricity production generated by the two buildings. In this season, the loads are higher and need more energy to be satisfied, therefore the energy demand can be covered buying electricity from the external grid. The other two graphical elements, pictured in purple and brown, are the active power from the building 1 and 2, both of them are importing electricity from the transition bus most of the time. For several instances, such as hours 22, 33, and 36, energy is shared among different buildings acting as an energy community. Conversely, during hours 61 to 63, energy is sold to the external grid.

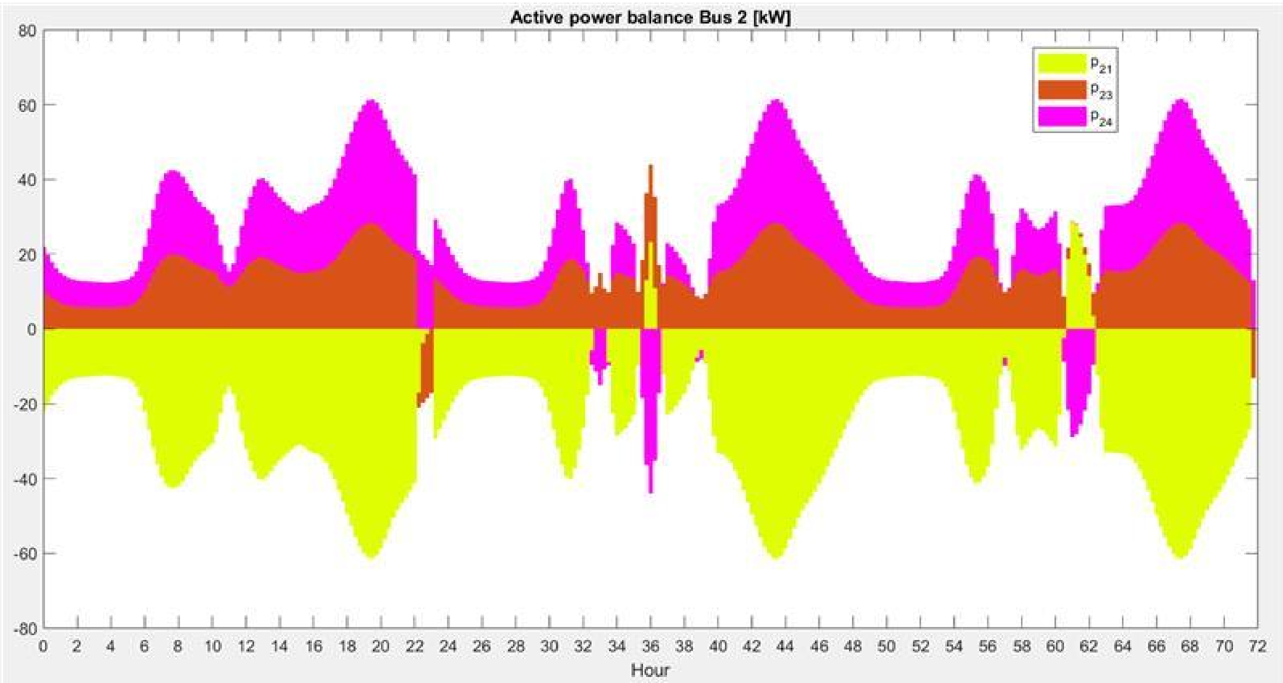

Figure 47: Active power balance for bus 2 during winter period (yellow: active power exchanged between grid and transition bus, red: active power exchanged between transition bus and building 1, purple: active power exchanged between transition bus and building 2)

In Figure 48, representing the summer season, the situation is the opposite. The energy demand is lower, and the energy productions are the highest during the year, hence the excess of electricity is delivered to the transition bus and then to the transmission grid. This is true especially for the building 2 where the PV power installed is more than double with respect to the other building. The building 1 is not always able to send the energy produced to the transition bus, between 5h and 16h the active power enters instead of leaving from the bus 3.

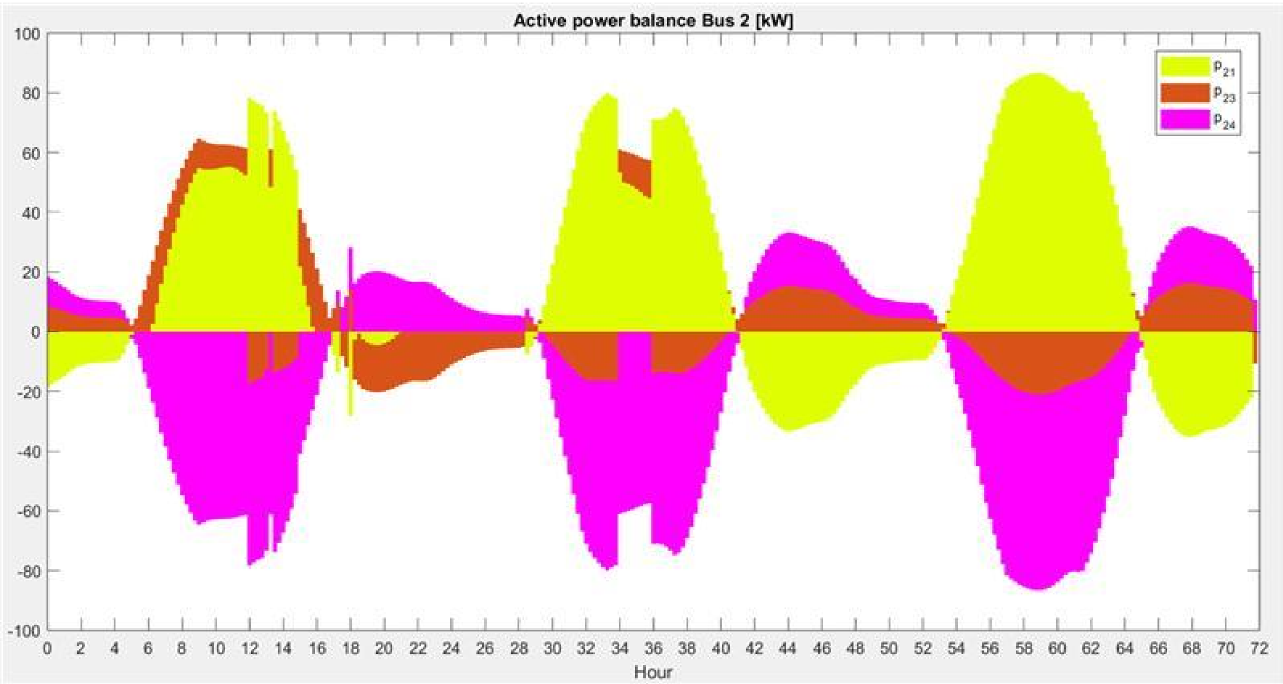

Figure 48: Active power balance for bus 2 during summer period (yellow: active power exchanged between grid and transition bus, red: active power exchanged between transition bus and building 1, purple: active power exchanged between transition bus and building 2)

4.5.3 Active power balance: bus 3

The bus 3 is refers to the building 1, equipped with hybrid system. The yellow part represents the PV building's energy production, which is higher in summer than in winter as expected. During the winter season (Figure 49), active power is transferred from bus 2 to 3, apart from occasional flow reversals such as that at the 23rd hour.
In contrast, during summer period (Figure 50), greater fluctuations in power exchange probably occur due to the use and the management of the BESS.

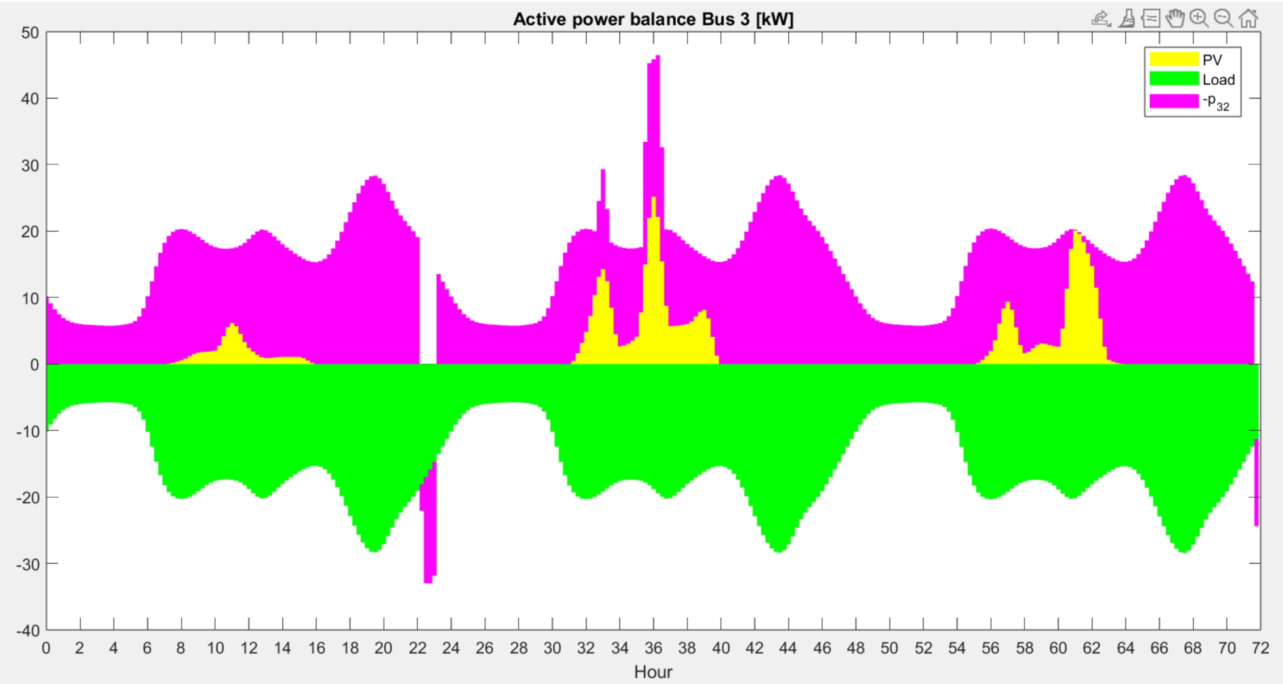

Figure 49: Active power balance for bus 3 during winter period (purple: active power exchanged between transition bus and building 1)

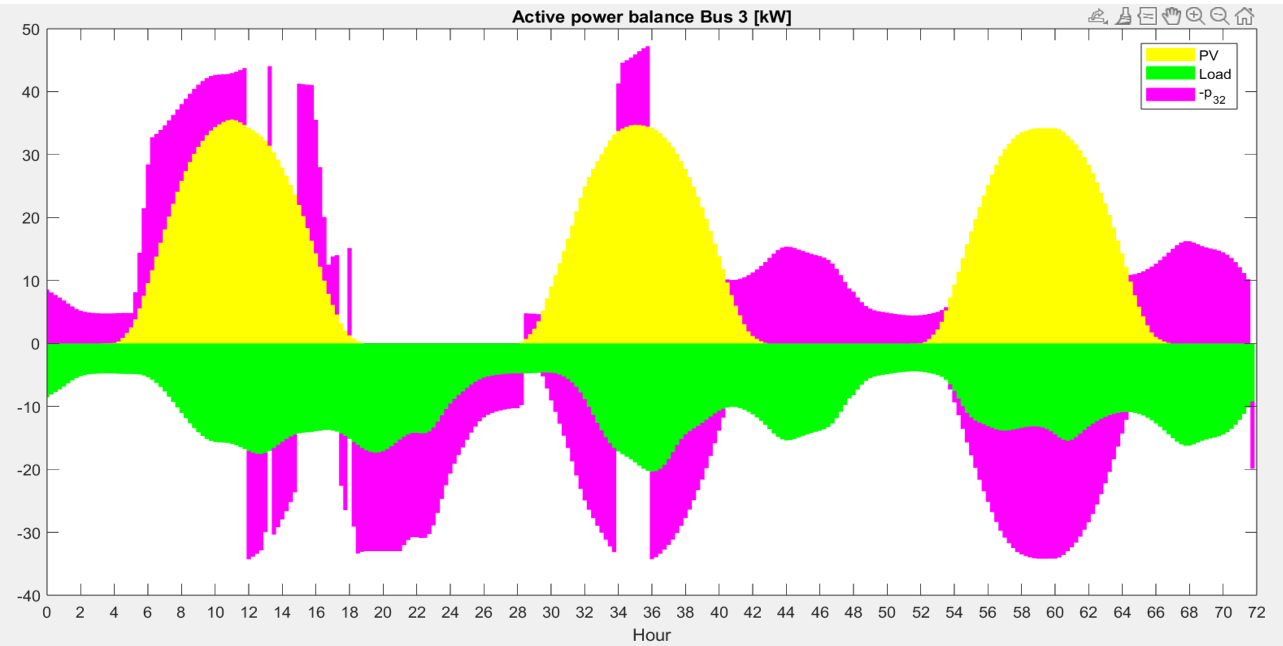

Figure 50: Active power balance for bus 3 during summer period (purple: active power exchanged between transition bus and building 1)

4.5.4 Active power balance: bus 4

Bus 4 refers to the building 2 and the cases displayed in Figures 51 and 52 are similar to those in the previous paragraph, but without the fluctuations due to the battery packs. In fact, the representations are smoother and more predictable.

During the winter period (Figure 51), energy is imported almost completely from the transition bus (2) apart from when the power peaks occur. In that case, the active power is sent the transition bus to be injected in the electrical grid.

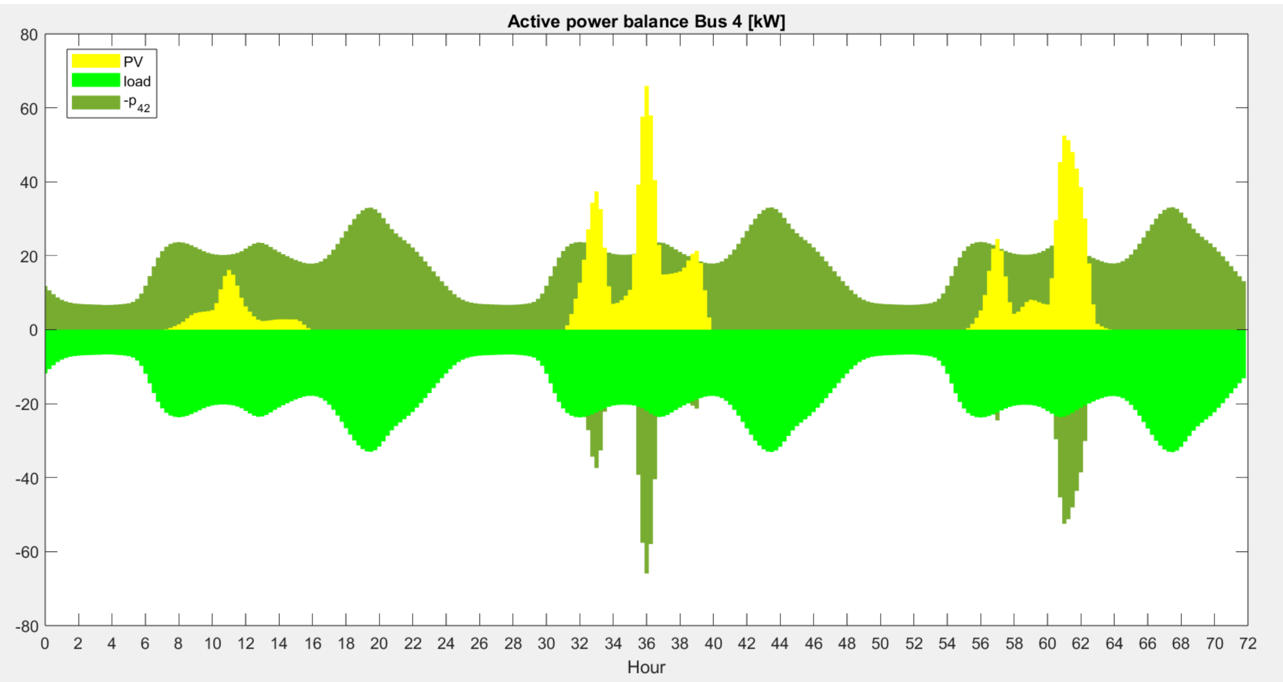

Figure 51: Active power balance for bus 4 during winter period (dark green: active power exchanged between transition bus and building 2)

In the summer case shown in Figure 52, when the PV system produces energy, this is sent outside the building (dark green). During the hours of darkness, the system does not work, and the building imports the energy required to meet the electrical load from the transition bus.

Obviously, due to the high electrical output of PV modules, the active power transferred is much higher than that purchased. This is also advantageous from an economical point of view, as it allows to make profit from the surplus energy produced.

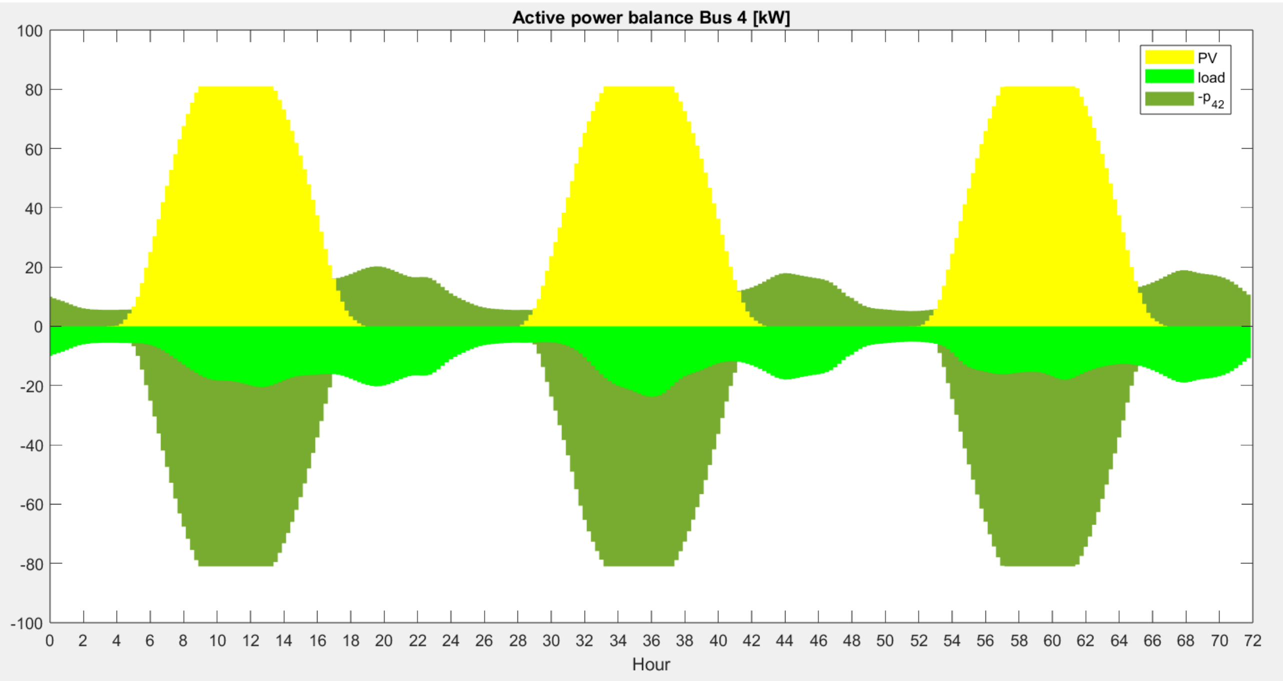

Figure 52: Active power balance for bus 4 during summer period (dark green: active power exchanged between transition bus and building 2)

4.5.5 Battery storage system

In this concluding section, the powers and the state of charge (SOC) of the BESS, relative to the building 1, are given in Figure 53 and Figure 54. Also in this case, the best and the worst cases are considered, namely the summer and the winter seasons. The analysis of these batteries parameters is crucial to understanding the behaviour of the battery system within this microgrid.

During the winter season (Figure 53), battery use is low. Indeed, it is easily visible that both power and SOC remain almost constant except for two specific moments of charging and discharging of the battery packs. The increase in power at the 23rd hour leads to a decrease in SOC from 20% to 9%, while at the 36th hour the exact opposite behaviour occurs.

In the summer season (Figure 54), the situation is completely different. The charge and discharge cycles are repeated more frequently, especially in the first 36 hours of analysis. In the periods where the solar production is in excess, the batteries are charged, and the SOC increases to the maximum (100%). When the PV energy production fails to fully meet the electrical load, the batteries completely release the electricity, and the SOC reaches the minimum value (0%).

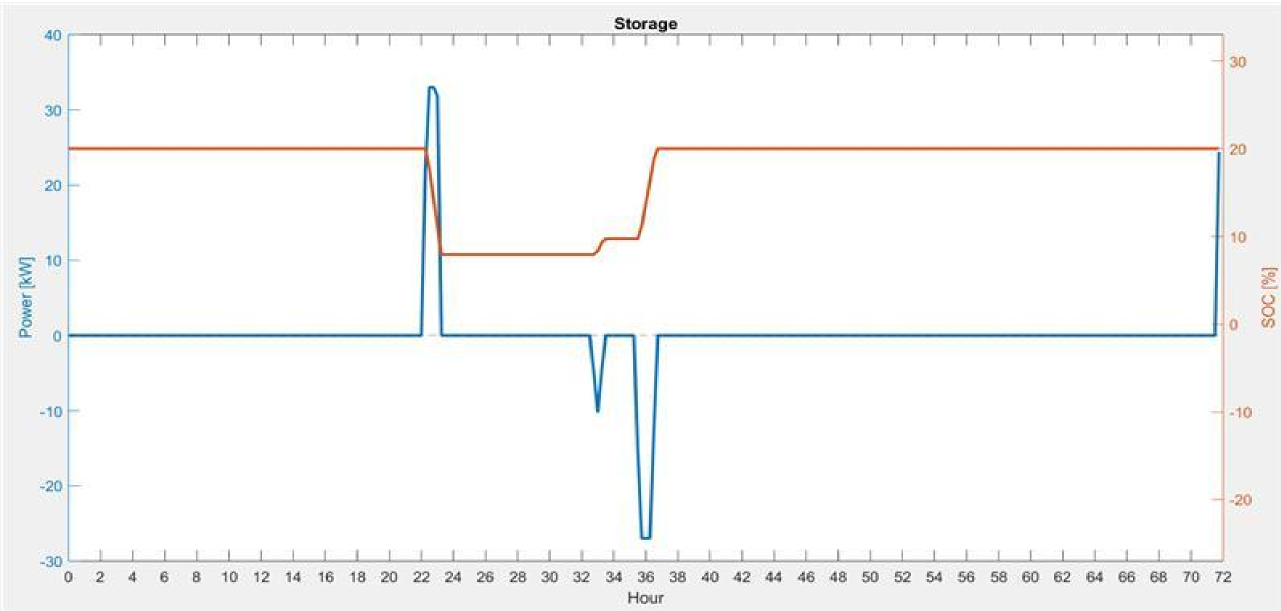

Figure 53: Power and SOC of BESS during winter period

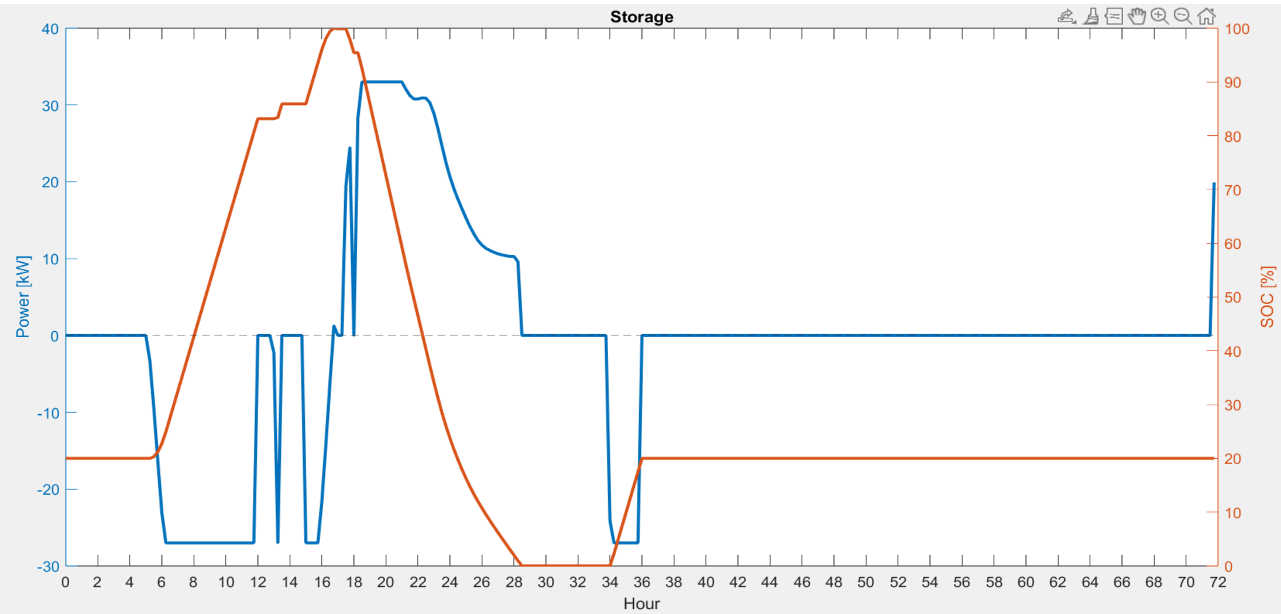

Figure 54: Power and SOC of BESS during summer period

5 Conclusions

This thesis aims to provide a general overview on how energy is produced and managed by the two buildings taken into account, simulating a small-scale energy community. The first building is equipped with a hybrid system, composed of a less powerful PV system (55,1 kWp) and a storage system. The second building is characterized by a higher nominal power (136 kWp), but the BESS is absent. The two buildings interact with each other and with the external grid in order to minimize the total costs and optimize the energy management. The results show that the users' energy needs are mainly covered by PV and battery storage systems, especially in summer, when solar energy production is maximized. In addition, the surplus energy can be sold to the external grid, contributing to increase the community's revenue. In practice, this model may be economically sustainable and suitable for all geographical areas where access to the national electric grid is not guaranteed. Moreover, the clean energy produced can contribute to the reduction of CO_2 while limiting the community's dependence on the external grid.

The model analyzed in the previous chapter can be further expanded by adding more types of participants, such as power plants and industry plants. The number of buildings used is rather limited and the simulation was carried out not taking into consideration the most efficient technological elements on the market. Furthermore, the hybrid system fully described in chapter 3 does not represent the only technological choice for a building in the city context. In fact, the photovoltaic and the battery storage systems provide a well-known and reliable energy solution, but also other technologies are suitable for the same purpose. For instance, in particular cases, small wind turbines can be implemented on a flat roof and produce energy in combination with PV modules. In future applications, even solid oxide fuel cells (SOFC) and electrolyzers could be implemented in RECs. The electrolyzers could convert the surplus electricity production into hydrogen (H_2) as a storage medium, while SOFCs could use the hydrogen produced to obtain electricity when needed or when electricity demand peaks occur.

The price of electricity is another relevant factor that could be crucial for the energy trading, especially in the years to come. These renewable communities, which promote local energy production and consumption through renewable sources, are highly

influenced by market fluctuations and regulatory frameworks. In the event of high electricity prices from the grid, the self-consumption of energy within the community becomes a more attractive strategy. This, therefore, results in greater incentives for investment in renewable energy infrastructure, such as solar panels, battery storage and smart EMS. In contrast, lower electricity prices from traditional sources may reduce the economic benefits of self-produced energy, potentially slowing down new investments in renewable projects and contributing to increase the CO_2 global emissions.
A major factor influencing energy prices in recent years has been geopolitical instability and armed conflicts, such as the one started between Ukraine and Russia in 2022, which is still in progress. Wars and geopolitical tensions have historically contributed to price increases by disrupting global energy supply chains, causing uncertainty in markets, leading to higher costs for fossil fuels and natural gas.

As energy prices rise due to these conflicts, RECs can become even more beneficial by reducing dependence on expensive and imported energy sources.
Energy price volatility also impacts the financial planning and management strategies of RECs. Higher energy costs can encourage community members to optimize consumption patterns, invest in energy efficiency solutions and adopt demand-side management practices. In contrast, unpredictable price drops could lead to financial instability, particularly for projects reliant on feed-in tariffs or other market-based compensation schemes.

Finally, innovative topic like artificial intelligence (AI) and machine learning (ML) could enhance remarkably the features of EMS by optimizing energy generation, distribution, consumption and storage.
One of the key applications of AI in RECs is demand forecasting. Machine learning models can analyze historical energy consumption data, weather patterns, and external factors such as electricity market prices to predict future energy demand with high accuracy. This enables RECs to optimise their self-consumption strategies, reduce reliance on the external grid, and minimize energy loss.
The EMS can also improve real-time energy distribution by adjusting power flows within the community. The integration of smart meters devices can balance efficiently supply and demand using AI, ensuring that renewable energy is used when and where it is needed most. For instance, when peaks of solar production occur, excess of energy can

be stored or shared among community members instead of being sold at low prices. Hence, the battery system managed through the use of AI could improve the overall efficiency of batteries by predicting when to charge or discharge batteries based on energy demand and market prices.

Moreover, the optimization of market participation can be improved through the implementation of AI. Smart EMS will be able to analyse energy market trends and determine the most suitable time for the purchase and sell of energy, taking advantage of price fluctuations in order to ensure the maximization of purchase.

6 References

[1] International Energy Agency, "Word Energy Outlook 2024," IEA, 2024.

[2] "Our World in Data," [Online]. Available: https://ourworldindata.org/co2-emissions. [Accessed January 2025].

[3] C. H. F. v. T. J. Lowitzsch, "Renewable energy communities under the 2019 European Clean Energy Package- governance model for the energy clusters of the future?," 2020. [Online]. Available: https://www.sciencedirect.com/science/article/pii/S1364032119306975?via%3Dihub.

[4] E. V. G. Doci, "Vasileiadou, Let's do it ourselves' Individual motivations for investing in renewables at community level," [Online]. Available: https://www.sciencedirect.com/science/article/pii/S1364032115003214?via%3Dihub.

[5] A. M. M. Sajjad Ahmed, "Renewable Energy Communities: Towards a new sustainable model of energy production and sharing," 2024.

[6] E. P. a. C. o. t. E. Union, "Directive (EU) 2018/2001 of the European Parliament and of the Council of 11 December 2018 on the promotion of the use of energy from renewable sources (recast) (Text with EEA relevance.)," [Online]. Available: https://eur-lex.europa.eu/legal-content/EN/TXT/?uri=uriserv:OJ.L_.2018.328.01.0082.01.ENG.

[7] E. P. a. C. o. t. E. Union, "Directive (EU) 2019/944 of the European Parliament and of the Council of 5 June 2019 on common rules for the internal market for electricity and amending Directive 2012/27/EU (recast) (Text with EEA relevance.)," [Online]. Available: https://eur-lex.europa.eu/legal-content/EN/TXT/?uri=CELEX:32019L0944.

[8] "DECRETO-LEGGE 30 dicembre 2019, n. 162," [Online]. Available: https://www.gazzettaufficiale.it/eli/id/2019/12/31/19G00171/S.

[9] "Art. 42-bis," [Online]. Available: https://www.gazzettaufficiale.it/atto/serie_generale/caricaArticolo?art.progressivo=0&art.idArticolo=42&art.versione=1&art.codiceRedazionale=042U0262&art.dataPubblicazioneGazzetta=1942-04-04&art.idGruppo=6&art.idSottoArticolo1=10&art.idSottoArticolo=2&art.

[10] "DECRETO LEGISLATIVO 8 novembre 2021, n. 199," [Online]. Available: https://www.gazzettaufficiale.it/eli/id/2021/11/30/21G00214/sg.

[11] "decreto n. 414 del 7 dicembre 2023," [Online]. Available: https://www.gazzettaufficiale.it/atto/serie_generale/caricaDettaglioAtto/originario?atto.dataPubblicazioneGazzetta=2024-02-

07&atto.codiceRedazionale=24A00671&elenco30giorni=false#:~:text=414%20del%207%20dicembre%202023,legislativo%208%20novembre%202021%2C.

[12] P. G. Chicco, *Self-sustainable prosumer community in emerging distribution grids,* Smart Electricity Systems, A.Y. 2023-2024.

[13] K. K. A. M. I. P. A. Z. Sylvain Quoilin, "Quantifying self-consumption linked to solar home battery systems: Statistical analysis and economic assessment," [Online]. Available: https://www.sciencedirect.com/science/article/pii/S0306261916311643.

[14] N. S. Kelepouris et al.., "Impact of demand side management on the self-sufficiency and self-consumption of bulidings with photovoltaic and storage systems," pp. 1-6, 2021.

[15] P. G. Chicco, *Electrical distribution system structure and reliability,* Smart Electricity Systems, A.Y. 2023-2024.

[16] P. G. Chicco, *Distributed Energy Resources,* Smart Electricity Systems, A.Y. 2023-2024.

[17] C. V. R. V. S. E. Shravan, "Emulation of AC and DC subgrids using Power".

[18] K. S. H. B. T. M. N. Ameer Hamza, "Hybrid AC/DC Microgrid for Residential".

[19] "Solargis Prospect," [Online]. Available: https://solargis.com/. [Accessed February 2025].

[20] "BDEW Bundesverband der Energie- und Wasserwirtschaft," [Online]. Available: https://www.bdew.de/. [Accessed February 2025].